

**U.S. DEPARTMENT OF THE INTERIOR
U.S. GEOLOGICAL SURVEY**

**THE TRACK OF THE YELLOWSTONE HOTSPOT:
VOLCANISM, FAULTING, AND UPLIFT**

by
Kenneth L. Pierce¹ and Lisa A. Morgan¹

Open-File Report 90-415

This report is preliminary and has not been reviewed for
conformity with U.S. Geological Survey editorial standards.

Copies of this report are available from:

U.S. Geological Survey
Office of Open File Services, MS 517
Box 25046, Federal Center
Denver CO, 80225

¹U.S. Geological Survey, MS 913, Box 25046, Federal Center, Denver, CO 80225.

Table of Contents

ABSTRACT1	1
INTRODUCTION	2
VOLCANIC TRACK OF THE YELLOWSTONE HOTSPOT	4
Hotspot Track 0-10 Ma	4
Western Snake River Plain and Hotspot Track	5
NEOTECTONIC CLASSIFICATION OF FAULTING	5
Belt II, Defined By Major Holocene Faults	6
Teton Fault History	6
Belt II, Southern Arm	7
Belt II, Western Arm	7
Belt I, Lesser and Reactivated Faults Beyond Belt II	8
Belt I, Southern Arm	8
Belt I, Western Arm	8
Belt III, Defined By Major late Pleistocene Faults	9
Belt III, Southern Arm	9
Belt III, Western Arm	10
Belt IV, Defined by Major Tertiary Faults	10
NEOTECTONIC DOMAINS EMANATING FROM THE YELLOWSTONE HOTSPOT	10
The Present Cycle	10
Belt IV and Older Cycles of Faulting	11
Neotectonic Fault Belts and Historic Seismicity	12
ALTITUDE AND THE HOTSPOT TRACK	12
Possible Scales to Consider	12
Yellowstone Crescent Of High Terrain	13
Altitude Changes North of the Snake River Plain	13
Rugged Mountains of Readily Erodible Rocks	14
Pleistocene Glacier-Length Ratios and Altitude Changes	15
Big Horn Basin Region	16
Unidirectional Stream Migrations (Displacements)	16
Convergent/Divergent Terraces	16
Uplifted(?) Calcic Soils, Rock Creek	17
Areas more than 250 km from the hotspot track	17
Problems Relating Regional Uplift to the Yellowstone Hotspot	17
DISCUSSION	18
Alternative Models and their Problems	19
Eastward Propagating Rift	19
Crustal Flaws and the Origin of the SRP-YP Province	20
Transform Boundary Zone Origin for the SRP	20
A Meteorite Impact Origin for the SRP-YP Province	21
A Two-Phase, Mantle Plume Model For the SRP-YP Region	22
The Two Phase Model	22
Evidence from Volcanism and Rifting	23
Evidence from Faulting and Uplift	25
Other Discussion Of Extensional Faulting	26
Relation Between the Yellowstone Hotspot and Basin and Range Deformation	27
CONCLUSIONS	28
REFERENCES CITED	30
Plate 1 caption	39
Start of captions for figures 1-23	40
Start of tables (1, 2, and3)	45

THE TRACK OF THE YELLOWSTONE HOTSPOT: VOLCANISM, FAULTING, AND UPLIFT

Kenneth L. Pierce and Lisa A. Morgan

ABSTRACT*

The track of the Yellowstone hotspot is represented by a systematic NE-trending linear belt of silicic, caldera-forming volcanism that arrived at Yellowstone 2 Ma, was near American Falls, Idaho, about 10 Ma, and started about 16 Ma near the Nevada-Oregon-Idaho border. From 10-2 Ma, silicic volcanism migrated N 54° E towards Yellowstone at about 3 cm/yr, leaving in its wake the eastern Snake River Plain (SRP). The eastern SRP is a linear, mountain-bounded, 75-km-wide trench almost entirely floored by calderas that are thinly covered by basalt flows. From 16-10 Ma, particularly 16-14 Ma, volcanism was widely dispersed around the inferred hotspot track in a region that now forms a moderately high volcanic plateau. The current hotspot position at Yellowstone is spatially related to active faulting and uplift.

Basin-and-range faults in the Yellowstone-SRP region are classified into six types based on both recency of offset and height of the associated bedrock escarpment. The distribution of these fault types permits definition of three adjoining belts and a pattern of waxing, culminating, and waning activity. The central belt, Belt II, is the most active and is characterized by faults active since 15 ka on range fronts >700 m high. Belt II has two arms forming a "V" that joins at Yellowstone: one arm of Belt II trends south to the Wasatch front; the other arm trends west and includes the sites of the 1959 Hebgen Lake and 1983 Borah Peak earthquakes. Fault Belt I is farthest away from the SRP and contains relatively new and reactivated faults that have not produced new bedrock escarpments higher than 200 m during the present episode of faulting. Belt III is the innermost active belt near the SRP. It contains faults that have moved since 15-120 ka and which have been active long enough to produce range fronts more than 500 m high. A belt with inactive faults occurs only south of the SRP and contains late Tertiary range-front faults that experienced high rates of activity coincident with hotspot volcanism on the adjacent SRP. Comparison of activity based on these belts with that defined by modern seismicity is remarkably similar but differs in detail.

Uplift migrating outward from the hotspot track is suggested by (1) the Yellowstone crescent of high terrain that is about 0.5 km higher than the

surrounding terrain, is about 350 km across at Yellowstone, wraps around Yellowstone like a bow wave, and has arms that extend 400 km southerly and westerly from its apex, (2) readily erodible rocks forming young, high mountains in parts of this crescent, (3) geodetic surveys and paleotopographic reconstructions that indicate young uplift near the axis of the Yellowstone crescent, (4) on the outer slope of this crescent, glaciers during the last glaciation were anomalously long compared with those of the preceding glaciation, suggesting uplift during the intervening interglaciation, and (5) lateral migration of streams, apparent tilting of stream terraces away from Yellowstone, and, for increasingly younger terrace pairs, migration away from Yellowstone of their divergent-convergent inflection point.

We conclude that the neotectonic fault belts and the Yellowstone crescent of high terrain reflect heating that has migrated to distances as much as 200 km from the eastern SRP in 10 m.y, and that the only mechanism for such heat transport is flow of hot material within the asthenosphere, most likely by a thermal mantle plume rising to the base of the lithosphere and flowing outward horizontally for at least such distances.

The change in the volcanic track between 16-10 Ma and 10-2 Ma is readily explained by first the head (300 km diameter) and then the chimney (10-20 km across) phases of a thermal mantle plume rising to the base of the SW-moving North American plate. About 16 Ma, the bulbous plume head intercepted and mushroomed out at the base of the lithosphere, resulting in widespread magmatism and tectonism centered near the common borders of Nevada, Oregon, and Idaho. Starting about 10 Ma near American Falls and progressing to Yellowstone, the chimney penetrated through its less active head and spread outward at the base of the lithosphere, adding basaltic magma and heat to the overriding SW-moving lithospheric plate, and leaving in its "wake" the eastern-SRP-Yellowstone track of calderas, and forming, ahead and outward from this track, the outward-moving belts of active faulting and uplift.

We favor a mantle plume explanation for the hotspot track and associated tectonism and find problems with competing hypotheses that include the following: (1) for a rift origin, faulting and extension directions are at nearly right angles to that appropriate for a rift, (2) for a transform origin, geologic evidence requires neither a crustal flaw nor differential extension across the eastern SRP, and volcanic alignments on the SRP do not indicate a right-lateral shear across the SRP. The southern Oregon rhyolite zone is not analogous to the eastern SRP and therefore does not disprove formation of the Yellowstone hotspot track by a mantle plume.

The postulated rise of a mantle-plume head into the mantle lithosphere about 16 Ma corresponds in both time and space with the following geologic changes: (1) the start of the present pattern of basin-range extension, (2) intrusion of basalt and rhyolite

* Approved by the Director, 6/27/90. This report intended for publication by the Geological Society of America in a volume in honor of Steve Oriol.

along the 1,100-km-long Nevada-Oregon rift zone, (3) the main phases of flood basalt volcanism of the Columbia River and Oregon plateaus, and (4) a change from calc-alkaline volcanism of intermediate to silicic composition to basaltic and bimodal rhyolite/basalt volcanism.

INTRODUCTION

The track of the Yellowstone hotspot is defined by the time-transgressive centers of caldera-forming volcanism which since 16 Ma migrated 700 km northeastward to Yellowstone (Plate 1; Fig. 1). We compare the progression of silicic volcanism with the timing of late Cenozoic faulting and uplift in nearby areas and suggest that a V-shaped pattern of deformation is now centered on Yellowstone. We use the term "hotspot" to nongenetically describe this progression of silicic volcanism, although we favor its formation by a mantle plume. The hotspot track is 700 km long and the fault belts and associated Yellowstone crescent of high terrain extend more than 200 km from the hotspot track: we attribute these horizontal dimensions to thermal effects originating deeper than the 100(?) -km-thick lithosphere and conclude that the history of uplift, volcanism, and faulting since 10 Ma in eastern Idaho and parts of adjacent states is best explained by the WSW movement of the North American plate across a thermal mantle plume.

By tracking from the present location of the hotspot beneath Yellowstone back in time, we find a major change occurred about 10 Ma. We think the significance of the Yellowstone hotspot is best understood by backtracking volcanism, faulting, and uplift from the areas of present activity to older positions to the southwest. From 10 Ma to present, caldera-forming volcanism is responsible for the 80-km-wide trench of the eastern Snake River Plain; with increasing age prior to 10 Ma, volcanism was increasingly more dispersed back to the inception of the hotspot about 16 Ma. We think a reasonable explanation for this change can be related to a transition in the shape from a large plume head prior to 10 Ma to, after 10 Ma, a much narrower plume tail or chimney (Fig. 2; Richards and others, 1989). About 16 Ma, the head of a mantle plume about 300 km in diameter rose into the base of the southwest-moving North American plate. About 10 Ma, a narrower "tail" or chimney about 10-20 km across that was feeding the plume head rose through the stagnant plume head and intercepted the base of the lithosphere.

A mantle plume hypothesis represents one side of an ongoing controversy about the origin of the eastern Snake River Plain-Yellowstone Plateau (SRP-YP) province. Plate-tectonic, global-scale studies often simply state the province represents a hotspot track, and commonly include it in inventories of hotspots (for example, Morgan, 1973). However, several prominent researchers in the region have argued for lithospheric movements that drive asthenospheric processes such as upwelling, and argue against an active mantle plume

modifying a passive lithosphere (Christiansen and McKee, 1978; Leeman, 1982; Hamilton, 1989). Our acceptance of the mantle plume hypothesis comes after serious consideration of these models.

A hotspot/mantle plume mechanism, particularly the start of a hotspot track with a large-diameter plume head, has been rarely invoked in North American geology. On a global scale, the existence and importance of hotspots and mantle plumes have gained credibility through their successful application to such topics as plate tectonics, flood basalts associated with rifts, volcanic hotspot island chains and associated swells, and anomalies in the geoid (see Bercovici and others, 1989; Sleep, 1990; Wilson, 1990). J. Tuzo Wilson (1963) proposed that the Hawaiian Islands, as well as other volcanic island chains, are formed by a stationary heat source located beneath the moving lithosphere-- a hotspot. Morgan (1973) argued that hotspots were anchored by deep mantle plumes and showed that hotspot tracks approximated the absolute motions of plates. Based on simultaneous solution of interplate motions determined by sea floor spreading rates, fracture zone trends, and earthquake slip vectors, Minster and others (1974) and Minster and Jordan (1978) determined that hotspots are fixed within ± 1 cm/yr relative to each other, and therefore do, as postulated by Morgan, approximately define absolute plate motions in the overriding lithosphere.

Hotspots and their tracks are better displayed and more common in oceanic than in continental lithosphere. They are preferentially located near divergent plate boundaries and preferentially excluded near convergent plate boundaries (Weinstein and Olson, 1989). However, during the Mesozoic-earliest Cenozoic breakup of the supercontinent Gondwana, the continental lithosphere was greatly affected by the Reunion, Tristan, and probably the Marion hotspots (White and McKenzie, 1989). Mantle plumes feeding these hotspots rose into continental lithosphere-- probably starting with mantle plume heads-- and produced domal uplifts about 2000 km across, released voluminous flood basalts, and caused continental rifts, many of which evolved into the present oceanic spreading centers (Richards and others, 1989). During the dispersion of continents following breakup of Gondwana, including the outward movement of oceanic spreading ridges, some spreading ridges have apparently crossed hotspots; this suggests that hotspots have both a deeper origin and lesser absolute motion than the spreading centers (Duncan, 1984).

No continental analogues similar to Yellowstone-eastern Snake River Plain are known to us for a hotspot/mantle plume. The following special characteristics of the North American plate and the western U.S. are probably important in how the Yellowstone hotspot is manifest. (1) The speed of the North American plate is about 3 cm/yr southwestward, much faster than for postulated hotspots beneath the nearly stationary African Plate (Crough, 1979, 1983). The Yellowstone speed is only one-third that beneath the "type" Hawaiian hotspot, which penetrates oceanic

crust. (2) The present location of the Yellowstone hotspot is at the northeast edge of the northeast quadrant of the extending Basin and Range lithosphere bordered to the north and east by high terrain of the Rocky Mountains. (3) The Yellowstone mantle plume rose into crust thickened during the Mesozoic and earliest Tertiary orogenies (Sevier and Laramide) (Christiansen and Lipman, 1972; Wernicke and others, 1987; Molnar and Chen, 1983). (4) About 2 Ma, the Yellowstone hotspot left thickened crust of the thrust belt and passed beneath the stable craton. (5) The plate margin southwest of the hotspot track has been progressively changing from a subduction zone to a weak(?) transcurrent fault (Atwater, 1970) over a time span that overlaps the postulated activity of the Yellowstone hotspot since 16 Ma.

In comparison to some other postulated continental hotspots, the volcanic age progression of the Yellowstone track is rather systematic along its 700-km track, whereas that for other postulated continental hotspots is less systematic, such as for the White Mountain igneous province (Duncan, 1984), the Raton (New Mexico)-Springerville zone (Suppe and others, 1975), and the African hotspots (Crough, 1979, 1983). However, this may be merely an artifact of the style of volcanism and being able to distinguish among various volcanic products. We define the volcanic track of the Yellowstone hotspot using the onset of large-volume, caldera-forming ignimbrite eruptions. However, within any one volcanic field of the SRP-YP province, volcanism (in the form of basalt and rhyolitic lava flows and small-volume rhyolitic pyroclastic deposits) may precede the major caldera-forming event by several million years and continue for several million years after (see Morgan and others, in press, Fig. 10). Thus, if it were not for the distinctive onset of the large-volume ignimbrite volcanism, Yellowstone would have a much less systematic age progression, more like the case for the above-mentioned postulated hotspots.

The length of this paper reflects an integration of volcanology, neotectonics, geomorphology, plate tectonics, and mantle plume dynamics. As such, this preliminary synthesis involves testable hypotheses in each of these disciplines as well as a potential framework for future studies. If our explanation is valid, studies in the Yellowstone region present unusual opportunities to study continental lithospheric response to such a large-scale disturbance.

Chronology of investigations and acknowledgements

This paper expands on a concept conceived in 1984 by Pierce relating the neotectonic deformation pattern of Idaho and adjacent states to the Yellowstone hotspot (Scott, Pierce, and Hait, 1985a, b) and briefly elaborated later (Pierce and Scott, 1986; Pierce and others, 1988). Bob Smith and Mark Anders have come to similar conclusions about deformation related to the Yellowstone hotspot based mostly on epicenter locations and undifferentiated Quaternary

faulting (Smith and others, 1985, written commun., 1989; Anders and Geissman, 1983; Anders and Piety, 1988; Anders and others, 1989).

In their analysis of the 1959 Hebgen Lake earthquake, Myers and Hamilton (1964) suggested that on-going faulting on both the Teton and Centennial Ranges is related to the SRP-Yellowstone volcanic rift zone. Armstrong and others (1975) documented a northeast progression of rhyolitic volcanism along the eastern SRP at a rate of 3.5 cm/yr. Suppe and others (1975) considered the Yellowstone hotspot responsible for both the on-going tectonic activity between Yellowstone and the Wasatch front, and updoming 350 km wide centered on Yellowstone. High rates of faulting between 4.3 and 2 Ma followed by quiescence in the Grand Valley area were described in an abstract by Anders and Geissman (1983) and attributed to a "collapse shadow" possibly related to a northeast shift of SRP volcanic activity. Scott, Pierce, and Hait (1985a, 1985b) recognized a V-shaped pattern of the most active neotectonic faults that converged on Yellowstone like the wake of a boat about the track of the Yellowstone "hotspot"; they also related earlier phases of late Cenozoic deformation to older positions of the hotspot. This report is a fuller development of ideas published in 1985 and later abstracts (Pierce and Scott, 1986; Pierce, Scott, and Morgan, 1988). Smith and others (1985; in preparation) noted two belts of seismicity and late Quaternary faulting that converge on Yellowstone and a "thermal shoulder" zone of inactivity inside these belts. Piety and others (1986, p. 108-9) conclude that the locus of faulting in the Grand Valley-Swan Valley area has moved along and outward from the track of the Yellowstone "hotspot". Anders and others (1989) define inner and outer parabolas that bound most of the seismicity in the region and model how underplated basalt increases in strength through time that elegantly explains both lithospheric softening and hardening upon passage of the mantle plume. In a summary on heat flow of the Snake River Plain, Blackwell (1989) concluded that the volcanic track resulted from a mantle plume. Westaway (1989) argued that the V-shaped convergence of seismicity and faulting on Yellowstone could be explained by shearing interactions of an upwelling mantle plume and WSW motion of the North American plate. Malde (in press) advocates the hot spot origin of the eastern Snake River Plain, and contrasts this with the graben origin of the western Snake River Plain. Acknowledgements-- Major help in review as well as stimulating discussion were freely given by Karl Kellogg, Scott Lundstrom, Dean Ostenaar, Marith Reheis, and Bob Duncan. We thank the following for discussions over the past years quite important to developing the arguments presented in this paper: Mark Anders, Ernie Anderson, Fred Barker, Clem Chase, Jim Case, Bob Christiansen, John Good, Tim Hait, Bill Hackett, Mel Kuntz, Bill Locke, Dave Love, Mike Machette, Ann McCafferty, Jim McCalpin,

Grant Meyer, Bob Palmquist, Bill Scott, Bob Smith, Mike West, Mary Lou Zoback.

VOLCANIC TRACK OF THE YELLOWSTONE HOTSPOT

The age of late Cenozoic caldera-filled silicic volcanic fields along the SRP increases systematically from 0-2 Ma on the Yellowstone Plateau to 15-16 Ma near the common borders of Idaho, Nevada and Oregon (Armstrong and others, 1975) (Plate 1). Figure 2 shows the time progression of volcanism, based on the oldest caldera within a particular volcanic field. Many consider this volcanic progression to represent the trace of a mantle plume (for example see Minster and others, 1974; Suppe and others, 1975; Crough, 1983; Anders and others, 1989; Richards and others, 1989; Blackwell, 1989; Wilson, 1990; Rodgers and others, 1990; Malde, in press). Alternatively, this volcanic progression has been attributed to a rift (Myers and Hamilton, 1964, p. 97; Hamilton, 1987), a propagating crack along a transform fault boundary separating greater basin-range extension south of the plain from lesser extension to the north (Christiansen and McKee, 1978), or a melting anomaly located in the lithosphere (Leeman, 1989).

HOTSPOT TRACK 0-10 MA

The onset of caldera-forming eruptions for the three younger volcanic fields of the SRP-YP province define a systematic spatial and temporal progression (Plate 1, Figs. 3 and 4, Table 1). The post-10 Ma hotspot track is also well defined by topography. From the Picabo to the Yellowstone fields, the 80 ± 20 -km-wide, linear, mountain-bounded trough of the eastern SRP-YP is floored by nearly continuous, overlapping calderas over its entire width. The 0-10 Ma volcanic fields and the caldera-forming ignimbrites from them are: (1) the Yellowstone Plateau volcanic field which produced the 2.0-Ma Huckleberry Ridge Tuff, the 1.2-Ma Mesa Falls Tuff, and the 0.6-Ma Lava Creek Tuff (Christiansen and Blank, 1972); (2) the Heise volcanic field, which produced the 6.5-Ma tuff of Blacktail Creek, the 6.0-Ma Walcott Tuff, and the 4.3-Ma tuff of Kilgore (Morgan and others, 1984; Morgan, 1988), and (3) the Picabo volcanic field, which produced the 10.3-Ma tuff of Arbon Valley (see footnote in Table 1).

Each volcanic field, commonly active for about 2 m.y., is defined by a cluster of several extremely large calderas. A systematic age progression is defined by the sequence of volcanic fields, but no systematic age progression is apparent within a field (Plate 1). In addition, a hiatus of at least 2 m.y. probably occurs between the youngest major ignimbrite in one field and the oldest major ignimbrite in the next younger field (Plate 1; Table 1; Fig. 3; see Morgan and others, 1984 for further discussion).

Location of calderas and their associated vents in the Yellowstone Plateau and Heise volcanic fields are

based on a variety of techniques including variations in ignimbrite thickness, grain-size distribution, ignimbrite facies and flow directions, mapped field relations of the ignimbrites with associated structures and deposits, and various geophysical techniques (Morgan and others, 1984; Morgan, 1988; Christiansen, 1984; Christiansen and Blank, 1972). The location of calderas and fields older than the Yellowstone field is hampered by a thin cover of basalt, thus requiring specialized studies of the tuffs to determine their origin (Morgan, 1988). The location of the Picabo field has been in part constrained by estimation of the location of the caldera for the 10.3-Ma tuff of Arbon Valley (Kellogg and others, 1989), an ignimbrite readily identified by phenocrysts of biotite and bipyramidal quartz.

In addition to the known volcanic geology, the boundaries of the Picabo and Twin Falls fields (Plate 1) are drawn on the basis of similar Bouguer and isostatic gravity anomalies and of aeromagnetic and apparent-magnetic-susceptibility-contrast anomalies; these anomalies are both similar to those displayed by the Heise and Yellowstone volcanic fields based on maps provided by V. Bankey (written communication, 1989) and A.E. McCafferty (written communication, 1989). Further stratigraphic and volcanic studies are needed, however, to better define the Picabo and Twin Falls volcanic fields.

For that part of the hotspot track younger than 10 Ma, the inception of caldera-forming eruptions has migrated at 2.9 ± 0.5 cm/yr to the $N 54 \pm 5^\circ E$ (Figs. 3 and 4; errors empirically determined). This rate is 15% slower than the 3.5-cm/yr rate first proposed by Armstrong and others (1975), based on the west-to-east longitudes. The vector we determine is similar to those resulting from plate-tectonic models: (1) $N 72^\circ E$ at 2.7 cm/yr (Minster and others, 1974), (2) $N 67^\circ E$ at 4.5 cm/yr (Smith and Sbar, 1974), and (3) $N 34^\circ E$ at 2.4 cm/yr (Minster and Jordan, 1978) referenced to oceanic plumes beneath the Pacific Plate, and (4) $N 54^\circ E$ at 2.76 cm/yr (Pollitz, 1988).

HOTSPOT TRACK 10-16 MA

Southwestward on the general trend of the post-10 Ma hotspot track, about 20 calderas are known that range in age from 16 to 10 Ma (Plate 1). As noted by Malde (in press), the oldest set of the calderas along the hotspot track is the 16.1-Ma peralkaline rhyolites of the McDermitt field (Rytuba and McKee, 1984; Plate 1). Silicic volcanic rocks with ages between 25 and 16 Ma are uncommon in this area, contrasting with widespread silicic volcanism from 13-16 Ma (Ludke and Smith, 1981; Ludke and Smith, 1982; McKee and others, 1970). The 15-16 Ma ignimbrites in the northern Nevada-southwest Oregon area commonly overlie and immediately post-date Oregon Plateau basalts (Fig. 3, shown by triangle) dated generally no older than 17 Ma.

From the Picabo field to the southwest, the calderas tend to increase in age along a centerline

drawn between the 10.3 Ma Picabo field and the 16.1-Ma caldera of the McDermitt field (Fig. 3; Plate 1). Silicic volcanic centers are dispersed more widely about this centerline than they are about the post 10 Ma hotspot track (Fig. 4). Silicic centers dated between 13 and 16 Ma lie as much as 160 km north of this centerline. South of this centerline, rhyolitic volcanism between 13-16 Ma is common within 50 km and extends as much as 100-180 km south of this centerline (Luedke and Smith, 1981). In addition, the topography does not define a mountain-bounded linear trough like that of the post-10-Ma hotspot track.

The Twin Falls field is the most speculative of the fields; its approximate location is based on the distribution of 8- to 11-Ma ignimbrites exposed on both sides of the plain (Williams and others, 1982; Armstrong and others, 1980; Wood and Gardner, 1984), and gravity and magnetic expressions similar to the better known volcanic fields.

Rates of migration are difficult to calculate because of the wide dispersal of silicic volcanic centers between 16.1 and 13.5 Ma. For the 350 km from the 16.1-Ma McDermitt volcanic field to the 10.3 Ma Picabo field, the apparent rate was about 7 cm/yr on a trend of N 70-75°E, not accounting for any basin-range extension increasing the rate and rotation to a more east-west orientation (Rodgers and others, 1990). Reasons for the contrasts in rate and other differences between the 16-10 Ma and 10-0 Ma volcanic centers are discussed later.

WESTERN SNAKE RIVER PLAIN AND HOTSPOT TRACK

The western Snake River Plain trends northwest and has a different origin than the eastern SRP (Mabey, 1982; Malde, in press; see Figures 1 and 24 for locations of western plain compared to hotspot track). The western Snake River Plain is a graben bounded by NNW- to NW-trending normal faults (Figures 1 and 24) and which is filled with more than 4 km of late Cenozoic deposits that consist of sedimentary and volcanic rocks, including at least 1.5 km of Columbia River basalt (Wood, 1984, 1989; Malde, in press; Mabey, 1982; Blackwell, 1989). This NNW-trending graben has generally been thought to have formed starting about 16 Ma (Malde, in press; Zoback and Thompson, 1978; Mabey, 1982). However, Spencer Wood (1984; 1989; written commun., 1989) suggests that available evidence indicates the western SRP graben may be as young as 11 Ma and that it transects obliquely older, more northerly trending structures that are also parallel to dikes associated with the Columbia River basalts. Faulted rhyolites demonstrate offset between 11 and 9 Ma and after 9 Ma, there was 1.4 km offset along the northeast margin and at least 1 km offset along the southwest margin of the western SRP (Wood, 1989, p. 72). No such faulting is known for the eastern SRP.

Therefore, the physiographic Snake River Plain has two structurally contrasting parts: the eastern SRP is a NE-trending lowland defined by post-10-Ma

calderas now thinly covered by basalts, and the western SRP is a NNW-trending late Cenozoic graben filled with a thick sequence of primarily basalt and sediments. Major differences between the eastern SRP and the western SRP are also reflected in regional geophysical anomalies as pointed out by Mabey (1982). The continuous physiographic province formed by linking of the volcanic eastern SRP and the graben of the western SRP does not appear to be fortuitous. Instead, graben formation of the western SRP occurred during and after passage of the eastward migrating hotspot.

A major arcuate gravity high suggests a large, deep mafic body trends southeast along the axis of the western SRP and then to an easterly orientation near Twin Falls (Mabey, 1982). North of the SRP, the Idaho batholith forms a relatively massive and unextended block that interrupts basin and range development for about 200 km from the western SRP to the basin-and-range east of the batholith. When hotspot volcanism moved east of the western SRP about 12 Ma but extension north of the SRP continued only in the western SRP graben, a local right-lateral shear couple with an east-west tension gash orientation would result, producing a local transform fault similar to the regional transform of Christiansen and McKee (1978); mafic filling of this tensional shear opening could thus explain the arcuate gravity high.

NEOTECTONIC CLASSIFICATION OF FAULTING

We define 6 types of normal faults based on two criteria (Plate 1, Table 2): (1) recency of offset and (2) height of the associated bedrock escarpment, which includes range fronts. We use the terms major and lesser to designate the size of the bedrock escarpment, which reflects the late Cenozoic structural relief on the fault, followed by a time term such as Holocene, Pleistocene (for late Pleistocene) to designate the recency of offset (Table 2). Most of the faults shown on Plate 1 are associated with sizable bedrock escarpments, primarily range fronts; faults with little or no bedrock escarpments are generally not shown unless scarps have been seen in surficial materials which also generally signifies Holocene or late Pleistocene offset. We use <15 ka for the youngest category of fault activity because 15 ka is the age of the youngest widespread alluvial fan deposits in the region near the SRP-YP province (Pierce and Scott, 1982).

1. *Major Holocene faults* (Scott and others, 1985b) occur along precipitous mountain fronts >700 m high and have had at least 1 m offset since 15 ka. This category is intended to locate faults that have had hundreds of meters offset in Quaternary time as reflected by the high, steep, mountain front, and that continue to be active, as attested by offsets in the last 15 ka. These faults generally have relatively high levels of activity, mostly >0.2 mm/yr and locally >1.0 mm/yr.

2. *Lesser and reactivated Holocene faults* are new and reactivated faults that have offsets in the last 15 ka.

Lesser Holocene faults are not along high, precipitous range fronts, suggesting that activity on a million-year time scale has been low (<0.03 mm/yr) whereas offset in the last 15 ka suggests either that the rate of activity has increased in latest Quaternary time or activity just happens to have occurred in the last 15 ka on a fault with a much longer recurrence interval. Reactivated faults may occur on sizable range fronts, but are thought to have been reactivated in the Quaternary following an interval of late Cenozoic quiescence. The intent of this category is to include faults newly started or reactivated in later Quaternary time.

3. Major Pleistocene faults have last been active between about 100 and 15 ka. The associated range fronts are more than 500 m high, but are generally neither as high nor as steep as those associated with *major Holocene* faults. They generally have low levels of activity (<0.1 mm/yr). The intent of this category is to define areas with late Quaternary rates near 0.1 mm/yr, but which have accumulated kilometers of structural offset.

4. Lesser Pleistocene faults are new and reactivated faults that have recognizable scarps or other evidence of movement in the last 100 ka, but associated topographic escarpments are less than 200 m high. Like lesser Holocene faults, this category isolates relatively young faults and provides a designation separate from the "major Pleistocene faults" which are more significant because of their much greater late Cenozoic offset.

5. Major Tertiary faults occur on range fronts with muted escarpments more than 500 m high. The most recent offset may be either Tertiary or older Quaternary. The escarpments suggest more than 1 km vertical offset, but absence of scarps in surficial materials indicates little or no Quaternary activity and rates probably <0.01 mm/yr based on <3 m offset since 300 ka. The intent of this category is to identify faults that had moderate to high levels of late Cenozoic activity (last 15 m.y.) but have subsequently ceased movement or decelerated to much lower levels of activity.

6. Lesser Tertiary faults do not have scarps in surficial materials, and are not known to have evidence of late Pleistocene offset. Associated bedrock escarpments are absent or less than 200 m high. The intent of this category is to separate these faults from the "major Tertiary faults". Many faults that fit this category are not shown on Plate 1.

Plate 1 shows these 6 faults types for the eastern SRP region: the darker the line representing a fault, the greater the ongoing activity on that fault. Four belts of faults having contrasting neotectonic character are distinguished based on the 6 fault types shown on Plate 1. The belts of faulting are designated by roman numerals with Belt I forming the outside zone farthest from the SRP-YP province and Belt IV the innermost zone. The faulting in each belt is discussed next, starting with Belt II, because it is the best defined and most active belt.

In the study area, many faults have a history of extensional tectonism older than the current episode of extensional faulting. The Montana Basin-Range, the Idaho Basin-Range north of the SRP, and the Jackson Hole area of Wyoming all have Miocene normal faulting that pre-dates the current activity (Reynolds, 1979; Fields and others, 1985; Love, 1977, p. 590; Barnosky, 1984; Burbank and Barnosky, 1990).

BELT II, DEFINED BY MAJOR HOLOCENE FAULTS

This belt is characterized by *major Holocene* faults, which define the most active Quaternary structures. We use the history of the Teton fault to represent the kind of activity that illustrates *major Holocene* faulting with high rates of activity sustained over a few million years.

Teton Fault History

Post-glacial vertical offset on the Teton fault is largest in the middle part of the fault, reaching 20 m offset since about 15 ka near String Lake, for a rate of 1.3 mm/yr (Gilbert and others, 1983; Susong and others, 1987). The range-front escarpment locally exceeds 1500 m in height (total relief is 2140 m) with slopes of 28° on triangular facets that extend about half way up the range front (Fig. 5). Offset on the Teton fault diminishes to no recognized scarps in surficial materials 30 km to the south and 20 km to the north of String Lake.

The available control on the history of the Teton fault suggests most faulting occurred since 6 Ma and that the rate of faulting has increased into Quaternary time. On Signal Mountain, 12 km east of the Teton fault at the outlet of Jackson Lake, the 2-Ma Huckleberry Ridge Tuff dips into the fault at 11° . Gilbert and others (1983) studied the fault geometry defined by the Huckleberry Ridge Tuff. Provided that there are no major faults between Signal Mountain and the Teton fault, they estimated a post-Huckleberry Ridge offset of 2.5 ± 0.4 km for a rate of 1.25 mm/yr. These values would increase if uplift of the Teton Range, as indicated by dips of several degrees of the Huckleberry Ridge Tuff on the west side of the range, are included and would decrease if part of the dip of the Huckleberry Ridge Tuff is primary. Rather than significant primary dip for the Huckleberry Ridge Tuff at Signal Mountain, an horizontal attitude is suggested because (1) the tuff maintains a uniform thickness basinward, (2) it was deposited on a quartzite-rich gravel which has a planar upper surface and not a dissected surface appropriate for a terrace tilted several degrees to the west (Gilbert and others, 1983, p. 77; Pierce, field notes) and (3) bedding features in the gravel appear conformable with the dip of the tuff.

A lithophysae-rich tuff exposed beneath the Huckleberry Ridge Tuff on Signal Mountain dips 22° W, has a fission track age of 5.5 ± 1.0 Ma (Nancy Naeser, written commun., 1990), and probably correlates with either the 4.2-Ma tuff of Kilgore

(Morgan, 1988) or the 5.99 ± 0.06 Ma Conant Creek Tuff (Christiansen and Love, 1978; Naeser and others, 1980; Gilbert and others, 1983). This ignimbrite was erupted from the Heise volcanic field (Morgan, 1988). Near Signal Mountain, dips on the Miocene Teewinot Formation are 17° , 20° , and 27° , for an average dip of 21.3° that is essentially the same as the 22° dip of the older tuff (Love and others, in press). Obsidian from the upper part of the Teewinot Formation yielded a K-Ar age of 9 Ma (Love, 1977; Evernden and others, 1964), that from the middle part yielded a K-Ar age of 10.3 ± 0.6 Ma (sample R-6826, Douglas Burbank, oral commun., 1990).

The vertical offset at String Lake, which is 13 km directly towards the fault from Signal Mountain, can be converted to a basin-tilting rate compatible with the tilting rates at Signal Mountain (Fig. 5). Assuming planar tilting of the basin into the fault out to a hinge zone 18 km from the fault, an offset rate of 20 m/15 ky at String Lake translates to a tilt rate at Signal Mountain of $4.2^\circ/\text{m.y.}$, remarkably similar to the $5.5^\circ/\text{m.y.}$ defined by 11° dip of the 2-Ma tuff.

Assuming the dip of the three units is tectonic, Figure 6 shows the rate of tilting was high from 0 to 2 Ma, either high or moderate from 2 to about 5 ± 1 Ma, and low to virtually nonexistent prior to that. Because rates of $5.5^\circ/\text{m.y.}$ from 0 to 2 Ma and $4.2^\circ/\text{m.y.}$ from 0 to 15 ka are similar (Fig. 6), it is reasonable to predict that this rate will continue for at least several thousand years into the future.

Older normal faulting in and near Jackson Hole--Based on studies of the Miocene Coulter Formation, Barnosky (1984) concluded that the onset of extensional-type bimodal basalt/rhyolite volcanism sometime between 18 and 13 Ma also heralded the start of extensional faulting in northern Jackson Hole, perhaps on the Teton fault. But the Teewinot Formation, younger than the Coulter Formation, indicates no significant uplift on the Teton fault until after 9 Ma (Love, 1977). In addition, the older tuff on Signal Mountain indicates pyroclastic flow from the Heise volcanic field across the area now occupied by the Teton Range, thus indicating a much lower Teton Range about 5 Ma than now. On the Hoback fault along eastern side of southernmost Jackson Hole, the Miocene Camp Davis Formation forms a half-graben fill which indicates more than 1.6 km of Miocene faulting (Love, 1977, p. 590; Schroeder, 1974).

Belt II, Southern Arm

The southern arm of Belt II extends S 20° W from Yellowstone about 400 km to the Salt Lake City area where the belt of Quaternary faulting becomes broader and trends north-south (Plate 1). The fault pattern is generally an echelon, right stepping with a notable gap between the Teton and Star Valley faults (Plate 1). The *major Holocene faults* are, from north to south: (1) the east Sheridan fault, which offsets more than a meter post-glacial (15 ka) talus along a 1000 m range front (Love and Keefer, 1975),

(2) the Teton fault, with up to 20 m offset since 15 ka (Gilbert and others, 1983), (3) the Star Valley fault, which has 9-11.6 m offset since 15 ka (Piety and others, 1986; Piety and others, this volume), (4) the Bear Lake fault, with as much as 10 m since 12.7 ka (McCalpin and others, 1990), (5) the east Cache fault, with 4 m offset since 15 ka (McCalpin, 1987), and (6) the Wasatch fault, where the middle 6 segments have Holocene activity and as much as 7 m offset since 6 ka (Machette and others, 1987). A gap in recognized Quaternary faulting occurs between Teton and Star Valley faults, although historic seismicity does occur in this gap (C.J. Langer, written commun., 1985; Wood, 1988).

Belt II, Western Arm

From Yellowstone, the northern belt of *major Holocene faults* extends S 70° W for about 300 km to the Lost River fault but loses definition further west in the Idaho batholith (Plate 1). Historic seismicity continues on this trend for 100 km further west (Smith and others, 1985), but Quaternary faulting is only locally recognized (Schmidt and Mackin, 1970; Fischer and others, 1983; D.L. McIntyre, oral commun., .

Faults along the western arm of Belt II are, from east to west: (1) Hebgen Lake earthquake faults which had surface offsets during 1959 of up to 5 m and absolute subsidence of as much as 7 m and consist of the 12-km Hebgen Lake and 22-km Red Canyon faults (Witkind, 1964; Myers and Hamilton, 1964); (2) the southern Madison fault, which had 5 m offset since 15 ka, including minor offset during the 1959 Hebgen Lake earthquake and we estimate roughly 800-900 m of downfaulting of the 2-Ma Huckleberry Ridge Tuff (Lundstrom, 1986; Mathiesen, 1983); (3) the eastern and central parts of the Centennial fault, which had up to 20 m offset since 15 ka (rate 1.3 mm/yr) (Witkind, 1975a) and a minimum of 1500-to-1800 m offset of the 2-Ma Huckleberry Ridge Tuff (rate >0.75 mm/yr) (Sonderegger and others, 1982); (4) the 16-km Sheeps Creek and 11-km Timber Butte segments of the Red Rock fault, which had two offsets totaling 4 m and one offset of about 2 m, respectively, since 15 ka (Stickney and Bartholomew, 1987a; Haller, 1988); (5) the 42-km Nicholia (perhaps late Pleistocene), the 23-km Leadore, and the 20-km Mollie Gulch (possibly late Pleistocene) segments of the Beaverhead fault (Plate 1, N, L, and M), which had no more than one 1-2 m offset since 15 ka (Haller, 1988); (6) segments of the Lemhi fault, consisting of the 43-km Sawmill Gulch segment with two offsets since 15 ka, and the 12-km Goldburg and 23-km Patterson segments with one offset each since 15 ka (Plate 1, S, G, and P; Haller, 1988), (7) the 22-km Thousand Spring and the 22-km Mackay segments of the Lost River fault (Plate 1, T and K) have two offsets each totaling up to 4 m since 15 ka, whereas the Warm Spring segment had only one offset since 15 ka (Plate 1, W; Scott and others, 1985b; Crone and others, 1987); (8) the Boulder fault, 30 km east of the south end of the Sawtooth fault, with

several meters offset of Pinedale moraines (<20 ka) over a distance of >5 km (Scott, 1982; A.J. Crone, oral commun., 1988), and (9) at least the northern part of the Sawtooth fault, which appears to have offset since 15 ka (Fisher and others, 1983).

The western arm is not as linear as is the southern arm and is divisible into two parts: an irregular eastern part 30-60 km wide from Yellowstone to the Red Rock fault and a western part about 75 km wide that is roughly parallel to the SRP. The eastern part is the least systematic part of Belt II, including both north-south and east-west trending faults, and involves foreland uplifts exposing Archean rocks of the craton. The faults further west in the western belt trend northwest parallel to thrust-belt structures, and the active normal faults are in a row, rather than having an en echelon pattern as in the southern part of Belt II (Plate 1).

BELT I, LESSER AND REACTIVATED FAULTS BEYOND BELT II

Belt I occurs outside Belt II and is characterized by *lesser Holocene faults*, *lesser Pleistocene faults*, as well as, for the western arm, reactivated Miocene faults. An important attribute of *lesser Holocene and lesser Pleistocene faults* is the absence of high, steep range fronts. Although characterized by relatively young activity, these faults are thought to be early in their present cycle of activity for they have not accumulated large Quaternary offsets.

Belt I, Southern Arm

The southern arm of Belt I is characterized by *lesser Holocene* as well as *lesser Pleistocene faults* in a belt 30-70 km wide and 400 km long, and are discussed from north to south. The Mirror Plateau faults occur immediately northeast of the Yellowstone caldera (Plate 1). This arcuate fault belt includes both *lesser Holocene* and *lesser Pleistocene faults* that parallel the caldera margin at distances of 10-15 km from it. About half the faults have post-glacial movement (Love, 1961; Pierce, 1974) and total offset on these faults is generally less than 100 m.

Southward from the Mirror Plateau, the largest post-glacial fault occurs inside the 0.6 Ma Yellowstone caldera between the East Sheridan fault and the upper Yellowstone faults (Plate 1). There, a *lesser Holocene fault* with a post-glacial fault scarp nearly as high as its associated topographic escarpment offsets Holocene shorelines of Yellowstone Lake and continues southward for 20 km (Pings and Locke, 1988; Richmond, 1974). Twenty km further south, another *lesser Holocene fault* extends 10 km along the ridge just NE of Bobcat Ridge, locally dams small lakes, and has nearly equal scarp heights and bedrock escarpment heights of 5-20 m (K.L. Pierce and J.M. Good, field notes, 1987).

East of the above-listed faults, the upper Yellowstone faults (Plate 1) bound a graben bounded

mostly by *major Pleistocene faults* and including two short segments of *major Holocene faults* included here in Belt I although they might be considered a short outlier of Belt II.

About halfway between the upper Yellowstone faults and the town of Jackson (Plate 1), two *lesser Holocene faults* offset Pinedale glacial deposits: (1) on Baldy Mountain a 5 m high scarp occurs in Pinedale glacial deposits on Baldy Mountain (Fig. 7: K.L. Pierce and J.D. Good, unpublished data, 1985) and (2) 10 km further east is a 10 m high scarp offsets in Pinedale glacial deposits (Love and Love, 1982, p. 295; Pierce, field notes, 1989).

Between Jackson and the Grays River fault Belt II crosses into the thrust belt where a 2-km section of the Miocene Hoback fault may have been reactivated in Holocene time (Love and de la Montagne, 1956, p. 174). The Grays River fault (Plate 1) has Holocene offset with a postulated *lesser-Holocene-fault-length* of 40 km and a total structural relief of about 500 m; (Rubey, 1973; Jim McCalpin, written commun., 1990) the 500-m-high range front is a dip-slope thought to exaggerate late Cenozoic offset. Further south in the Wyoming thrust belt, the Rock Creek fault has a *lesser-Holocene-fault-length* of 44 km, along which Rubey and others (1975) note scarps 16-18 m high in alluvium at the base of a bedrock escarpment about 200-300 m high.

The Crawford Mountain fault in northeast Utah is included in Belt I (Plate 1; Gibbons and Dickey, 1983). The most recent offset is probably late Pleistocene (Susanne Hecker, oral commun., 1990). Although the range front is 500 m high and thus qualifies this fault as a *major Pleistocene fault*, the range front is actually a dip slope and Quaternary offset may be more like that of a *minor Pleistocene fault*.

In southwest Wyoming and still in the thrust belt, the Bear River fault zone is 37 km long and has 2 offsets since 5 ka (West, 1986). Surface offsets and total escarpment heights are 4-10 m suggesting total offset is late Holocene for these new or *lesser Holocene faults*. About 10 km to the east, *lesser Pleistocene faults* offset mid-Pleistocene terrace deposits. West (1986) suggests that these *lesser Pleistocene faults* relate to backsliding above the sub-Tertiary trace of the Darby thrust whereas the *lesser-Holocene* Bear River fault propagated to the surface above a ramp accompanying backsliding on the Darby thrust.

Belt I, Western Arm

The western arm of Belt I trends across basin-range structure initiated in middle Miocene time (Reynolds, 1979, p. 190). The western arm of Belt I includes a rather dispersed band 50-100 km wide containing *lesser Pleistocene and lesser Holocene faults* in the Miocene basins and reactivated faults along the Miocene range fronts. Perhaps contrasting, diffuse pattern results from both the differences between the

Miocene and currently developing stress regimen and the inhomogeneities introduced by Miocene normal faulting.

In Belt I between the Emigrant fault and the Yellowstone caldera, no Holocene (post-glacial) faulting is documented on important normal faults such as the east Gallatin fault (Plate 1). The Norris-Mammoth corridor (Eaton and others, 1975) occurs east of the east Gallatin fault and contains 17 volcanic vents younger than 0.6 Ma thought to have related subsurface dike injection. Extension that otherwise would surface on the east Gallatin fault may be accommodated by dike injection along the Norris-Mammoth corridor (Pierce and others, in preparation). Active tectonism along the Norris-Mammoth corridor is indicated by historic level-line changes and by historic seismicity (Reilinger and others, 1977; Smith and others, 1985; Fig. 12).

About 70 km north of the Yellowstone caldera, 4- to 6 m offset on the Emigrant fault since 15 ka indicates a late Quaternary slip rate of about 0.25 mm/yr (Personius, 1982). Because basalt flows on the basin floor are 8.4 and 5.4 Ma (Montagne and Chadwick, 1982; Burbank and Barnosky, 1990) are tilted no more than 0.5°, faulting at the late Quaternary rate is limited to the last 0.5 Ma, preceded by quiescence to before basalt deposition 8 Ma (Fig. 8). Prior to the 8 Ma basalt, Barstovian sediments beneath the basalts are tilted 8-10° into the fault (Barnosky and Labar, 1989; Burbank and Barnosky, 1990) and require more than 1 km of Miocene faulting (Fig. 8). These relations require two pulses of activity, one between 8 and at least 15 Ma and another after 0.5 Ma, with quiescence in between (Fig. 8). A steep, fresh facet about 100 m high occurs immediately above the Emigrant fault, above which is a much higher but gentler escarpment; these landforms support the above history of activity on the Emigrant fault. Elsewhere in the western arm of Belt I, we suggest that Quaternary(?) reactivation of Miocene faults may be indicated by Tertiary sediments tilted towards muted range fronts with late Quaternary scarps.

Similar to the Emigrant fault, the Madison fault exposes Precambrian crystalline rocks in its high bedrock escarpment, and the thick Tertiary fill shown by gravity surveys suggests large offset during the Tertiary. The northern segment of the Madison fault is less active and appears to have experienced less Quaternary reactivation than the southern segment (Mayer and Schneider, 1985) and thus may also be a recently reactivated Miocene fault.

Westward from the Madison fault, definition of Belt I is problematic. Although Quaternary faulting appears to form a fringe zone outside Belt II, two problems exist: (1) immediately west of the Madison fault, faulting is disperse and difficult to separate from activity further north near Helena (Stickney and Bartholomew, 1987a, and (2) further west, later Quaternary faulting is poorly documented.). In Belt I westward from the Madison to Blacktail fault, disperse, low activity Quaternary faults occur in a 100

km wide zone commonly not along range fronts. The Blacktail fault occurs on a range front 600 m high and is therefore classified as a *major(?) Pleistocene fault* (Stickney and Bartholomew, 1987), although the scarp occurs at the edge of the piedmont rather than on the muted range front (Dean Ostenaar, oral commun., 1990) suggesting it may be a reactivated *lesser Pleistocene fault*. Twenty km southwest of the Blacktail fault, a *lesser Pleistocene fault* occurs across the valley from and north of the Red Rock fault (Dean Ostenaar, oral commun., 1990). Twenty km northeast of the Blacktail fault, the *lesser Holocene Sweetwater fault* has a long history of activity for it offsets 4-Ma basalt 250 m (Stickney and Bartholomew, 1987a, b). Further north, the *lesser Holocene Georgia Gulch fault* and *lesser Pleistocene Vendome horst* have muted scarps in old (150 ka) deposits, and indicate low rates of late Quaternary activity on these non-range-front faults (Stickney and Bartholomew, 1987a, b; 1990).

West from the Blacktail fault, Quaternary faulting is poorly known and the definition of Belt I becomes questionable. *Major late Pleistocene faults* near the northern ends of the Beaverhead, Lemhi, and Lost River Ranges (Haller, 1988) are tentatively assigned to Belt I (Plate 1). The last offset on these northern segments was older than 15 ka, and may have been in late Pleistocene time (Haller, 1988; Stickney and Bartholomew, 1987a). These faults occur on muted range fronts thought to be relict from Miocene faulting and associated basin deposition common in the Idaho and Montana Basin and Range (Fields and others, 1985; Reynolds, 1979). Moderate levels of historic seismicity (Smith and others, 1985) are compatible with the hypothesis that these faults may be in the process of reactivation, but active at low levels.

BELT III, DEFINED BY MAJOR LATE PLEISTOCENE FAULTS

Belt III is characterized by *major late Pleistocene faults* that last moved between 15 and 125 ka and occur on range fronts that are more than 500 m high, but are neither as high or steep as those associated with *major Holocene faults*. Because Belt II is the most clearly defined, the delimiting of Belt III is aided by its outer boundary conforming with the inner boundary of Belt II. Sedimentation related to the next-to-last (Bull Lake) glaciation was ending about 125 ka, thus providing the limiting age for this fault category.

Belt III, Southern Arm

In the southern arm of Belt III, the two northern *major late Pleistocene faults* are the northern segment of the Bear Lake fault (McCalpin, 1990) and a range-front 20 km to the west which is associated with late Pleistocene basaltic vents (Oriol and Platt, 1980; Bright, 1967; McCoy, 1981). Further south, the northern East Cache fault and Pocatello valley faults (McCalpin and others, 1987) and the northern three segments of the Wasatch fault (Machette and others,

1987) have late Pleistocene offsets on range fronts that are not as high, as steep, nor as freshly faceted as those associated with *major Holocene faults*.

The southern arm of Belt III includes *lesser late Pleistocene faults* out in basin flats in the Grays Lake-China Hat-Soda Springs area, all associated with late Quaternary volcanism which at China Hat is as young as $61,000 \pm 6,000$ years (G.B. Dalrymple, written commun. in Pierce and others, 1982). Southwest from here, Belt III includes *lesser late Pleistocene faults* active since 15 ka in the Hansel Valley-Pocatello Valley corridor (McCalpin and others, 1987): the 1934 Hansel Valley earthquake fault and a fault at the west side of the North Promontory Range

Belt III, Western Arm

The western arm of Belt III starts south of the Centennial fault; the northern boundary of this arm stays within 50 km of the eastern SRP for 150 km to the area north of Craters of the Moon National Monument. Beyond Craters of the Moon to the Boise area, *major late Pleistocene faults* may exist but are not well documented.

The most studied fault in the western arm of Belt III is the southern part of the Lost River fault, the Arco segment, which last moved 30 ka (Fig. 9). Back tilt within 100 m of the fault results in a tectonic offset rate of about 0.07 mm/yr, 30% less than the rate 0.1 mm/yr based on offset datums at the fault (Fig. 9; Pierce, 1985; Scott and others, 1985b). Compared to the *major Holocene* part of the Lost River fault further north (Plate 1), the late Quaternary slip rate is more than three times slower, the range front is lower and less precipitous, and the facets are more dissected. Neotectonic studies (Malde, 1987; Haller, 1988) of the southernmost segment of the Lemhi fault, the Howe segment, suggest late Quaternary activity similar to that seen in the Arco segment. The morphology of both scarps is similar.

Few details of the late Cenozoic history of *major late Pleistocene faults* north of the SRP are currently known. Ignimbrites older than 4.2 Ma but mostly not older than 6.5 Ma, occur on the eastern slopes in the southern Lost River and Lemhi Ranges and Beaverhead Mountains and, in general, form east-facing dip slopes of 5-15° (McBroome, 1981). A gravel beneath a 6.5-Ma ignimbrite contains clasts of distinctive quartzite and carbonate known only in the White Knobs area across two basin-ranges and 70 km to the west (M.H. Hait, Jr. oral commun., 1988; Scott and others, 1985b). Taken together, all these relations suggest that the present cycle of faulting started between 6.5 and 4.3 Ma (Scott and others, 1985b, p. 1058) and continued after 4.3 Ma (Rodgers and Zentner, 1988). For faults in the western arm of Belt III, structural relief of 1.5-2 km (Scott and others, 1985b) inferred to have developed between 6.5 Ma and present would result in an average rate of offset of 0.2-0.3 mm/yr, about twice the late Quaternary rate. This suggestion that the present cycle of basin-range

faulting started 6.5 Ma and decelerated to lower rates in the Quaternary needs to be further evaluated.

BELT IV, DEFINED BY MAJOR TERTIARY FAULTS

Belt IV is present only on the south side of the plain, and from a vanishing point near Yellowstone widens to 50-to-80 km southwest from Yellowstone (Plate 1). Belt IV is characterized by *major Tertiary faults*, range-front faults that were active in late Tertiary time but show little or no evidence of Quaternary activity (Plate 1; Greensfelder, 1976). The ages of several of the faults in Belt IV is described in more detail in the next section. Range fronts are generally muted with no planar triangular facets and relief less than in Belts II and III suggesting geomorphic degradation in a manner similar to scarp degradation.

NEOTECTONIC DOMAINS EMANATING FROM THE YELLOWSTONE HOTSPOT

THE PRESENT CYCLE

Belt II is the central, most neotectonically active belt. From Yellowstone, its two arms extend more than 350 km to the south and to the west and have widths of 30-50 km (Plate 1). These arms diverge about the volcanic track of the Yellowstone hotspot in a V-shaped pattern analogous to the wake of a boat now at Yellowstone (Scott, Pierce, and Hait, 1985b). Belt I occurs outside Belt II, is 20-100? km wide, and wraps around the northeast end of the 0.6-Ma Yellowstone caldera (Plate 1). The southern arm of Belt I is characterized by lesser Holocene or "new" faults whereas the western arm has reactivated Tertiary(?) and lesser Holocene faults, as well as some major Pleistocene faults. Belt III occurs inside Belt II and from a width of 50 km narrows or vanishes towards Yellowstone. This belt is characterized by major Pleistocene faults, which have moved in the last 15-120 ky and whose bedrock escarpments at least 500 m high and associated basin fill suggest structural relief of more than 1 km. Structural relief is comparable to faults in Belt II yet low offset rates of <0.1 mm/yr in late Quaternary time suggest neotectonic activity in Belt III may have waned over the last several million years.

The overall pattern of Belts I, II, and III suggest the following progression of neotectonic activity moving outward from the track of the Yellowstone hotspot. Faults in Belt I are presently active but have small amounts of structural offset in the southern arm, and small amounts of offset since reactivation in the western arm. Thus, they are in a waxing state of development compared to those in Belt II. Faults in Belt II have high rates of offset that continue into the present and have produced ranges about 1 km high with large fresh triangular facets, and are in a culminating state of activity. Faults in Belt III have structural offsets similar to Belt II, but have longer

recurrence intervals between offsets and have less boldly expressed facets and range heights, and thus are in a decelerating or waning state of activity. Belt IV was active in late Tertiary time, but is now dead. Taken together, the spatial arrangement of the belts suggests the following neotectonic cycle moving outward from the hotspot track: Belt I-- an initial waxing phase, Belt II-- the culminating phase, Belt III-- a waning phase, and Belt IV-- a completed phase.

We conclude that the strong spatial and sequential tie of all three belts of faulting to the present position of the Yellowstone hotspot suggests that the same deep-seated process responsible for the volcanic track of the hotspot is also responsible for this spatial and temporal progression of faulting.

BELT IV AND OLDER CYCLES OF FAULTING

If the neotectonic fault belts are genetically related to the Yellowstone hotspot, then faulting in areas adjacent to older positions of the Yellowstone hotspot should be similar in age to the older hotspot activity. On the southern side of the plain in Belt IV (Plate 1, age of faulting increases with distance from Yellowstone and roughly correlates with the age of silicic volcanic fields on the SRP. On the northern side of the plain, a northeast-younging progression of fault activity and cessation has not been recognized, in part because faulting there has continued into the late Pleistocene, although the effects of the hotspot may be indicated by inception of faulting roughly similar in age with the age of silicic volcanism on the SRP followed by *waning rates* of faulting. The limited data on the late Cenozoic history of faulting north of the SRP suggests higher rates of activity prior to the late Quaternary and after about 6.5 Ma (see discussion under Belt III). South of the SRP in Belt IV, evidence for faulting and other deformation, from northeast (younger) to southwest (older) is as follows.

Grand Valley-Star Valley fault system-- For Grand Valley fault (Plate 1), Anders and others (1989) used offset and tilted volcanic rocks to define an episode of deformation between 4.3 and 2 Ma that resulted in 4 km total dip-slip displacement at an average rate of 1.8 mm/yr (Plate 1, Fig. 10). This 2-m.y. burst of activity was an order of magnitude more active than the interval before (0.15 mm/yr), and two orders of magnitude more active than the interval after it (0.015 mm/yr) (Anders and others, 1989). High rates of offset on the Grand Valley fault occurred after the 6.5-4.3 Ma interval of caldera-forming eruptions on the adjacent SRP in the Heise volcanic field 30-100 km to the northwest (Plate 1). Gravity-sliding of bedrock blocks into Grand Valley probably results from normal faulting and oversteepening of the range-front. Emplacement of these slide blocks thus date times of maximum structural activity; one block was emplaced between 6.5 and 4.4 Ma, another after 7 Ma, and another prior to 6.3 Ma (Anders, 1990; Moore and others, 1987).

Blackfoot Mountains-- For the Gateway fault, on the west side of the Blackfoot Mountains (Plate 1), Almendinger (1982) concluded that most activity occurred between emplacement of ignimbrites dated 5.86 ± 0.18 Ma and 4.7 ± 0.10 Ma. These relations yield nearly 1 km vertical offset in about 1 m.y. for an offset rate of 0.8 mm/yr (Almendinger, 1982). The timing of this deformation falls in the middle of the 6.5-4.3 Ma interval for caldera-forming eruptions in the Heise volcanic field on the adjacent SRP (Plate 1).

Portneuf Range-- For normal faulting within and on the west side of the Portneuf Range, Kellogg and Marvin (1988, p. 15) concluded that "a very large component of Basin and Range faulting occurred between 7.0 and 6.5 Ma" as indicated by bracketing ages on a boulder conglomerate at the northern end of the range. This age corresponds closely with the 6.5-Ma caldera of the Heise field on the adjacent SRP (Plate 1). Only minor subsequent faulting is recorded by 50 m offset of 2.2-Ma basalt.

Rockland Valley-- Southwest of Pocatello, extensional faulting was largely over by 8-10 Ma (Plate 1). The Rockland valley fault along the west side of the Deep Creek Mountains and several other nearby Basin-Range normal faults have vertical displacements of more than 1 km (Trimble and Carr, 1976). Trimble and Carr (1976, p. 91) conclude that "movement on basin-and-range faults was largely completed before the outpouring of the middle Pliocene volcanic rocks that now partly fill the structural valleys." The most prominent of these volcanic rocks is the 10.3-Ma tuff of Arbon Valley (see footnote, Table 1). This ignimbrite is locally offset 100 m by younger faulting at the northern end of the Deep Creek Mountains, but Quaternary fault scarps have not been recognized in the area (Greensfelder, 1976). Thus, although the time of inception of faulting is not well defined, faulting was largely over by 10 Ma, roughly coincident with the 10.3 Ma caldera on the adjacent SRP (Plate 1).

Sublett Range-- Extensional deformation for the northern part of the Sublett Range was completed by 10 Ma (Plate 1), as determined by relations to the 10.3-Ma tuff of Arbon Valley (R.L. Armstrong, oral commun., 1988). But near the southeastern end of the Sublett Range, a biotite-bearing ignimbrite tentatively correlated with the tuff of Arbon Valley is deformed into anticlinal folds (M.H. Hait, oral commun., 1988). This shows that deformation 50 km south of the margin of the SRP continued somewhat after 10 Ma, consistent with movement of deformation through time outward from the SRP (Plate 1).

Raft River valley region-- The ranges on the west side of the Raft River valley are composed of rhyolitic Jim Sage Volcanic Member (9 to 10 Ma) whose pod-like form and extensive brecciation indicates accumulation on a wet valley floor (Covington, 1983; Williams and others, 1982; Armstrong, 1975). Because these rocks are now 1 km above the Raft River Valley, large tectonic movements must have occurred after 10 Ma (Plate 1). Based on mapping, extensive geothermal

drilling, extensive seismic reflection and other geophysical studies, Covington (1983) concluded that the rocks that now form the ranges on the east side of the Raft River valley (Sublett and Black Pine Ranges) slid eastward on a detachment fault from an original position on the flank of the Albion Range, which now forms the west side of the valley (Fig. 11). Some valley opening by detachment faulting and filling of this valley by tuffaceous sediments occurred prior to eruption of the volcanics of the Jim Sage Member 9-10 Ma, but after this time about 15 km of eastward movement on detachment-fault is inferred (Covington, 1983, Fig. 5; Williams and others, 1982). When detachment faulting ceased is poorly known, but only minor Quaternary deformation is present (Williams and others, 1982; K.L. Pierce, unpublished data). The presence on the margins of the Raft River valley of a 7-Ma ignimbrite (west margin), an 8 to 10-Ma ignimbrite (northeast margin), and two 8-Ma shallow dome-like intrusions (west and south east margin) suggest basin evolution to a form similar to the present by 7-8 Ma, thus suggesting about 15 km detachment faulting occurred between 10 and 7 Ma. The emplacement of 1-km-thick Jim Sage Volcanic Member of the Salt Lake Formation about 10 Ma correlates with passage of the Yellowstone hotspot on the adjacent SRP between about 12 and 10 Ma (Plate 1). The time of deformation from prior to 10 Ma to between 10 and 7 Ma is younger than for the Sublette Range and Rockland valley areas discussed above rather than older, perhaps due to detachment faulting relating to uplift on the west of the Albion Range core complex.

NEOTECTONIC FAULT BELTS AND HISTORIC SEISMICITY

Our belts of faulting, based on surficial geology and geomorphology, form an asymmetric V-shaped bands that converge on Yellowstone and flair outward about the track of the Yellowstone hotspot (Plate 1). This V-shaped pattern based on geologic assessment of fault activity was first pointed out by Scott, Pierce, and Hait, (1985b. Smith and others (1985) independently observed that earthquake epicenters showed a similar relation to the SRP-Yellowstone hotspot trend (Fig. 12). Anders and Geissman (1983) noted a southward progression of late Cenozoic faulting in the Grand Valley-Star Valley area that they related to migration of volcanism along the SRP. Later, Anders and others (1989) determined that two parabolas, arrayed about the path of the Yellowstone hotspot, bounded most of the earthquake activity in the SRP region (Fig. 12).

The neotectonic fault belts parallel but do not exactly correspond with concentrations of earthquake epicenters in the region (Fig. 12). These differences most likely arise from the contrasting time windows of observation; historical seismicity spans only several decades whereas the geologic record spans 10,000 to several million years. For example, most of the *major*

Holocene faults show little or no historic activity such as the Lemhi, Beaverhead, Red Rock, Teton, and Wasatch faults, Plate 1 and Fig. 12. The western belt of Quaternary faulting and particularly the activity in Belt II had a sparsity of historic earthquakes over a width of about 200 km prior to the 1983 Borah Peak earthquake which filled in the western 40 km of this belt.

We note the following differences and similarities between our neotectonic belts and boundaries suggested by others:

1. Immediately north of the SRP, an aseismic zone north and east of Mackay, Idaho is defined by Smith and others (1985) as a "thermal shoulder", and by Anders and others (1989) as a "collapse shadow" (Fig. 12). Their suggestion of inactivity is based on historical seismic quiescence, but this area contains late Pleistocene fault scarps and long-term fault histories that suggest continued activity in this belt (Pierce, 1985; Malde, 1987; Haller, 1988).
2. Immediately south of the plain, Smith and others' (1985) "thermal shoulder" and Anders and others' (1989) "collapse shadow" lie within a zone of seismic quiescence. Our Belt IV (rundown faults) also indicates cessation of tectonic activity.
3. Unlike the symmetric parabolas defined by the seismic zones, our neotectonic classification does not show bilateral symmetry across the plain. The late Cenozoic tectonic belts flair more outward south than north of the plain. This asymmetry results from the presence of Belt IV (rundown faults) only south of the plain.
4. North of the plain, the western arms of Belts I and II make up Anders and others' (1989) "active region", but south of the plain, Anders and others' (1989) "active region" includes all of the southern arms of Belts II and III, and parts of Belts I and IV. South of the plain, historic earthquakes have occurred in the Pocatello Valley, Soda Springs, and Hansel Range areas in Belt III; our classification suggests zone of greatest activity over time spans of thousands of years lies about 50 km to the east. The outer parabola bounding the southern band of historical seismicity (Anders and others, 1989) trends across Belt I and part of Belt II (Fig. 12). These differences are most likely due to the several orders of magnitude difference between the time-window of historic activity compared to that of the geologic record. Given an earthquake record of thousands of years, we suggest their greatest concentration and maximum energy release would parallel the trend of Belt II.

ALTITUDE AND THE HOTSPOT TRACK

POSSIBLE SCALES TO CONSIDER

If the neotectonic belts and caldera-forming volcanism that converge at Yellowstone are the result of the North American plate moving across a relatively stationary mantle plume, then by analogy with oceanic hotspots, a large elevated region or swell is predicted

(Crough, 1979, 1983; Okal and Batiza, 1987). Figure 13 shows profiles across three oceanic hotspot swells that range between 1-2 km high and 800-1200 km wide. The height of oceanic swells increases with the age and therefore the cooler temperature of the associated oceanic crust: the 2-km-high Cape Verde swell is in 140-Ma crust whereas the 1.2-km high Hawaiian swell is in 90 Ma crust (Crough, 1983, Fig. 5). The Hawaiian swell has a broad arcuate front, sub-parallel sides, and an elevated trailing margin more than 2,000 km long.

The uniform composition and simple thermal history of the oceanic crust, as well as generally minor erosion and sedimentation, facilitate simple morphologic expression of oceanic swells. Continental swells would not have a simple morphology because of the more complicated history and increased thickness of the associated continental crust. In the nearly static African plate, five postulated continental hotspot swells are about 1000 km across, between 700-2500 m high, and have associated volcanism (Morgan, 1981; Crough, 1983, Fig. 5).

Four other processes that might be related to a hotspots centered beneath Yellowstone are given here to suggest scales of uplift and subsidence one might consider in addition to the swell diameter: (1) radial flow of a plume and resulting dynamic uplift about 500 km across (Sleep, 1990), (2) extensive basaltic intrusion or underplating near the base of the crust at about 40 km depth may have a width of 100-400 km (Leeman, 1982, Fig. 5; Anders and others, 1989); (3) intrusion (timing uncertain) and cooling of mid-crustal basaltic magmas between 8-18 km depth may have a width of about 100 km (Sparlin and others, 1982; Braille and others, 1982); and (4) intrusion and cooling of granitic magmas at 2-10 km depth that also produced ignimbrite eruptions and rhyolite flows may have a width of 40-80 km (Lehman and others, 1982; Christiansen, 1984).

YELLOWSTONE CRESCENT OF HIGH TERRAIN

In the Yellowstone region, a crescent-shaped area about 350 km across stands about 0.5-1 km higher than the surrounding region (Fig. 14; Plate 1). This crescent has southern and western arms that extend more than 400 km from the apex of the crescent. The crest of the western arm of the crescent (long-dashed line) coincides with the belts of neotectonic faulting, whereas the crest of the southern arm (long dashed line) is just east of these belts (Plate 1). Definition of the greater Yellowstone elevation anomaly is complicated by mountains and basins of Laramide age (formed roughly 100-50 Ma), but others have recognized this altitude anomaly including Suppe and others (1975) who describe it as "updome" about 350 km across indented on the southwest by the Snake River Plain and by Smith and others (1985) as a lithospheric bulge 400 km across centered on the Yellowstone Plateau. The boundary and crest of the Yellowstone crescent shown on Plate 1 were drawn by Pierce on a subjective basis, attempting to account for

Laramide uplifts. Assuming the crescent is moving northeast at a plate tectonic rate of 30 km/m.y., the magnitude of associated uplift can be estimated based on bulge height of 0.5 to 1 km and an outer slope-length, measured parallel to plate motion, of 60-150 km. Thus, 0.5-1 km uplift on the outer slope of the Yellowstone crescent would last 2-5 m.y., yielding regional uplift rates of 0.1-0.5 mm/yr.

A large part of the altitude anomaly is formed by the Absaroka Range (Fig. 1), extends along the eastern boundary of Yellowstone and consists of post-Laramide volcanic rocks. The Laramide Wind River Range (Fig. 1) tilts southeasterly away from the Yellowstone hotspot, as shown by the 1-km-altitude decrease of both the range crest and a prominent bench (erosion surface?) on the east side. The central and western part of the head of the Yellowstone crescent is largely formed by the combined Beartooth (Snowy), Gallatin, and Madison Ranges (Fig. 1), all of which stand high and have youthful topography.

Ignimbrite sheets suggest differential altitude changes with uplift on the outer slope of the crescent and subsidence on the inner slope. North of the Yellowstone Plateau volcanic field near the crest of the Yellowstone crescent, the 2-Ma Huckleberry Ridge Tuff (Table 1) now reaches altitudes of 2800 m, 400-800 m higher than it is around its caldera (Fig. 14). Ignimbrites from the Heise volcanic field (plate 1), originally emplaced on a flat, relatively smooth topographic surface, now dip 20° toward the plain for the oldest unit and become progressively less for the younger ignimbrites (Morgan and Bonnicksen, 1989) suggesting regional tilting towards the Heise field during its period of activity.

Stream terraces are common on the outer, leading margin of the Yellowstone crescent, suggesting uplift. Terraces are much less well developed on the trailing edge of the crescent and on the SRP, and suggest subsidence and also tilting against the direction of flow.

ALTITUDE CHANGES NORTH OF THE SNAKE RIVER PLAIN

An historic level line across the western arm of the Yellowstone crescent shows a broad uplift about 200 km across (Fig. 15; Reilinger and others, 1977). Maximum uplift of about 2 mm/yr occurs both near the axis of the Yellowstone crescent and near the boundary between neotectonic fault Belts I and II.

Contours of the rates of historic uplift are based on highway survey lines along topographic lows and show three domes of uplift that roughly coincide with fault Belts I and II (Fig. 15B; Reilinger, 1985). The domes of historic uplift occur in downfaulted basins of the *major Holocene* Red Rock, Madison-Hebgen, and Emigrant faults. These rates are much greater than the estimated long-term regional rate of uplift associated with the "wings" of the Yellowstone crescent of roughly 0.2 mm/yr assuming 500 m uplift in 3 Ma. Basin uplift may be reflect regional interseismic uplift

of the Yellowstone crescent plus local interseismic uplift; during an earthquake absolute subsidence of 1-2 m occurs (Barrientos and others, 1987). For the Teton fault, Smith and others (1990) observed 0.8 mm/yr interseismic uplift of the basin block relative to the range.

For the area between the Red Rock and Madison faults, Fritz and Sears (1989) determined that a south-flowing drainage system more than 100 km long was disrupted at the time of emplacement of rhyolitic eruptions from the SRP, most likely from the 6.5 to 4.3-Ma Heise volcanic field, then reversed by northward tilting as demonstrated by a 4-Ma basalt that flowed northward down this reversed slope. This paleodrainage system was subsequently broken by basin-range faulting. The northward tilting may reflect the outer slope of the Yellowstone paleocrescent associated with the hotspot during the 6.5-4.3 Ma Heise volcanism (Plate 1), whereas disruption of the drainage reflects faulting associated with northward migration of Belts I and II after 4 Ma.

The three domes of historic uplift along the western arm of the Yellowstone crescent also coincides with a postulated the axis of arching represented by the modern drainage divides. For the three basin-range valleys east of the Beaverhead, Lemhi, and Lost River Ranges, Ruppel (1967) summarized evidence that the north half of three south-flowing drainages had been reversed from south flowing to north flowing. This reversal supports the postulate of late Cenozoic arching along the present crest of the west arm of the Yellowstone crescent (Fig. 14).

RUGGED MOUNTAINS OF READILY ERODIBLE ROCKS

Most of the Rocky Mountains are formed of erosionally resistant rocks such as granites, gneiss, and Paleozoic limestones and sandstones. But much of the mountainous terrain forming the head of the Yellowstone crescent is underlain by relatively young, erosionally incompetent rocks. Late Cenozoic uplift is required to explain the high, steep slopes underlain by such rocks, and the high rates of erosion in these areas.

The mountains that form the northern and much of the eastern margin of Jackson Hole and extend in a belt 30-40 km wide north to Yellowstone Lake, are underlain by weakly indurated sandstones, shales, and conglomerates mostly of Mesozoic and early Cenozoic age. Relief in this terrain is as great as 700 m over 2.4 km (16° slope) and more commonly 600 m over 1.4-2 km (17-24° slope). Landsliding is common; stream valleys are choked with alluvium and have broad, active, gravel-rich channelways. Streams draining into Jackson Hole from the east, such as Pilgrim, Pacific, Lava, Spread, and Ditch Creeks, have built large post-glacial alluvial fans. East of a remnant of 2-Ma ignimbrite on Mt. Hancock (alt. 3,112 m), local erosion of about 800 m of Mesozoic sediments has occurred since 2 Ma. West of Mt Hancock, structural relief on this tuff of 775 m in 6 km also demonstrates large-scale Quaternary deformation (Love and Keefe, 1975).

The Absaroka Range occurs along and east of the east boundary of Yellowstone Park and extends for about 70 km to the southeast. This range is formed largely of erodible Eocene volcanoclastic and volcanic rocks. The highest, most precipitous part of the Absaroka Range is 75-100 km from the center of the 0.6-Ma Yellowstone caldera. Peaks in the range reach above 3,700 m and peak-to-valley relief is as much as 2000 m. Mountain sides have dramatic relief, locally rising 1000 m in 1.9 km (27°), 800 m in 1.3 km (31°), and 670 m in 1.1 km (31°). Almost yearly, snowmelt and/or flash floods result in boulder-rich deposits on alluvial fans at the base of steep slopes. The upper parts of stream courses are commonly incised in bedrock whereas the larger streams commonly flow on partly braided floodplains with year-to-year shifts of gravel bars. Runoff is commonly turbid during snowmelt and flash floods with audible transport of boulders. The bedrock is dangerous to climb or even walk on because of loose and detached rock fragments. Compared to other parts of the Rocky Mountains formed of Precambrian crystalline rocks, the Absaroka Range is rapidly eroding and the deep, young canyons suggests late Cenozoic uplift of a 1 km magnitude.

A widespread, low relief erosion surface is well preserved on uplands of the Absaroka Range. In the southern Absaroka Range, basalt was erupted on this surface prior to cutting the modern canyons (Ketner and others, 1966); one of these flows has been dated as 3.6 Ma (Blackstone, 1966).

An obsidian-bearing gravel occurs 80 km east of Jackson Lake, Wyoming, high in the Absaroka Range (alt. 3350 m) (Fred Fisher, written commun., 1989; W.R. Keefe, oral commun., 1989; J.D. Love, oral commun., 1988). Obsidian pebbles from this gravel have a K-Ar age of 6.26 ± 0.06 Ma (Naeser and others, 1980). The possible sources of this obsidian include Jackson Hole (Love and others, in press), the Heise volcanic field (Morgan, 1988), or two silicic volcanic deposits in the Absaroka Range (Smedes and others, 1989; Love, 1939). If the obsidian originates from either the Heise volcanic field or Jackson Hole, this gravel indicates more than a kilometer of westerly tilting since 6.3 Ma, with subsidence to the west in the Jackson Hole/Heise area on the inside of the crescent, and uplift to 3350 m and associated deep incision near the crest of the crescent. If the source is from late Tertiary rhyolites in the Absaroka range, the present deep canyons have been carved since 6 Ma, indicating > 1 km uplift.

For the high Absaroka Range extending from the above area about 50 km to the north, formation of a late Cenozoic syncline with 600 m structural relief over about 40 km is described by Fisher and Ketner (1968). This deformation is on an order of magnitude smaller scale than the Yellowstone crescent. South of the Absaroka Range, major late Cenozoic tilting along the western front of the Gros Ventre Range is described by Love and others (1988). The Pliocene Shooting Iron Formation (about 2-3 Ma) age contains fine-grained lacustrine sediments and was deposited in a

topographic low. Love and others (1988) conclude that westward tilting of the Shooting Iron Formation since 2-3 Ma has resulted in the 1.2 km altitude difference between remnants in Jackson Hole and those on the Gros Ventre Range.

PLEISTOCENE GLACIER-LENGTH RATIOS AND ALTITUDE CHANGES

In the Rocky Mountains, terminal moraines of the last (Pinedale) glaciation normally are found just up valley from those of the next-to-last (Bull Lake) glaciation. Pinedale terminal moraines are between 20 and 35 ka whereas most Bull Lake moraines are near 140 ka, for an age difference of about 120 ± 20 ky (Pierce and others, 1976; Richmond, 1986). The end moraine pattern is consistent with the Oxygen-18 record from marine cores, where the estimated global ice volume of stage 2 time (Pinedale) was 95% that for stage 6 time (Bull Lake) (Shackleton, 1987). The ratio of the length of Pinedale glaciers to Bull Lake glaciers, Pd/BL ratio, is typically between about 88% and 96%. For example, in the Bighorn Mountains, 11 valleys mapped by Lon Drake and Steven Eisling (written commun., 1989) have Pd/BL ratios of $88 \pm 6\%$ (Fig. 15). In the Colorado Front Range, glacial reconstructions in five valleys yield a Pd/BL length ratio of $96 \pm 3\%$.

Departures from the normal ratio of glacier length during the last two glaciations may indicate areas of uplift or subsidence (Fig. 16). Uplift places a glacier area at higher altitude during the Pinedale that it was at an older time during the Bull Lake glaciation, and this higher altitude would increase the Pd/BL ratio. Subsidence would produce a change in the opposite sense. Factors other than uplift or subsidence may be responsible for changes in the Pd/BL ratio such as: (1) local responses to glacial intervals having differing values of precipitation, temperature, and duration; (2) different altitude distributions of the glaciated areas; (3) differing storm tracks between Pinedale and Bull Lake time, perhaps related to different configurations of the continental ice sheets; and (4) orographic effects of upwind altitude changes.

Figure 16 was compiled to see if high (>96%) or low (<88%) values of Pd/BL ratios define a pattern that can be explained by uplift or subsidence. In the head and southern arm of the Yellowstone crescent, the Beartooth Mountains, the Absaroka Range, and the central part of the Wind River Range have high Pd/BL ratios: of 30 Pd/BL ratios, 24 exceed 96% and 17 exceed 100% (Fig. 15). Only one low ratio was noted: a ratio of 79% based on a moraine assigned to Bull Lake glaciation along Rock Creek southwest of Red Lodge, Montana. The belt of high values is 70 to 140 km from the center of the 0.6-Ma Yellowstone caldera, and lies between the crest and outer margin of the crescent (Plate 1, Fig. 14). Uplift is expected in this area based on the northeastward migration of the Yellowstone hotspot.

For the western arm of the Yellowstone crescent of high terrain, Pd/BL ratios generally are from ranges where active faulting may result in *local* rather than regional uplift. Mountains not associated with active, range-front faulting occur east of Stanley Basin (Fig. 1) and have ratios of >100% suggesting uplift (Fig. 16).

The magnitude of the amount of uplift that might produce a 5% increase in the Pd/BL ratio can be calculated based on valley-glacier length and slope at the equilibrium line (line separating glacial accumulation area and ablation area). A vertical departure from the normal difference between Pinedale and Bull Lake equilibrium line altitudes (ELA's) would approximate the amount of uplift. The 5% increase in Pinedale glacier length from normal displaces the equilibrium line downvalley a distance equal to about half the increase in length of the glacier. For a valley glacier 15 km long, a typical slope at the ELA is about 3° (see Porter and others, 1983, Fig. 4-23). A 5% change in length is 750 m, indicating a 375 m downvalley displacement of the ELA, which for a glacier-surface slope of 3° decreases the ELA by 20 m. On the outer slope of the Yellowstone crescent, the Pd/BL ratios are about 5-10% above normal (Fig. 16). These glaciers are of geometry noted above. Thus, uplift of Pinedale landscapes by several tens of meters relative to Bull Lake ones could explain this belt of high Pd/BL ratios. Uplift of 20-40 m in 100-140 ky (Bull Lake to Pinedale time) results in a rate of 0.15-0.4 mm/yr similar to 0.1 to 0.5 mm/yr assuming northeast, plate-tectonic motion of the Yellowstone crescent.

A dramatic contrast in Pd/BL ratios occurs around the perimeter of the greater Yellowstone icemass and suggests northeast moving uplift followed by subsidence (Fig. 165). The Pd/BL ratios are >100% for glacial subsystems that terminated along the Yellowstone River and the North Fork of the Shoshone River and were *centered* to the north and east of the 0.6 Ma caldera. But Pd/BL ratios for glacial subsystems located on and south or west of the 0.6 Ma caldera are, from south to north, 59%, 77%, 69%, and 49% (from Jackson Hole via Fall River to the Madison River and Maple Creek). These ratios are among the lowest Pd/BL ratios in the Rocky Mountains. Because the Yellowstone icemass was an icecap commonly more than 1 km thick, any calculation of the apparent change in ELA is much more uncertain than for valley glaciers. Nevertheless these extremely low values for the southern and western parts of the Yellowstone icemass are compatible with perhaps 100 m *subsidence* at perhaps 1 mm/yr, whereas the high Pd/BL ratios in the northern and eastern Yellowstone region suggest *uplift* at perhaps .1-4 mm/yr.

We wish to caution that the possible uplift and subsidence based on departures from the "normal" in the size of different-aged Pleistocene glaciations is built on an inadequate base of observations. Most of the Pinedale and Bull Lake age assignments and the Pd/BL ratios calculated therefrom generally are not

based on measured and calibrated relative-age criteria. Additional studies are needed to verify and better quantify the pattern apparent in Figure 16.

With the above caution in mind, Figure 16 shows that high ratios suggesting uplift occur in an arcuate band largely coincident with the outer slope of the Yellowstone crescent of high terrain. Inside the crescent, few ratios were determined and are mostly from ranges with active range-front faults. A concentration of low Pd/BL ratios at about the position of Twin Falls suggest subsidence near the Snake River Plain and on the inner, subsiding slope of the Yellowstone crescent. For the Yellowstone icecap, low ratios suggest subsidence in and south of the 0.6 Ma caldera, whereas to the north and east of this caldera, high values suggest uplift.

BIG HORN BASIN REGION

Unidirectional Stream Migrations (Displacements)

Abandoned terraces of many drainages east and north of Yellowstone record a history of stream displacement, either by capture or slip-off, that tends to be away from the Yellowstone crescent (Fig. 17). The main exception to this away-from-Yellowstone-pattern was the capture of the 2.2 Ma Clark Fork and the subsequent migration of the 2 Ma Clark Fork (Fig. 17; Reheis and Agard, 1984). The capture appears to have been favored by the readily erodible Cretaceous and younger sediments at the northern, open end of the Big Horn Basin, but the subsequent migration is an example contrary to the overall trend of movement away from the Yellowstone crescent..

Three main processes have been evoked to explain unidirectional stream migration: (1) greater supply of sediment, particularly coarse gravel, by tributaries on one side of a stream; (2) migration down-dip, particularly with interbedded erodible and resistant strata; and (3) tectonic tilting with lateral stream migration driven by either sideways tilt of the stream or as suggested by Karl Kellogg (written commun., 1990) by increased or decreased sediment supply to the trunk stream depending on whether tributary streams flow in or opposed to direction of tilt. Palmquist (1983) discussed reasons for the eastward migration of the Bighorn River in the Bighorn Basin and rejected all but tectonic tilting. Morris and others (1959) considered that sediment and water supply from the north was responsible for southward migration of two tributaries of the Wind River (Muddy and Fivemile Creeks) near Riverton. However for the southeastward migration of the Wind River, the size of tributary drainage basins flowing into the Wind River from the north (Muddy and Fivemile Creeks) compared with those from the south invalidate this mechanism. For drainages north of the Bighorn Mountains, migration due to unequal sediment contribution by tributaries on either side of the river is not reasonable for the northward migration of the Yellowstone River or the eastward migration of the

Bighorn River and two of its tributaries (Lodge Grass and Rotten Grass Creeks).

The effect of tilting on erosion and sediment supply by tributary streams seems a more potent mechanism than the tilting of the trunk stream itself. For tributaries flowing away from Yellowstone into the trunk stream, tilting would increase both their gradient and sediment delivery, whereas for tributaries flowing towards Yellowstone, both would be decreased: the combined effect would produce migration of trunk streams away from Yellowstone.

The effect of sideways tilting of the trunk stream seems too small to produce the observed lateral migration. One km of uplift over the distance from the Yellowstone crescent axis to the east side of the Bighorn Basin, 200 km, produces a total tilt of only 0.3°. This small amount of tilting at a plate motion rate of 30 km/m.y. would occur over an interval of nearly 7 m.y., or at a rate of 0.00005° per thousand years.

Although the mechanism is poorly understood, a relation to the Yellowstone hotspot is suggested by the pattern of displacement of streams courses generally away from the axis of the Yellowstone crescent of high terrain.

Convergent/Divergent Terraces

Terrace profiles from some drainages in the Bighorn Basin (Fig. 17; Plate 1) suggest uplift of the western part of the basin and tilting towards the east. If tilting is in the same direction as stream flow, stream terraces will tend to diverge upstream, whereas if tilting is opposed to stream flow, terraces will tend to converge upstream. Streams flowing west into the Bighorn River and towards Yellowstone have terraces that tend to converge upstream with the modern stream, as illustrated by the terrace profiles of Paint Rock and Tensleep Creeks (Figs. 17, 18). Streams flowing east into the Bighorn River have terraces that tend to diverge upstream (Mackin, 1937, p. 890) as shown by the terrace profiles for the Shoshone River, particularly the Powell and the Cody terraces, which appear to diverge at about 0.1 m/km (Fig. 18). For the Graybull River (Fig. 17), terraces show a lesser amount of upstream divergence (Mackin, 1937; Merrill, 1973).

Isostatic doming of the Bighorn Basin due to greater erosion of soft basin fill than the mountain rocks (McKenna and Love, 1972; Mackin, 1937) would tend to produce upstream convergence of terraces for streams flowing from the mountains towards the basin center. This effect would be add to hotspot-related upstream convergence of west-flowing streams such as Paint Rock Creek and Tensleep Creek but would subtract from hotspot-related upstream divergence of east-flowing streams such as the Shoshone and Greybull Rivers, perhaps explaining the stronger upstream convergence than upstream divergence noted for in the west- and east flowing streams (Fig. 18).

Rock Creek (Fig. 17) flows northeast past the open, northern end of the Bighorn Basin. Terrace profiles for Rock Creek first converge and then diverge downstream. For any two terraces, the convergence/divergence point is defined by the closest vertical distance on terrace profiles. A plot of this convergence/divergence point against the mean age of the respective terrace pairs (Fig. 19) shows that this point has migrated northeastward throughout the Quaternary at an irregular rate, but overall not incompatible with hotspot and the plate-tectonic rates. The convergence/divergence point might be thought of as the inflection point between slower rates of uplift to the northeast and higher rates of uplift to the southwest towards the Yellowstone crescent.

The change from an apparent rate between 1300 and 300 ka of < 10 km/m.y. to an apparent rate of 110 km/m.y. after 300 ka (Fig. 19) may suggest irregularities associated with the deep processes responsible for the inferred uplift and tilting. Whether the change in rate or even the overall trend of the plot itself has tectonic significance is open to question, for climatic, lithologic, or stream-capture factors might also relate to changes in gradient through time.

In the Bighorn Basin, the Bighorn Basin parallels the crest of the Yellowstone crescent and its terraces are remarkably parallel (Palmquist, 1983). Northeastward from the Bighorn Mountains, the Bighorn flows away from the Yellowstone crescent. Here, Agard (1989) notes the lower 4 terraces converge with the river, but the upper 4 terraces diverge from it with an overall pattern of migration of convergence/divergence points away from the Yellowstone crescent.

The maximum thickness of Quaternary gravels along the Greybull River has migrated about 25-45 km eastward in about 800-900 ky but with one reversal in direction (data from R.C. Palmquist, written commun., 1989), yielding overall rates not incompatible with plate tectonic rates.

Uplifted(?) Calcic Soils, Rock Creek

The upper limit of carbonate accumulation in soils is primarily controlled by (1) some maximum threshold value of precipitation, which increases with altitude, and (2) temperature, which decreases with altitude at a lapse rate of typically $5.7^{\circ}\text{C}/1000$ m. In her study of the terraces of Rock Creek, Montana, Reheis (1987) determined that the upper altitude limit of calcic soils on each terrace increases with terrace age. Calcic soils occur in the 600-ka lower Roberts terrace at altitudes 300 m higher than the highest such soils in the 20-ka Pinedale terrace, and 250 m higher than such soils in the 120-ka Bull Lake terrace (Fig. 20). The highest calcic soils forming on the 20-ka Pinedale terrace are continuing to accumulate carbonate, but the highest calcic soils forming on older terraces are relict and tending to lose their carbonate, particularly those at the highest, moister altitudes.

If the increase in altitude of relict calcic soils is due solely to uplift, uplift at 0.5 m/ky (0.5 mm/yr) is indicated (Fig. 20). On the other hand, the increase in altitude of the upper limit of calcic soils may be due to factors other than uplift, including (1) climatic differences between interglaciations wherein some older interglacials were increasingly arid (Richmond, 1972), (2) effect of the build-up of fine material in the soil through time, discussed in Reheis (1987, p. D24), and (3) a time- and cycle-dependent process that may enhance carbonate buildup once CaCO_3 nucleation sites are established. Concerning factor (1), evidence for older interglacials being increasingly warmer is not supported by global oxygen-isotope records of ice volumes. For the about 7 interglacials that post-date the 600 ka Roberts terrace, none are clearly isotopically lighter (lesser ice volumes, warmer?) than stages 1 or 5 which are the interglacials following the 20-ka Pinedale and the 120-ka Bull Lake terraces, only two others are isotopically similar, and the other 5 interglacials were isotopically heavier (greater ice volumes, colder?) than stages 1 and 5 (Shackleton, 1987).

At present, it is not possible to decide among these explanations. Uplift has not been previously considered, yet ongoing epeirogenic uplift is commonly thought to be occurring for much of the Rocky Mountains. If explained by uplift, the estimated rate of 0.5 mm/yr assuming uplift is at the upper end estimated range of 0.1 to 0.5 mm/yr based on plate tectonic motion of the Yellowstone crescent (0.5 to 1 km uplift in 2 to 5 m.y.).

Areas more than 250 km from the hotspot track

At distances beyond the Yellowstone crescent, a boundary to high terrain can be drawn at distances of 300 to 400 km north and east of Yellowstone (Fig. 14). Regrettably, we have not been able to draw a line around to the south of Yellowstone and thus define a topographic feature comparable to the 400-600 radius (800-1200 km diameter) oceanic swells. This problem is greatest southeast from the Yellowstone crescent across the Green and Wind River Basins and in southern Wyoming and Colorado. There is no clear boundary between high and lower topography between northwest Wyoming and southern Colorado. Suppe and others (1975) proposed the intriguing suggestion that tandem northeastward migration of the Yellowstone and Raton (New Mexico) "hotspots" have caused arching on an axis that extends between the hotspots and is responsible for the epeirogenic uplift of the Rocky Mountains-Colorado Plateau-Great Plains region.

PROBLEMS RELATING REGIONAL UPLIFT TO THE YELLOWSTONE HOTSPOT

Uplift is most clearly defined for the Yellowstone crescent on the leading margin of the Yellowstone hotspot (Fig. 14; Plate 1). The distance from the crest

of the crescent to its outer margin is about 100 ± 40 km. At a migration rate of 30 km/m.y. indicated by the Yellowstone hotspot, uplift on the outer margin of the Yellowstone crescent would therefore take about 3 m.y.; uplift of 0.5 to 1 km would therefore occur at a rate of 0.1-0.3 mm/yr.

Quantitative separation of the Yellowstone crescent from Laramide block uplifts presents a major challenge. These uplifts, presently expressed by the Gros Ventre, Beartooth, Wind River, and Blacktail-Snowcrest-Madison Ranges, are mountains that expose older bedrock that has been uplifted, in part, by Laramide crustal shortening. Late Cenozoic normal faulting, however, has broken parts of these uplifts. For example, the Teton fault has broken the Gros Ventre Range (Lageson, 1987), the Madison fault has broken the west side of the Madison Range, and the Emigrant fault has broken the northwest side of the Beartooth uplift (Personius, 1982).

The 350-km width of the Yellowstone crescent is much smaller than the generally 1000 ± 200 km oceanic hotspot swells (Fig. 13; Crough, 1983). Higher terrain extends as far as 350 km north and northeast of Yellowstone (Fig. 14; see also Godson, 1981), compatible with a swell 700 km across. But southeasterly from Yellowstone, an outer margin to uplift is difficult to draw because average altitude remains high. At 350 km from Yellowstone in south-central Wyoming, regional altitudes are high and then to increase in Colorado.

Quaternary incision rates were examined to see if any pattern emerges (Fig. 26). These rates are determined from terraces dated by volcanic ashes that range in age from 0.6-2 Ma (Izett and Wilcox, 1982; Reheis and others, in press). Relatively high incision rates extend from the Yellowstone region southeast to Colorado and New Mexico. Assuming these incision rates might approximate uplift rates, uplift in this region has been approximately 100-200 m/m.y.. For a hotspot swell 1000 m high and 1000 km wide in a plate moving 30 km/m.y., uplift of 60 m/m.y. is predicted, a factor of 2-3 less than the 100-200 m/m.y. rates of incision. In summary, the altitude distribution and the distribution of high incision (uplift?) rates prevents the objective definition of a swell centered on Yellowstone because the "swell" is markedly enlarged on its southeast margin.

Suppe and others (1975) ingeniously surmounted this difficulty by suggesting that the Yellowstone and proposed Raton hotspots operated in tandem to produce a broad northeastward-migrating arch that extends from Montana to New Mexico. This tandem hotspot arch is basically the same late Cenozoic uplift previously known as epirogenic uplift of the Rocky Mountain-High Plains-Colorado Plateau area. The Raton hotspot is much less credible than the Yellowstone hotspot, having neither a systematic volcanic progression (Lipman, 1980) nor associated belts of neotectonic faulting. Consequently, the Raton hotspot, if real, is weaker and less able to affect and

penetrate the continental lithosphere than the Yellowstone hotspot.

Late Cenozoic uplift and tilting of southwestern Wyoming is shown by several studies. For the Pinedale anticline area of the northern Green River Basin, studies of thermal histories of materials from a deep oil well indicate uplift started around 2-4 Ma and resulted in at least 20°C cooling, which is equivalent to about 1 km of uplift and erosion (Naeser, 1986; Pollastro and Baker, 1986). Further south, Hansen (1985) noted that an eastward course of the Green River across the present Continental Divide was captured about 0.6 Ma, and gravels of this eastward course were subsequently tilted so they now slope to the west. This indicates uplift along and east of the present continental divide and/or subsidence to the west of it. The tandem Yellowstone-Raton hotspot hypothesis of Suppe and others (1975) explains the The Great Divide Basin (Red Desert on Fig. 1) by arching in the headwaters of a previously east-flowing drainage, thereby creating a closed basin on the continental divide.

DISCUSSION

Models to explain the SRP-YP volcanic province include: (1) an eastward propagating rift (Myers and Hamilton, 1964; Hamilton, 1987), (2) volcanism along the SRP-YP localized by a crustal flaw (Eaton and others, 1975) (3) a plate-interaction model with the SRP-YP trend being a "transitional transform boundary zone [at the northern margin] of the Great Basin" (Christiansen and McKee, 1978), (4) volcanism initiated by a meteorite impact (Alt and others, 1988), and (5) a deep-seated mantle plume leaving a hotspot track in the overriding plate (Morgan, 1973, 1981; Suppe and others, 1975; Smith and Sbar, 1974; Smith and others, 1977; Zoback and Thompson, 1978; Anders and others, 1989; Blackwell, 1989; Westaway, 1989; Rodgers and others, 1990; Malde, in press).

All these explanations require heat from the mantle, but in models 1, 2, and 3, the lithosphere is the operative (driving) process which causes changes in the mantle, whereas in model 5, a thermal mantle plume is the operative (driving) process which causes magmatism and deformation in the overriding plate. In model 1 asthenosphere upwelling into the space vacated by the moving lithosphere may release melts needed to provide the heat for volcanism, but models 2 and 3 are not based primarily on lithospheric spreading across the SRP, so upward transport of heat by melts generated by strongly upwelling asthenosphere would not be available.

A mantle plume explanation may seem to have an ad hoc quality because such plumes are remote from direct observation and straight-forward testing. Explanations based on driving by lithospheric processes may be more appealing to geologists because they rest on firmer ground and tie more closely to the kind of information that can be directly observed. We think mantle plumes are real based on

the success of hotspot tracks in defining absolute plate motions, the more than 1000 km dimension of swells associated with hotspots, and the apparent need for mantle plumes in the deeper of the two convective systems operating in the mantle/lithosphere. Thus, although mantle plumes are remote from the top of the lithosphere, difficult to examine, and not well studied in continental lithosphere, we think the mantle plume model merits serious consideration as an explanation for the volcanic track, neotectonic faulting, and uplift in the SRP-YP region.

ALTERNATIVE MODELS AND THEIR PROBLEMS

Eastward Propagating Rift

Hamilton (1987, 1989) considers the lower terrain of the eastern SRP-YP province bounded by higher mountains (Plate 1) to be a rift that has propagated eastward through time. By this explanation, rifting or necking of the lithosphere has created this lower terrain; movement of asthenosphere upward into the volume vacated by lithospheric spreading results in depressuring and melt generation. However, both the extension directions and the late Cenozoic fault trends seem incompatible with this mechanism.

If the SRP were a rift, extension directions of a rift should be perpendicular to its margins. But for the SRP-YP region, extension directions are subparallel to or at low angles to the margins of the SRP-YP trench (Fig. 22; Malde, in press). The only exceptions are a few observations near the Montana-Wyoming-Idaho border where some extension directions are nearly perpendicular to the northern margin of the SRP-YP trench. We assume the craton east of the Basin-Range is fixed thus permitting us to give only the extension vector away from this fixed craton. South from the SRP to the Wasatch front, extension is west to west-northwest. North of the SRP, excepting the Madison-Centennial area, the extension direction is $S45^{\circ}W \pm 15^{\circ}$. This extension direction continues to the northern boundary of the Basin and Range Province in the Helena area (Stickney and Bartholomew, 1987a; Reynolds, 1979, Fig. 10). In the Madison-Centennial area, extension is both $S4^{\circ}W \pm 10^{\circ}$ and about west, compatible with the westerly trends of the Centennial-Hebgen faults and the northerly trend of the Madison fault respectively (Stickney and Bartholomew, 1987a, Fig. 10). Fissures associated with Quaternary basalt eruptions on the SRP mostly indicate extension to the west-southwest (Kuntz, in press).

Extension is approximately normal to the trend of active faults in the area, as demonstrated statistically by Stickney and Bartholomew (1987a) for the area north of the plain. In addition, extension on the SRP parallels that in the nearby Basin-Range. Interestingly, the Great Rift fissure system (Kuntz and others, 1983) arcs through an angle of about 30° thus paralleling faults north and south of the SRP.

In the Yellowstone area at the active end of the SRP-YP trend, fault orientation and earthquake

extension directions are inconsistent with a rift origin (Fig. 22, Plate 1). Post-glacial faults trend north-south across the caldera margin and nearly perpendicular to the margins of the SRP-YP trend. On the Mirror Plateau, numerous post-glacial faults trend northeasterly in a broad arc. Their orientation is 90° off the predicted trend of faults at the tip of a propagating rift on the SRP-YP trend.

Thus, actual extension directions are incompatible with a rift origin, for they generally depart more than 45° and many are near 90° from their orientation predicted by a rift origin. In addition, paleogeographic reconstructions of Paleozoic and Proterozoic facies show that opening of the SRP by rifting since the Paleozoic is not required to account for the present distribution and thicknesses of these units (Skipp and others, 1979; Skipp and Link, in press).

From his study of late Cenozoic faulting in the Blackfoot Mountains, south of and adjacent to the Heise volcanic field, Almendinger (1982, p. 513) concluded "that no normal faults paralleling the SRP appear to have formed prior to or synchronous with the earliest phase of magmatic activity" and therefore concluded that the SRP is better explained by magmatic rather than rifting processes. Elsewhere, some faults are parallel to the plain although some of these faults may be associated with caldera margins rather than rift structures (Pankratz and Ackerman, 1982; Malde, in press). In the southern Lemhi Range and southern Centennial Mountains, adjacent to the Blue Creek and Kilgore calderas, respectively, arcuate faults locally parallel to the plain margin apparently formed synchronously with collapse of the calderas (McBroome, 1981; Morgan, 1988). Zones of autobrecciation (poorly sorted, angular clasts of the ignimbrite within a matrix of fine-grained, vapor-phase matrix) are concentrated along some faults and appear restricted to the caldera margins (Morgan and others, 1984).

Hamilton (1989) considers magmatism on the SRP-YP province to be clearly rift related on the basis of its bimodal volcanic assemblage, its extensional setting, and its crustal structure. He suggests that the premagmatic crust beneath the SRP has been thinned, that in much of the province it may be absent, and that the present crust consists of mantle-derived basalt. These features and their causes are debatable as to their distinct rift signature. According to Hamilton (1989; personal communication, 1990), other models proposed for the origin of the SRP-YP province, including a hotspot origin, require that magmatic material has been added to the crust which would result in the plain becoming a topographically high area, rather than being its present characteristic topographic low. However, several factors may explain the 500-700 m decrease in average altitude from the adjacent mountains down to the eastern SRP. These factors include gabbroic underplating, the plain-wide extend of the calderas and volcanic fields (Morgan and others, 1989), post-volcanic thermal contraction (Brott

and others, 1981), and transfer of crustal material from beneath the SRP to sites outside of the plain by eruption of ignimbrite and co-ignimbrite ash (> 1000 km³ each event), and possible changes in the mantle lithosphere. Neither the eastern SRP nor the Yellowstone Plateau appears to require a rift origin to isostatically compensate for the decrease in altitude at their margins.

In addition, the mountains at the edge of the SRP from Yellowstone to the 10.3-Ma caldera do not have the characteristic rift-rim topography; rather than the highest mountains being near the rift margin, the mountains near the edge are relatively low and increase in altitude for about 100 km away from the margin.

Crustal Flaws and the Origin of the SRP-YP Province

The parallelism of the northeast-trend of the SRP with that of the Late Cretaceous-early Tertiary Colorado Mineral Belt and the late Cenozoic Springerville-Raton lineament was noted by Lipman (1980) who suggested that these NE-trends reflect a pre-existing "structural weakness" in an ancient Precambrian crust along which younger activity was concentrated. Others (Eaton and others, 1975), Mabey and others, 1978; Christiansen and McKee, 1978) suggest that the location of the SRP-YP province was controlled by a crustal flaw aligned with the NE-trending regional aeromagnetic lineament that extends from Mono Lakes, California into Montana (the Humboldt zone of Mabey and others, 1978). However, upon examination of regional magnetic and gravity maps, we see no strong expression of a crustal boundary along the northeast projection of the Yellowstone hotspot track. The hotspot track itself is well expressed in the magnetics as the rhyolitic and basaltic rocks have relatively high magnetic susceptibilities but this only reflects the late Cenozoic magmatism, and not some pre-existing crustal boundary. The projection of the Humboldt magnetic zone to northeast of Yellowstone (Eaton and others, 1975; Mabey and others, 1978) has dimensions that seem peculiar for a crustal weakness exploited by Yellowstone-type volcanism. First, rather than a single boundary, it is commonly two lineaments nearly 100 km apart; why would two such lineaments be exploited simultaneously rather than the failing of one lead to all the activity there. The Madison mylonite zone locally represents one of these lineaments, but was not exploited by the Yellowstone trend. No crustal flaw is known to cross the Beartooth Mountains on the projection of the centerline of the hotspot track (Barker, oral commun., 1990). Second, these lineaments as drawn are absolutely straight over a distance of 1000 km, which seems odd for a geologic boundary that is typically arcuate over such distances.

Major crustal boundaries defined by both geologic and geophysical studies do occur both north and south of the plain and appear more significant than any pre-Miocene crustal flaw coincident with the

plain for which there is no geologic evidence. The Great Falls tectonic zone, a major Archean structure active from Precambrian to Quaternary time, is subparallel to the SRP and is about 200 km north of it (O'Neill and Lopez, 1985). Similarly, the Madison mylonite zone, a major Proterozoic shear zone, is also subparallel to the SRP-YP margin but is about 30 km north of it (Erslev, 1982; Erslev and Sutter, in press). The southern margin of the Archean Wyoming province, a major crustal boundary, is also subparallel to the plain and is 200-300 km south of it (J.C. Reed, written communication, 1989). A Late Proterozoic to Early Cambrian rift basin is postulated by Skipp and Link (in press) to trend NNE from the Portneuf Range across the plain to the Beaverhead Mountains. Analyses of the distribution and thicknesses of Paleozoic sedimentary facies by Skipp and others (1979) show that strike-slip offset across the SRP is not necessary, although both left-lateral (Sandberg and Mapel, 1967) and right-lateral strike-slip faulting (Sandberg and Poole, 1977) have been proposed based on similar information. Woodward (1988) presents structural and facies data to argue that no faulting is indicated across the Snake River Plain, and states "There is no reason to postulate major changes [across the Snake River Plain] in Tertiary extension either". In summary, major crustal boundaries are known both north and south of the plain whereas a major pre-Miocene boundary coincident with the plain is doubtful. If exploitation of crustal flaws is the controlling process, why were not the crustal flaws north of the plain (the Great Falls tectonic zone and the Madison mylonite zone) exploited. We conclude that the location of the Yellowstone hotspot track probably reflects a sub-lithospheric process rather than a crustal flaw within the lithosphere. Preexisting crustal flaws do not have a unique relationship to the SRP and a transcurrent fault along the SRP is not required from either stratigraphic or structural studies.

Transform Boundary Zone Origin for the SRP

In their plate-interaction model for the basin-range, Christiansen and McKee (1978) suggested the SRP-YP was a "transitional transform boundary zone [at the northern margin] of the Great Basin". They suggest transform motion is indicated by a greater amount of basin-range extension south of the 1000-km-volcanic lowlands formed by the combined Snake River Plain and southern Oregon rhyolite belt (Christiansen and McKee, 1978, Fig. 13-8; McKee and Noble, 1986).

However, for the eastern Snake River Plain, evidence published after Christiansen and McKee (1978) does not support right-lateral offset. As discussed under "Crustal Flaws", Skipp and others (1979) and Woodward (1988) argue against any strike-slip offset based on stratigraphic facies and structural trends. The widespread basin-range extension north of the plain (Plate 1) that became *generally* known following the 1983 Borah Peak earthquake, suggests

that extension north of the plain is of similar magnitude to that south of the plain, and that no right-lateral offset need be occurring.

If there were right lateral shear across the plain, the orientation of aligned and elongated volcanic features should be in the orientation of tension gashes and orientated in a direction 30° clockwise to the trend of the SRP. As indicated by elongations and alignments of volcanic features (Fig. 22), the volcanic rift zones trend nearly perpendicular to the margins of the SRP (Kuntz, in press, Fig. 4), about 60° clockwise from the tension gash orientation. Of the 9 rift zones shown by Kuntz (in press, Fig. 4), only the Spencer-High Point rift zone has an orientation close to that of tension gashes that would be related to right lateral shear along the SRP.

Southern Oregon Rhyolite Belt--. Christiansen and McKee (1978) define the High Lava Plains as extending from the eastern SRP to the Brothers fault zone and parallel zones to the west. They postulate that right-lateral shear was localized in the area of the High Lava Plains because the plains are located along "the approximate northern boundary of maximum cumulative extension" of the basin and range. In Christiansen and McKee's (1978) model, the eastern SRP represents an ancient crustal flaw while the Brothers fault zone and parallel zones in the west represent a symmetrical tear. According to Christiansen and McKee (1978), coeval bimodal volcanism along both the eastern and western arms of the High Lava Plains originated approximately 14 to 17 Ma at the common borders of Oregon, Nevada and Idaho and propagated symmetrically from this point. Although the timing of volcanism, rates of volcanic migration, volcanic compositions, and length of the volcanic track of volcanism in southeast Oregon has been compared with that on the eastern SRP (Christiansen and McKee, 1978), we do not concur with these conclusions. Beginning in the late Miocene, silicic volcanism along the eastern SRP differs from that of the southeastern rhyolite belt in 8 ways listed in Table 3. The earliest volcanism associated with the southeast Oregon belt is dated about 14.5 Ma and is limited to 3 randomly spaced events at 14.7 Ma, 14.7 Ma, and 13.5 Ma (MacLeod and others, 1976). These older volcanic events show little, if any, spatial relationship to the younger events which began on a regular basis at about 8 Ma. Although three events occurred about 10 Ma, there is a significant lull in volcanic activity 6 m.y. long from the time volcanism was weakly expressed 14.5 Ma until about 8 Ma when a volcanic progression becomes apparent in southeast Oregon. Based on the differences summarized in Table 3, we conclude that the silicic volcanism in southeast Oregon bears little, if any, relationship to that on the eastern SRP and that the two volcanic provinces should be considered as separate and having different origins.

We accept the interpretation that volcanic activity in southern Oregon is related to transform or right-

lateral offset along the Brothers fault zone as advocated by Christiansen and McKee (1978), but do not extend this explanation to the eastern SRP Yellowstone area.

A Meteorite Impact Origin for the SRP-YP Province

Many investigators have noted that flood basalt volcanism occurs at the start of hotspot tracks and, following this pattern, suggest the Columbia Plateau flood basalts relate to the Yellowstone hotspot (see, for example, Morgan, 1972, 1981; Duncan, 1982; Richards and others, 1989; White and McKenzie, 1989). However, Alt and others (1988, 1990) go one step farther and suggest meteorite impacts are responsible for the initiation of flood basalt volcanism. By analogy with the Deccan Plateau flood basalts and the later Reunion (Chagos-Laccadive) hotspot track, Alt and others (1988) suggest that the initiation of the Columbia Plateau flood basalts and the Yellowstone hotspot track are the result of a meteorite impact located in southeast Oregon that somehow initiated a deep-seated mantle plume. The sudden appearance of large lava plateaus erupting over a short interval of time without any apparent tectonic cause is offered as a main criterion (Alt and others, 1988) to support an impact hypothesis. Alt and others (1988) suggest that the presence and distribution of felsic lavas in the plateaus mark the approximate location of impact.

We question an impact hypothesis for the origin of the SRP-YP province for the following reasons: (1) The chosen impact site in southeast Oregon is not supported by any evidence in pre-Steens Basalt strata such as in the Pine Creek sequence where evidence of impact might be expected (Scott Minor, U.S.G.S., personal communication, 1990). Established impact sites are characterized by shatter cones, shocked quartz and feldspar, high pressure mineralogical phases, breccia-filled basins, and high Ni content in the associated magmatism. (2) At sites accepted as having a meteorite impact origin, such as the Manicouagan and Sudbury craters in Canada, associated magmatism has occurred for approximately a million years. However, these established sites have neither voluminous flood basalts nor protracted volcanism to produce a systematic volcanic track like that of a hotspot. In Alt and others' (1988) model, "volcanism at the surface maintains the mantle plume at depth -- the hotspot continues to erupt because it continues to erupt" (Sears, Hyndman, and Alt, 1990), a mechanism we find unconvincing. (3) Alt and others' (1988) argument for an impact producing the Deccan Plateau flood basalts may be erroneous on several accounts. First, no impact crater has been defined for the Deccan Plateau site. Second, although the Deccan Plateau basalts date from near the time of the Cretaceous/Tertiary boundary, (Courtillot and others, 1986; Alt and others, 1988), studies of the boundary layer and the size of its contained shock quartz suggest impact in the Western Hemisphere (Izett, 1990), possibly in the Caribbean Basin

(Hildebrand and Boynton, 1990; Bohor and Seitz, 1990). (4) Alt and others (1988) attribute an impact origin to felsic rocks that we think are associated with the southern part of the Columbia Plateau (better known as the Oregon Plateau) 5) Finally, no major faunal extinction event occurs at about 17 Ma as is thought to be associated with other postulated meteorite impacts. In conclusion, we do not accept the impact hypothesis because evidence expected to accompany such an impact in southeast Oregon has not been found.

A TWO-PHASE, MANTLE PLUME MODEL FOR THE SRP-YP REGION

We find a thermal mantle plume model best accounts for the large-scale processes operating at asthenospheric and lithospheric depths that are responsible for the observed systematic volcanic progression, regional uplift, and localization of late Cenozoic basin-range faulting. Several investigators have proposed a deep-seated mantle plume or hotspot origin for the SRP-YP province (Morgan, 1973, 1981; Suppe and others, 1975; Smith and others, 1977, 1985; Zoback and Thompson, 1978; Anders and others, 1989; Blackwell, 1989; Westaway, 1989; Rodgers and others, 1990; Malde, in press) to account for the various volcanic and tectonic features present. In this section, we first explain a model and then discuss how geologic evidence supports this model, particularly based on the large horizontal scale of processes operating at lower crustal and lithospheric mantle depths that are responsible for the observed systematic volcanic progression, regional uplift, and localization of late Cenozoic basin-range faulting.

The Two Phase Model

Richards and others (1989) suggest that hotspots start with very large "heads" ($>10^2$ km diameter) capable of producing melting, rifting, doming, and flood basalts (White and McKenzie, 1989a). Following a path pioneered through the mantle by this head is a much narrower chimney that feeds hot mantle material up into the head. Richards and others (1989) calculate that 15-28 m.y. are required for a plume head to rise from the core-mantle interface through the mantle to the base of the lithosphere. The head phase contains more than an order of magnitude more heat than the heat carried by 1 m.y. of chimney discharge. In addition, the central part of the head may be 50-100°C hotter (White and McKenzie, 1989a) than the chimney. Richards and others (1989) note that rifting may actually result from the encounter of the plume head with the lithosphere and that large amounts of continental lithospheric extension may not necessarily precede flood basalt eruptions. After the head flattens against the base of the lithosphere and partially melts, the chimney eventually intercepts the lithosphere and produces a migrating sequence of volcanism and uplift in the overriding plate, a hotspot track (Richards and

others, 1989; Whitehead and Luther, 1975; Skilbeck and Whitehead, 1978). The chimney phase of the Hawaiian and other hotspot tracks have lasted longer than 100 m.y. Although some investigators agree with a core-mantle source region for plumes (Tredoux and others, 1989), others suggest mantle plumes originate from higher in the mantle, perhaps at the 670-km seismic discontinuity (Ringwood, 1982) or at possibly even shallower depths (Anderson, 1981). Recent evidence suggests the 670-km discontinuity may be an abrupt phase change (Ito and Takahashi, 1989; Wood, 1989) and not a constraint to plume flow from the core-mantle boundary to the lithosphere.

We suggest a mantle-plume head about 300 km in diameter first encountered the base of the lithosphere 16-17 Ma near the common borders of Nevada, Oregon, and Idaho based on volcanic and structural features in this region (Figs. 23, 24). Zoback and Thompson (1978) suggested that the mantle plume associated with the Yellowstone hotspot first impinged on the lithospheric base of the North American plate around 16-17 Ma along a NNW-trending rift zone herein called the Nevada-Oregon rift zone. The chimney, which was about 10-20 km in diameter and had been feeding the now stagnating head, intercepted the lithosphere about 10 Ma near American Falls, Idaho, 200 km southwest of Yellowstone (Plate 1; Figs. 23, 24). Volcanism along the hotspot track is more dispersed during the head phase than the chimney phase (Fig. 3).

Figure 24 is a schematic representation of the development of the thermal plume that formed the Yellowstone hotspot track, based on other investigators' models proposed for thermal mantle plumes. The following 4 paragraphs explain the relations we envisage for the 4 parts of Figure 24.

1. The plume began deep in the mantle, perhaps at the core/mantle boundary, as a thin layer of hotter, less viscous material converging and flowing upward at a discharge of perhaps $0.4 \text{ km}^3/\text{yr}$ (Richards and others, 1989) through cooler, more viscous mantle (Whitehead and Luther, 1975). To rise 3,000 km from the core/mantle boundary, (Richards and others, 1989) calculate the plume head took 28 M.y. to reach the lithosphere, rising at an average rate of 0.1 m/yr. As it rose, the plume head was constantly supplied with additional hot mantle material through its plume chimney, a conduit only about 10 or 20 km across whose narrow diameter and greater velocity (perhaps 1 m/yr, Richards and others, 1989 or 2-5 m/yr, Loper and Stacey, 1983) reflects the established thermal chimney where the increased temperatures result in much higher strain rates. As the plume head rose, continued feeding of it by its chimney inflated it to a sphere about 300 km in diameter by the time it intercepted the lithosphere (Richards and others, 1989).
2. About 16 Ma, the plume head intercepted the base of the SW-moving North American lithospheric plate and mushroomed out in the asthenosphere to a diameter of perhaps 600 km. Doming and

lithospheric softening above this plume head resulted in east-west extension along the 1100-km-long NNW-trending Nevada-Oregon rift zone. Decompression melting accompanying the rise of the plume generated basaltic material that rose into the lithosphere, produced flood basalts in the more oceanic crust of Washington and Oregon, and mafic intrusions in northern Nevada (Fig. 23). Near the common boundary of Nevada, Oregon, and Idaho, basaltic melts invaded and heated more silicic crust, producing rhyolitic magmas that rose upward to form upper crustal magma chambers, from which ignimbrites were erupted that now cover extensive terrain near the Nevada-Oregon-Idaho border region (Fig. 23). The plume head may have domed the overriding plate, with increased temperatures in the asthenosphere lessening drag on the overriding plate. On the west side of the dome, extension in the overriding plate would be favored whereas on the east side compression seems likely.

3. Sometime between about 14 to 10 Ma, a transition from the head phase to the chimney phase occurred (Fig. 24). As the plume head spread out horizontally and thinned vertically at the base of the lithosphere, the heat per unit area beneath the lithosphere became less and the plume material became more stagnant. The chimney continued to feed upward at a relatively high velocity and carried material into the thinning, stagnating but still hot, plume head. This transition from plume head to chimney is reflected in better alignment of calderas after 13 Ma (Plate 1).

4. By 10 Ma, continued upward flow of the chimney established a path through the flattened plume head and encountered the base of the lithosphere. Continued decompression melting of material rising up the chimney released basaltic melts that invaded and heated the crust to produce silicic magmas. These silicic magmas moved upward to form magma chambers in the upper crust, from which large-volume ignimbrites were erupted, forming the large calderas of the Yellowstone Plateau and eastern Snake River Plain. The linear, narrow volcanic track defined by the eastern SRP-YP volcanic province reflects the narrower, more focused aspect of the chimney phase of the plume (Plate 1, Figure 4). As with the Hawaiian hotspot, flow of plume material carries heat outward for hundreds of kilometers in the asthenosphere and results in swell uplift and other lithospheric changes (Figs. 23, 24; Courtney and White, 1986; White and McKenzie, 1989a). Because of the elevated temperature in the asthenosphere due to the hotspot, drag in the asthenosphere at the base of the North American plate would be lessened. Due to doming associated with the Yellowstone hotspot, perhaps including other hotspots to the south (Suppe and others, 1975), the plate on the west side may readily move westward favoring basin-range extension whereas that on the east side continues under compression. The axis of this dome approximates the eastern margin of the Basin and Range.

Evidence from Volcanism and Rifting

The most prominent feature associated with the start of the hotspot is a volcanic rift zone, consistent with the observations that rifting may accompany interception of a plume head with the lithosphere (White and others, 1987), and that large amounts of continental lithospheric extension do not necessarily precede flood basalt eruptions (Richards and others, 1989).

The 1100-km-long Nevada-Oregon rift zone is associated with 17- to 14-Ma basaltic and silicic volcanism and dike injection (Fig. 23) and is part of the 700-km-long Nevada rift zone defined by Zoback and Thompson (1978) as extending from central Nevada to southern Washington. The distinctive, linear, positive aeromagnetic anomaly associated with the central part of this rift, the northern Nevada rift, results from mafic intrusions about 16 Ma. The northern Nevada rift has recently been extended 400 km further to southern Nevada (Blakely and others, 1989) (Fig. 1), where 16-14 Ma rhyolitic fields are also present (Luedke and Smith, 1981). The feeder dikes for the Oregon Plateau flood basalts (including the basalts at Steens Mountain, Carlson and Hart, 1986, 1988) and the Columbia River flood basalts (Hooper, 1988; Smith and Luedke, 1984) have the same age and orientation as the northern Nevada rift and are considered by us a northern part of it. The eruptive volume of these flood basalts totals about 220,000 km³ (Figs. 23, 24), based on about 170,000 km³ for the Columbia River Basalt Group (Tolan and others, 1989) and perhaps about 50,000 km³ for the Oregon Plateau basalts (Carlson and Hart, 1988).

White and McKenzie (1989a, b) conclude that if mantle plumes (hotspots) coincide with active rifts, exceedingly large volumes of volcanic material can extend along rifts for distances of 2000 km. The main pulse of eruption of the Columbia River-Oregon Plateau flood basalts at the northern end of the 1100-km-long Nevada-Oregon rift zone and the mid-Miocene location of the Yellowstone hotspot near the center of this rift are consistent with this pattern.

The Columbia River basalts have been referred to as the initial expression of the Yellowstone hotspot (Morgan, 1981; Zoback and Thompson, 1978; Duncan, 1982; Leeman, 1989; Richards and others, 1989) although this genetic tie has been questioned by others (Leeman, 1982, 1989; Carlson and Hart, 1988; Hooper, 1988), in part because of the lopsided position of the Columbia River basalts and feeder dikes 400 km north of the centerline of the projected hotspot track (Fig. 23). Morgan (1981) points out that many continental flood basalts (Table 2) are associated with the initial stages of hotspot development and cites the following examples where flood basalts are not centered on the younger hotspot track: the Deccan Plateau flood basalts and the Reunion track, the Parana basalts and the Tristan track, and the Columbia River basalts and the Yellowstone track. The 1100-km length of the Nevada-Oregon rift zone is actually bisected by the

hotspot track (Fig. 23), indicating that there is no asymmetry in structure, but only in the volume and eruptive rates of basalts that surfaced north of the bisect line, perhaps due to crustal differences. The eruptive rate calculated for the Columbia River and Oregon Plateau basalts (Figs. 23, 24) is based on the fact that more than 95% of the total estimated volume of 200,000 km³ erupted in about a 2-m.y. interval (Carlson and Hart, 1986; Baksi, 1990).

The sharp contrast in style and amount of 17- to 14-Ma volcanism along the 1100-km-long, Nevada-Oregon rift zone correlates with the nature of the crust affected by the thermal plume (Figs. 24 and 25). The Columbia River and Oregon Plateau flood basalts occur in accreted oceanic terrains (Figs. 23, 24; Vallier and others, 1977; Armstrong and others, 1977) having relatively thin, dense crust (Hill, 1972), whereas south of the Oregon Plateau basalt province into northern Nevada and southeast of the 0.704 isopleth (i.e., the initial ⁸⁷Sr/⁸⁶Sr = 0.704 isopleth referred to by Kistler and Peterman, 1978) (Fig. 23), much of the accreted crust is somewhat thicker than to the north and is underlain by early Paleozoic or younger mafic crust having oceanic or transitional affinities (Kistler, 1983; Elison and others, in press). This thicker (Mooney and Braile, 1989) and more brittle crust responded to the mantle plume by producing peralkaline rhyolitic volcanism in the region near the common boundaries of Nevada, Oregon, and Idaho, and MUCH less voluminous bimodal volcanism farther south along the 500-km-long Nevada rift (Blakely and others, 1989) in contrast to the voluminous flood basalts to the north (Fig. 23).

About 17 Ma, basin-range faulting became widely active. McKee and others (1970) note a hiatus in volcanic activity from about 17-20 Ma in the Great Basin. In addition volcanism prior to 17 Ma was calc-alkaline of intermediate to silicic composition whereas that after 17 Ma was to basaltic and bimodal rhyolite/basalt volcanism (Christiansen and Lipman, 1972; Christiansen and McKee, 1978; McKee and Noble, 1986). Also at about 17 Ma, ashes erupted from this area changed from dominantly W-type (white, low iron, biotitic) to dominantly G-type (gray, high iron, non-biotitic) (G.A. Izett, 1981, written commun., 1990). Both these changes may be associated with the head of the Yellowstone hotspot encountering and affecting the lithosphere.

The hotspot track from 10 Ma to present is described next, followed by that older than 10 Ma. Transecting thrust belt terrain 10 to 4 Ma, volcanism created the linear trench of the 80 ± 20-km-wide eastern SRP floored by calderas as wide as the SRP itself. From 2 Ma to present in cratonic terrain, the Yellowstone field consists of nested calderas forming a volcanic plateau rimmed by higher mountains and narrowed to only about 45 ± 10 km in width. A major heat source is present beneath Yellowstone as attested by the young volcanism and active geothermal systems. High geothermal gradients are indicated by estimates of the Curie temperature at about 5 km as well as the

absence of earthquakes below about 5 km suggesting the brittle/ductile transition at that depth (Smith and others, 1974). High helium-3/helium-4 isotope ratios occur in Yellowstone thermal waters and indicate a mantle magmatic source (Kennedy and others, 1987). Beneath the Yellowstone and Heise volcanic fields, teleseismic studies indicate high mantle temperatures. Based on P-wave delays, Iyer and others (1981) concluded that a large low-velocity body occurs beneath Yellowstone to depths of 250-300 km and may be best explained as a body of partial melt. The lower part of this low-velocity body extends southwestward along the SRP to the Heise volcanic field, where Evans (1982) noted a low-velocity zone to depths of 300 km. This low-velocity zone is inclined to the northwest and descends beneath the northern margin of the SRP as much as 150 km northwest of the SRP axis.

Caldera-forming silicic volcanism moved at a rate of about 30 km/m.y. to the N 54 ± 5°E between 10.3 and 2 Ma, resulting in the Yellowstone Plateau and Heise volcanic fields, which started at 2.0 and 6.5 Ma, respectively, and the less well-understood Picabo volcanic field, which probably started with the 10.3-Ma tuff of Arbon Valley.

The hotspot track older than 10 Ma contrasts with the younger-than-10-Ma track in that (1) no discrete trench like the eastern SRP was formed; (2) prior to 10 Ma, silicic volcanism was spread over an area as wide as 200 km (Fig. 4) and produced ignimbrites with higher magmatic temperatures (Ekren and others, 1984) than those observed in the younger ignimbrites (Hildreth, 1981) (Fig. 24); (3) the older track has a more easterly trend and progressed at an apparent rate of 7 km/m.y., a rate at least twice that for both the North American plate motion and the younger track (Plate 1, Figs. 2, 23). Some possible reasons for the different character of the older track are a change in the character of the thermal plume with time and differences in the compositions and thickness of the crust. Based on the Yellowstone hotspot track, Pollitz (1988) noted a change in apparent plate motion at 9 Ma, but only a minor change in velocity. Because of the change in plume geometry, we are hesitant to suggest a change in plate motion is indicated at 10 Ma. The apparent rate of 70 km/m.y. from the McDermitt to the Picabo field is about twice the plate motion and may result from: (1) crustal extension that post-dates the older track, (2) large imprecision in the location of the geographic center for the inception of volcanism within a volcanic field, and (3) lack of centering of the plume chimney beneath the plume head, particularly as these rising phases of the plume interacted with and were sheared WSW by the North American plate (Fig. 24). Factor 3 provides the better explanation because the effects of 1 and 2 appear minor compared to the total change. The mantle plume probably did not rise straight up because its angular velocity had to increase as it moved away from the earth's spin axis. The rising plume would deflect either to the west as it required acceleration to keep up with the spin rate or to the

north, in order to stay parallel to the spin axis and thus not require increased angular momentum.

Differences in the crust of the North American plate as it passes over the thermal plume are reflected in the character of the volcanic track of the Yellowstone hotspot. Along the 16-Ma Nevada-Oregon rift, the change from mostly silicic in the central area to flood basalts to the north has been discussed. The area of largest dispersion of silicic volcanic centers (Plate 1, Fig. 4) lies to the west of the 0.706 isopleth for Mesozoic and Cenozoic plutonic rocks, corresponding to the western edge of Precambrian sialic crust (Figures 24 and 25) (ie., the initial $87\text{Sr}/86\text{Sr} = 0.706$ isopleth referred to by Kistler and Peterman, 1978; Armstrong and others, 1977; Kistler and others, 1981; Kistler and Lee, 1989), and lies between the approximate boundaries of the Owyhee-Humboldt and Bruneau-Jarbridge volcanic fields (Figs. 23, 24). East of the 0.706 isopleth (Fig. 23), the old, relatively stable cratonic crust of the Archean Wyoming province (Leeman, 1982; J.C. Reed, written communication, 1989) may have helped restrict volcanism to the relatively narrow 10-0 Ma track we attribute to a plume chimney. Upon crossing from the thrust belt into the craton, the width of the volcanic belt narrows from 80 ± 20 km for the eastern SRP to 45 ± 10 km for the Yellowstone calderas.

Equilibration temperatures for units from the Owyhee-Humboldt field have been calculated to be in excess of 1090°C (Ekren and others, 1984); temperatures from the Bruneau-Jarbridge field are $>1000^\circ\text{C}$ (Bonnichsen, 1982) (Fig. 24). The $700\text{-}800^\circ\text{C}$ temperatures depicted for the Picabo volcanic field are for biotite-bearing ignimbrites (Hildreth, 1981) and extrapolated for the tuff of Arbon Valley (Table 1); this temperature is anomalously low for this province and reflects the hydrous nature of this unit. The Twin Falls, Picabo, and Heise volcanic fields are flanked on both sides of the SRP by Cordilleran fold-and-thrust belt terrain whereas the Yellowstone Plateau field has developed in cratonic crust deformed by Laramide foreland uplifts (Figs. 23, 24). This general decrease in equilibration temperatures eastward and with time may reflect crustal or plume differences (Fig. 24).

Evidence from Faulting and Uplift

The neotectonic belts of faulting, particularly the most active Belt II, converge on Yellowstone and define a pattern analogous to the wake of a boat that has moved up the SRP to Yellowstone (Plate 1, Scott and others, 1985b). The overall V-shaped pattern of the fault belts can be explained by outward migration of heating associated with the Yellowstone hotspot track (Scott and others, 1985b; Smith and others, 1985; Anders and others, 1989). Heat transferred from the same source responsible for the Yellowstone hotspot has weakened the lithosphere, thereby localizing extensional faulting in Belts I-III which are the most active structures for extension in the northeast sector of the Basin and Range. We suggest that Belts I, II,

and III represent waxing, culminating, and waning stages of fault activity respectively. Their spatial arrangement suggests a northeastward migration of a wake-like pattern of faulting, localized by lithospheric heating and weakening. Because the Belts of faulting appear related to the motion of the North American Plate, the Belts shown in Plate 1 will move to the N 55° E at 30 km/m.y. Because of this outward migration and implied sense of acceleration of activity in Belt I, culmination of activity in Belt II, and deceleration of activity in Belt III, the outer part of Belt II would have higher rate of ongoing faulting than the inner part.

The Yellowstone crescent of high terrain has a spatial relation to Yellowstone similar to the fault belts. Although the following supportive evidence is incomplete and selective, ongoing uplift on the outer slope of this crescent is suggested by high Pd/BL ratios, tilting of terraces, outward migration of inflection points along terraces, uplift of ignimbrite sheets, and uplift along historic level lines. The Yellowstone crescent is also predicted to be moving to the ENE at a rate of 30 km/m.y.

The association of both faulting and uplift with Yellowstone cannot be explained by lateral heat conduction within the lithosphere because 10-100 m.y. are required for temperature increases to effect ductility at distances of 50 km (Anders and others, 1989). We think the transport of heat as much as 200 km outward from the SRP-Yellowstone hotspot track (as reflected by the Yellowstone crescent of high terrain) occurs by outward flow in the asthenosphere of an upwelling hot mantle plume upon encountering the lithosphere (Crough, 1978, 1983; Sleep, 1987, 1990). However, the time available is not adequate for conductive heat transport to thermally soften the lithosphere (Houseman and England, 1986; Anders and others, 1989). Anders and others (1989) suggest that rising magmas transport heat into the lithosphere and lower the yield strength, particularly in the upper mantle portion of the lithosphere where much of the yield strength resides. The available heat from the outward motion of a mantle plume at the base of the lithosphere probably diminishes outward due to loss of heat and radial dispersal of the mantle plume.

That uplift precedes volcanism around Yellowstone indicates a process active in the mantle causes lithospheric deformation rather than lithospheric rifting or other deformation caused by passive mantle upwelling. For the Red Sea, Bohannon and others (1989) argue for a passive mantle model because uplift followed initial volcanism and rifting. But on the leading margin of the Yellowstone hotspot, the apex of the Yellowstone crescent of high terrain northeast of Yellowstone and geomorphic indicators of eastward tilting of the Bighorn Basin shows that uplift occurs several hundred kilometers in advance of the volcanism along the hotspot track.

Near the southern margin of the SRP, now inactive areas (Belt IV) have a late Cenozoic history of fault activity concentrated within a few million years. Extension at this time was similar to present and not

oriented perpendicular to the SRP margin as a rift origin of the SRP would predict. This activity has a time-transgressive pattern that correlates well with the volcanic activity along the hotspot track (Plate 1). This pattern is readily explained by the predicted ENE migration of the mantle plume. Faults north of the SRP are still active and initial ages of faulting are not well constrained. Nevertheless, activation of basin-range faulting since about 10 Ma and waning of activity along the faults marginal to the SRP may reflect activity associated with passage of the hotspot.

The eastern SRP and Belt IV, which flanks it on the south, are characterized by little or no Quaternary fault or earthquake activity. This paucity of activity does not result simply from lithospheric cooling, because heat flow from these areas remains high (Brott and others, 1981; Blackwell, 1989) and basalt eruptions have continued throughout the Quaternary. The absence of activity in Belt IV and the slowing of activity in Belt III do not depend on crustal strengthening by crystallization of a basaltic magma at mid-crustal depths. No such mid-crustal body is observed flanking the SRP (Sparlin and others, 1982).

The quiescent yet high-heat-flow in Belt IV and the SRP indicates that process related to passage of the hotspot have resulted in both strengthening and heating of the lithosphere, a combination that appears to require conversion of the lower crust to more mafic material (Anders and others, 1989).

Geophysical and petrologic studies indicate intrusions of basalt at two depths beneath the SRP. The deeper level represents intrusion of basaltic material near the base of the crust (crustal underplating) at a depth near 30 to 40 km (Leeman, 1982; Anders and others, 1989). The lower crust thickens southwestward along the SRP (Leeman, 1982; Braille and others, 1982). A mid-crustal basaltic intrusion beneath the SRP is indicated both by anomalously high velocities (6.5 km/sec) and by high densities (2.88 g/cc) between depths of 10 and 20 km (Sparlin and others, 1982; Braille and others, 1982). Anders and others (1989) outline a model whereby solidification of these mid- and lower crustal basaltic intrusions increases the strength of the crust, particularly deepening the depth of the brittle/ductile transition from a depth of about 15 km to a depth of about 20 km.

Some extension parallel to the ENE trend of the SRP is indicated by fissures and fissure eruptions. These fissures are formed by near-vertical injection of basaltic dikes from near the base of the crust (Leeman, 1982) and are locally marked by grabens (Smith and others, 1989). Although the surface trace of these fissures locally line up with basin-range faults marginal to the plain, they are not co-planar with the primary zone of faulting at depth; the basin-range faults dip at about 50° whereas fissures formed by dike injection are driven vertically upward from depth perpendicular to the minimum stress which in this extensional stress field is generally close to horizontal.

Spacing of faults becomes closer towards the SRP. For example, the Teton fault progressively splits into as many as 10 strands northward between the Teton Range and Yellowstone (Christiansen, 1984; and written commun., 1986). The same pattern occurs near the north end of the Grand Valley (Prostka and Embree, 1978), the northern part of the Portneuf Range (Kellogg, in press), the northern part of the Blackfoot Mountains (Almendinger, 1982), near the south end of the Arco Hills (Kuntz and others, 1984), the southern part of the Lemhi Range (McBroome, 1981), and from the southern end of the Beaverhead Range to the Centennial range (Skipp, 1985). This progression to smaller fault blocks suggests that the part of the crust involved in faulting became thinner because the depth to the brittle-ductile transition became shallower toward the SRP (Ernie Anderson, oral commun., 1988). Heating that could raise the brittle-ductile transition is likely from silicic and basaltic intrusions at depths of 5-20 km beneath the SRP.

For the southern belt of faulting, the surface topographic gradient may provide a mechanism driving and localizing faulting. There, Belts I, II and III are on the inner, western slope of the Yellowstone crescent. But for the western arm, neither the location or orientation of faults appears related to the inner, southern slope of the crescent.

OTHER DISCUSSION OF EXTENSIONAL FAULTING

The geometry of faults in the western and southern belts produces a markedly different kinematics. The en echelon arrangement of faults in the southern belt may produce an comparable amount of east-west extension because one fault takes over where the other dies out. But the western belt, the faults are arranged one behind the other such that late Quaternary extension is subparallel rather than perpendicular to the length of Belt II (Plate 1).

West of the active basin-range north of the plain is the relatively unfaulted Idaho batholith. This area has acted like a block, but one that has moved westward relative to the craton as the basin range east of it extended. West of the Idaho batholith is the Western Snake River Plain, the largest and best-formed graben in the entire region. The lack of extension within the batholith appears to be compensated by strong expression of basin-range extension east and west of the it.

The western Snake River Plain is a graben apparently associated with passage of the Yellowstone hotspot, but a fundamentally different structure from the hotspot track in spite of the geomorphic continuity of the two lowlands. In addition, the gravity anomaly that appears to join these features may represent a large tension-gash or riedel-shear opening formed by right-lateral shear when the hotspot had moved east of the western plain to adjacent to Idaho batholith which resisted extension which therefore continued on the western Snake River Plain.

RELATIONS BETWEEN THE YELLOWSTONE HOTSPOT AND BASIN AND RANGE DEFORMATION

The neotectonic fault belts that converge on Yellowstone are here explained by thermal effects associated with the Yellowstone mantle plume localizing basin-and-range extension, thereby deferring explanation of basin-and-range extension. But if we backtrack from Yellowstone to the 16-Ma start of the Yellowstone hotspot, the following geologic associations between the head phase of the hotspot and the origin of the basin and range suggest a strong interrelation:

1. The hotspot head intercepted the base of the lithosphere about 16 Ma, coinciding with the start of widespread basin-range extension and normal faulting.
2. The hotspot track started in about the center of the active Basin and Range structural province (Fig. 23).
3. The change in basin-and-range magmatism from calc alkalic to basalt and bimodal basalt/rhyolite (Christiansen and McKee, 1978) coincided in time and space with volcanic and structural penetration of the lithosphere we relate to the plume head.
4. The 1100-km-long Nevada-Oregon rift zone we associate with the plume head was active over a length comparable to the diameter of the basin and range (Fig. 23).
5. Associated with the northern part of the Nevada-Oregon rift, voluminous flood basalt volcanism of the Columbia River and Oregon plateaus were erupted 16 ± 1 Ma through a denser, more oceanic crust.
6. A spherical plume head 300 km in diameter if converted to a layer averaging 20 km thick would cover an area almost 1000 km in diameter, similar in scale to the active basin-and-range.
7. Assuming a plume takes 25 M.y. to ascend from the core mantle boundary, the plume head would store heat approximated by the total of 25 M.y. at the present Yellowstone rate. The hotspot buoyancy flux of the Yellowstone hotspot is estimated to be 1.5 Mgs^{-1} (Sleep, 1990). Much of the plume's original heat could still reside in the asthenosphere and lower lithosphere beneath the Basin and Range, the original heat approximated by 25 M.y. of the amount now feeding the Yellowstone hotspot.

Thus, the Basin and Range may have a causal relation with particularly the plume-head phase of the Yellowstone hotspot as indicated by their coincidence in time and space, and relate to the large amount of thermal energy stored in the plume head that could still be affecting the lithosphere and asthenosphere over an area perhaps as large as the Basin and Range (Fig. 23). Thus, the plume mechanism may merit integration with at least two other mechanisms thought important in the deformation of the western cordillera in late Cenozoic time.

First, the Yellowstone mantle plume rose into crust thickened during the Mesozoic and earliest Tertiary orogenies (Sevier and Laramide) and subsequently softened by radiogenic heating of a

thickened sialic crust (Christiansen and Lipman, 1972; Wernicke and others, 1987; Molnar and Chen, 1983).

Second, in Cenozoic time the plate margin southwest of the hotspot track has progressively changed from a subduction zone with possible back-arc spreading to a weak(?) transcurrent fault (Atwater, 1970) over a time span that overlaps the postulated activity (16-0 Ma) of the Yellowstone hotspot.

Thus, basin-range breakup of the continental lithosphere, which is a deformation pattern rather unusual on the earth, may involve at least three complimentary factors: (1) Sevier/Laramide orogenic thickening producing delayed radiogenic heating resulting in thermal softening of the crust, (2) a unconfined plate margin to the west permitting westward extension faster than North American plate motion, and (3) the Yellowstone plume head providing gravitational energy through uplift as well as thermal softening of the mantle lithosphere and lower continental crust. After 10 Ma, outward spreading at the base of the lithosphere of the much thinner chimney phase of the Yellowstone hotspot localized extension in the northeast quadrant of the Basin and Range in the SW moving North American plate.

Rise of a mantle plume would exert body forces consistent with westward pulling apart of the Basin and Range. Plume material rising away from the earth's spin axis would be accelerated to the higher velocity demanded by the greater spin radius. For asthenospheric positions at the latitude of Yellowstone (about 44° N), plume rise from a spin radius of 4300 to 4400 km would require an eastward increase in spin velocity of 628 km/day or 7.26 m/sec (an increase from 27,018 to 27,646 km/day). At a plume-head rise rate suggested earlier of 0.1 mm/yr, this 100 km rise from a spin radius of 4300 to 4400 km would take 1 M.y. The force needed to accelerate the huge plume-head mass to this higher eastward velocity would have to be exerted through the surrounding upper mantle and lithosphere producing an equal and opposite (westward) against the surrounding mantle/lithosphere, which if weak enough would deform by westward extension. Rise of the chimney phase of the Yellowstone plume would continue to exert westward drag on the mantle and lithosphere.

The high terrain of the western U.S. (largely shown on Fig. 23) can be divided into two neotectonic parts: a western part containing the Basin and Range and an eastern part consisting the Rocky Mountains and High Plains. Kane and Godson (1989, Fig 4) show that both the regional terrain and regional bouguer gravity maps define a this high 1500 to 2000 km across that centers in western Colorado. This high may in part relate to thermal effects associated with (1) heat remaining from the Yellowstone plume head, (2) heat from the chimney phase of the Yellowstone plume, and (3) perhaps other thermal plumes as suggested by Wilson (1990) and Suppe and others (1975).

The western part of this high is largely occupied by Basin and Range where the following (not inclusive) would favor westward extension: (1) a

topographic gradient towards the west, (2) plume material rising near the center of the high would spread outward and westward at the base of the lithosphere, (3) eastward acceleration due to plume rise, and (3) lithospheric softening due to thermal plume heating and previous orogenic thickening.

The Rocky Mountains-High Plains occupy the eastern part of this high where the following (not inclusive) would favor compression or non-extension: (1) plate tectonic motion of the American plate southwestward up the slope of the east side of this high, (2) outward and eastward flow of plume material from the center of this high, and (3) lack of sufficient heating to result in lithospheric softening.

A prominent difficulty relating this high with its extension on west and non-extension on east sides to the postulated Yellowstone thermal plume is that the geometric center of the topographic and gravitational high is in western Colorado (Kane and Godson, 1989). A grouping of plumes of which Yellowstone is the northern one (Wilson, 1990; Suppe and others, 1975), or the plume conduit that descends in the mantle both eastward and southward as favored by angular momentum considerations (see above) would move the center of the the regional high towards western Colorado. For the postulated Raton hotspot track, Lipman (1980) shows this volcanic trend has no systematic northeastward volcanic progression and concludes that the Raton volcanic alignment is more likely controlled by a crustal flaw than a hot spot.

CONCLUSIONS

We conclude that the temporal and spatial pattern of volcanism and faulting and altitude changes in the Yellowstone-Snake River Plain region require a large scale disturbance of the lithosphere best explained by a mantle plume, starting with a head phase and followed by a chimney phase.

Temporal and spatial pattern of volcanism and faulting--. After 10 Ma, inception of caldera-forming volcanism migrated ENE at 30 km/m.y, leaving the mountain-bounded SRP floored with a basaltic veneer on thick piles of rhyolite along its trace. Compared to after 10 Ma, migration of the Yellowstone hotspot from 16-10 Ma, (1) produced volcanism in a less systematic pattern, (2) had an apparent rate of 7 cm/yr in a more easterly orientation, (3) had a loci of volcanic eruptions that were more dispersed from the axis of migration, (4) left no trench-like analogue to the eastern SRP, and (5) was initially accompanied by extensive north-south rifts and contemporaneous flood basalts.

Neotectonic faulting in the eastern SRP region define four belts in a nested V-shaped pattern about the post-10-Ma, hotspot track.

1. Belt II has been the most active belt in Quaternary time. Faults in this belt have had at least one offset since 15 ka and range fronts are steep and >700 m high. From its convergence on

- Yellowstone, Belt II flairs outward to the southwest about the hotspot track (eastern SRP).
2. Belt I contains new small escarpments and reactivated faults. It occurs outside Belt II and appears to be waxing in activity.
 3. Belt III occurs inside Belt II. Compared to faults in Belt II, those in Belt III have been less recently active, and are associated with more muted, somewhat lower escarpments. Activity on these faults appears to be waning.
 4. The spatial pattern of Belts I, II, and III indicates a northeast-moving cycle of waxing, culminating, and waning fault activity, respectively, that accompanies the northeast migration of the Yellowstone hotspot. The pattern of these belts is arrayed like parts of a large wave: the frontal part of this wave is represented by waxing rates of faulting, the crestal part by the highest rates, and the backslope part by waning rates.
 5. Belt IV contains quiescent late Tertiary major range-front faults and occurs only on the south side of the SRP. In this belt, the timing of faulting correlates well with the time of passage of the Yellowstone hotspot along the SRP. Southwestward from Yellowstone, the ages of major range-front faulting at Belt II rates (or other deformation are as follows): (1) Teton fault, <6-0 Ma; (2) Grand Valley fault, 4.4-2 Ma; (3) Blackfoot Range-front fault, 5.9-4.7 Ma; (4) Portneuf Range-front fault, 7-6.7 Ma; (5) Rockland Valley fault, 10->8 Ma; (6) Sublett Range folding, >10 Ma; (7) Raft River valley detachment faulting, 10-8(?) Ma. This age progression increases but becomes less systematic to the southwest.
 6. The belts of faulting flair more on the southern than western side of the SRP. This asymmetry is due to the presence of Belt IV only on the south side of the eastern SRP.

Altitude changes--. Another type of deformation that may mark movement of the Yellowstone hotspot is change in altitude. The pattern is similar to that for Quaternary faulting but includes a large upland area ahead of the hotspot track. Several indicators appear to define an outward moving, wave-like pattern, although each of the individual components suggesting altitude changes are subject to alternate interpretations. Uplift appears to be occurring on the leading slope of the wave and subsidence on the trailing slope marginal to the SRP. Indicators of regional uplift and subsidence include the following:

1. An area of high terrain defines the Yellowstone crescent of high terrain 350 km across at the position of Yellowstone; the arms of the crescent extend from the apex more than 400 km to the south and to the west. The crests of these arms parallel the neotectonic fault belts, although the southern crest is more outside the fault belts than the western crest.

2. From Yellowstone southwestward, the altitude of the SRP decreases. Perpendicular to the axis, the ranges adjacent to the SRP are lower than ranges farther from the SRP.
3. The western arm of the Yellowstone crescent coincides with three domes of historic uplift, rising at several mm/yr, as well as the axis connecting the modern drainage divides. A 2-Ma ignimbrite also has been uplifted along the western arm and locally along the southern arm of the crest.
4. High, steep, deeply dissected mountains formed of readily erodible rocks within the Yellowstone crescent indicate neotectonic uplift. Such mountains include the Absaroka Range, the mountains of southern Yellowstone and the Bridger-Teton Wilderness area, the Mt. Leidy-northern Wind River highlands, the Gallatin Range, parts of the Madison Range, and the Centennial Range. This general pattern is complicated by mountains in the crescent, formed of resistant rocks, that were uplifted in Laramide time (about 100-50 Ma).
5. Departures from typical ratios for the length of glaciers during the last (Pinedale, Pd) compared to next to last (Bull Lake, BL) glaciation suggest uplift on the leading margin of the Yellowstone crescent and subsidence on the trailing margin. High Pd/BL ratios are common on the outer part of the Yellowstone crescent and suggest an uplift rate of perhaps .1-.4 mm/yr. Low Pd/BL ratios in the western part of the Yellowstone ice mass in the cusp of the trailing edge of the crescent suggest subsidence perhaps more than .1-.4 mm/yr.
6. Stream terraces are common on the outer, leading margin of the Yellowstone crescent, suggesting uplift. Terraces are much less well developed on the trailing edge of the crescent and on the SRP, and suggest subsidence and also tilting against the direction of flow.
7. Near the northeast margin of the Yellowstone crescent, migration of streams by both capture and by unidirectional slip-off has generally been away from Yellowstone in the direction of the outer slope of the crescent.
8. In the Bighorn Basin, tilting away from Yellowstone is suggested both by the upstream divergence of terraces of streams flowing away from Yellowstone and by the upstream convergence of terraces of streams flowing towards Yellowstone.
9. Near the Bighorn Basin, inflection points in stream profiles have migrated away from Yellowstone as shown by the downstream migration of the convergence and divergence point for pairs of terrace profiles along Rock Creek and perhaps the Bighorn River northeast of the Bighorn Mountains.

Regional late Cenozoic geologic effects require large-scale disturbance of the lithosphere--. The following

large-scale late Cenozoic geologic effects cover distances many times the thickness of the lithosphere and require a sub-lithospheric thermal source.

1. The hotspot track formed from 16-0 Ma is 700 km long whereas that from 10-0 Ma is 300 km long.
2. For Belts I and II, the distance from the western belt of faulting to the southern belt of faulting ranges from less than 100 km across Yellowstone to more than 400 km across the eastern SRP at the site of the 10.3-Ma Picabo volcanic field.
3. The Yellowstone crescent of high terrain is about 350 km across near Yellowstone; each arm of the crescent is more than 400 km long.
4. The present stress pattern indicates extension generally subparallel to and nearly always within 45° of the WSW trend of the SRP-YP province. Such a stress pattern is not consistent with either rifting parallel to the eastern SRP-YP province or right-lateral transform shear across the SRP-YP province. A crustal flaw origin for the SRP-YP province has the following problems: offset across the SRP is not required by structural or stratigraphic information and the most pronounced crustal flaws are located north or south of the SRP-YP trend, rather than down its axis.

Thermal processes are the only reasonable explanations for the late Cenozoic volcanic, faulting, and uplift/subsidence activity. We consider that the large scale of such activity is most reasonably explained by transport of heat by outward flow of asthenosphere beneath the lithosphere. The several-million-year time-scales involved are not adequate for lateral heat transport within the lithosphere over such distances. A deep-seated mantle plume best explains all these observations. A plume of hotter asthenosphere mushrooming out at the base of the lithosphere could intrude and heat the mantle lithosphere thereby (1) weakening of the mantle lithosphere (where most lithospheric strength resides) and (2) convert dense mantle lithosphere to lighter asthenosphere, resulting in isostatic uplift. Any heating and softening of the crust (upper 40 km of the lithosphere) probably is accomplished largely by upward transport of heat by magma.

We suggest that such thermal effects have localized the observed neotectonic extension pattern for the northwest quadrant of the Basin and Range. Although this explanation seems to suggest that extension relates to a separate process, we point out that the origin of Basin and Range activity has three strong ties with the postulated head phase of the Yellowstone hotspot: (1) the Basin and Range province is centered on the general area of the hotspot head, (2) Basin and Range activity started at about 16 Ma, the same age as rhyolitic volcanism we associate with the plume head, and (3) rifting and associated volcanism we attribute to the plume head extend over a distance of 1100 km, quite similar to the dimensions of the Basin and Range. Thus, we find no way to

clearly distinguish between formation of the Basin and Range from the plume-head origin of the Yellowstone hotspot affecting a large area near the common boundary of Nevada, Idaho, and Oregon.

In conclusion, we recognize that much more information is needed to convincingly demonstrate the histories of volcanism, faulting, and uplift/subsidence outlined in this paper. The region within 500 km of Yellowstone is a good candidate for studies of the effects of an inferred mantle plume on the lithosphere. The space/time history of volcanism, faulting, and uplift/subsidence presented here can be readily tested. We have a model which can be evaluated in many ways and which has important implications for the lithospheric responses to a deep-seated mantle thermal plume and as well as for the plume itself.

REFERENCES CITED

- Ach, J.A., Plouff, D., and R.L. Turner, 1987, Mineral Resources of the East Fork High Rock Canyon Wilderness Study Area, Washoe and Humboldt Counties, Nevada: U.S. Geological Survey Bulletin 1707B, p. B1-B14.
- Agard, S.S., 1989, Map showing Quaternary and late Tertiary terraces of the lower Bighorn River, Montana: U.S. Geological Survey Miscellaneous Field Studies Map MF-2094, scale 1:100,000.
- Almendinger, R.W., 1982, Sequence of late Cenozoic deformation in the Blackfoot Mountains, southeastern Idaho, in Bonnichsen, Bill, and Breckenridge, R.M., eds., *Cenozoic Geology of Idaho*: Idaho Bureau of Mines and Geology, Bulletin 26, p. 505-516.
- Alt, D., Sears, J.M., and Hyndman, D.W., 1988, Terrestrial maria: the origins of large basalt plateaus, hotspot tracks and spreading ridges: *Journal of Geology*, v. 96, n. 6, p. 647-662.
- Alt, David, Hyndman, D.W., and Sears, J.W., 1990, Impact origin of late Miocene volcanism, Pacific Northwest: *Geological Society of America Abstracts with Programs*, v. 22, No. 3, p. 2
- Anders, M.H., 1990, Late Cenozoic evolution of Grand and Swan Valleys, Idaho, in Shelia Roberts, editor, *Geologic Field Tours of Western Wyoming and parts of adjacent Idaho, Montana, and Utah*: Geological Survey of Wyoming Public Information Circular No. 29, p. 15-25.
- Anders, M.H., and Geissman, J.W., 1983, Late Cenozoic structural evolution of Swan Valley, Idaho: *EOS (Transactions of the American Geophysical Union)*, v. 64, no 45, p. 625.
- Anders, M.H., Geissman, J.W., Piety, L.A., and Sullivan, J.T., 1989, Parabolic distribution of circum-eastern Snake River Plain seismicity and latest Quaternary faulting: migratory pattern and association with the Yellowstone hot spot: *Journal of Geophysical Research*, v. 94, n. B2, 1589-1621.
- Anders, M.H., and Piety, L.A., 1988, Late Cenozoic displacement history of the Grand Valley, Snake River, and Star Valley faults, southeastern Idaho: *Geological Society of America Abstracts with Programs*, v. 20, no. 6, p. 404.
- Anderson, D.L., 1981, Hotspots, basalts, and the evolution of the mantle: *Science*, v. 213, p. 82-88.
- Andrews, D.A., Pierce, W.G., Eargle, D.H., 1947, Geologic map of the Bighorn Basin, Wyoming and Montana, showing terrace deposits and physiographic features: U.S. Geological Survey Oil and Gas Investigations, Preliminary Map 71.
- Armstrong, R.L., 1975, The geochronometry of Idaho: *Isochron/West*, n. 14, 50 p.
- Armstrong, R.L., Leeman, W.P., and Malde, H.E. 1975, K-Ar dating, Quaternary and Neogene volcanic rocks of the Snake River Plain, Idaho: *America Journal of Science*, v. 275, p. 255-251.
- Armstrong, R.L., Taubeneck, W.H., and Hales, P.O., 1977, Rb-Sr and K-Ar geochronometry of Mesozoic granitic rocks and their Sr isotopic composition, Oregon, Washington, and Idaho: *Geological Society of America Bulletin*, v. 88, p. 397-411.
- Armstrong, R.L., Harakal, J.E., and Neill, W.M., 1980, K-Ar dating of Snake River Plain (Idaho) volcanics rocks—new results: *Isochron/West*, no. 27, p. 5-10.
- Atwater, Tanya, 1970, Implications of plate tectonics for the Cenozoic tectonic evolution of western North America: *Geological Society of America Bulletin*, v. 81, p. 3513-3536.
- Baksi, A.J., 1990, Timing and duration of Mesozoic-Tertiary flood-basalt volcanism: *EOS*, v. 71, No. 49, p. 1835-6.
- Barnosky, A.D., 1984, The Coulter Formation: evidence for Miocene volcanism in Jackson Hole, Teton County, Wyoming: *Earth Science Bulletin*, Wyoming Geological Association, v. 17, p. 49-97.
- Barnosky, A.D., and Labar, W.J., 1989, Mid-Miocene (Barstovian) environmental and tectonic setting near Yellowstone Park, Wyoming and Montana: *Geological Society of America Bulletin*, v. 101, p. 1448-1456.
- Barrientos, S.E., Stein, R.S., and Ward, S.N., 1987, Comparison of the 1959 Hebgen Lake, Montana and the 1983 Borah Peak, Idaho, earthquakes from geodetic observations: *Bulletin of the Seismological Society of America*, v. 77, p. 784-808.
- Bercovici, D., Schubert, G., and Glatzmaier, G.A., 1989, Three-dimensional spherical models of convection in the Earth's mantle: *Science*, V. 244, p. 950-955.
- Blackstone, D.L., Jr., 1966, Pliocene volcanism, southern Absaroka Mountains, Wyoming: University of Wyoming, *Contributions to Geology*, v. 5, p. 21-30.
- Blackwell, D.D., 1989, Regional implications of heat flow of the Snake River Plain, northwestern United States: *Tectonophysics*, v. 164, p. 323-343.
- Blakely, R.J., 1988, Curie temperature isotherm analysis and tectonic implications of aeromagnetic data from Nevada: *Journal of Geophysical Research*, v. 93, p. 11817-11832.
- Blakely, R.J., Jachens, R.C., and McKee, E.H., 1989, The Northern Nevada Rift: a 500-km-long zone that resisted subsequent deformation: *EOS*, v. 70, no. 43, p. 1336.
- Bohannon, R.G., Naeser, C.W., Schmidt, D.L., and Zimmermann, R.A., 1989, The timing of uplift, volcanism, and rifting peripheral to the Red Sea: a case for passive rifting?: *Journal of Geophysical Research*, v. 94, p. 1683-1701.
- Bohor, B.F., and Seitz, Russell, 1990 Cuban K-T catastrophe: *Nature*, v. 344, April 12, p. 593
- Bond, J.G., 1978, Geologic Map of Idaho: Idaho Department of Lands, Bureau of Mines and Geology, Moscow, Idaho, Scale 1:500,000.
- Bonnichsen, Bill, 1982, The Bruneau-Jarbridge eruptive center, southwestern Idaho, in Bonnichsen, Bill, and Breckenridge, R.M., eds., *Cenozoic Geology of Idaho*: Idaho Bureau of Mines and Geology, Bulletin 26, p. 237-254.
- Bonnichsen, Bill, and Kauffman, D.F., 1987, Physical features of rhyolite lava flows in the Snake River Plain volcanic province, southwestern Idaho: *Geological Society of America Special Paper* 212, p. 119-145.
- Braille, L.W., Smith, R.B., Anson, J., Baker, R., Sparlin, M.A., Prodehl, C., Schilly, M.M., Healy, J.H., Mueller, S., and Oisen, K.H., 1982, The Yellowstone-Snake River Plain seismic profiling experiment: crustal structure of the eastern

Snake River Plain: *Journal of Geophysical Research*, v. 87, No. B4, p. 2597-2609.

- Breckenridge, R.M., 1975, Quaternary geology of the Wood River area, Wyoming: Wyoming Geological Association, Guidebook, 27th Annual Field Conference, p. 45-__
- Bright, R.C., 1967, Late Pleistocene stratigraphy in Thatcher Basin, southeastern Idaho: Tebiwa, *The Journal of the Idaho State University Museum*, v. 10, No 1, p. 1-7.
- Brott, C.A., Blackwell, D.D., and Ziagos, J.P. 1981, Thermal and tectonic implications of heat flow in the eastern Snake River Plain, Idaho: *Journal of Geophysical Research*, v. 86, No. B12, p. 11,709-11,734.
- Burbank, D.W., and Barnosky, A.D., 1990, The magnetostratigraphy of Barstovian mammals in southwestern Montana and implications for the initiation of Neogene crustal extension in the northern Rocky Mountains: *Geological Society of America Bulletin*, p. 1093-1104.
- Carter, B.J., Ward, P.A. III, and Shannon, J.T., 1990, Soil and geomorphic evolution within the Rolling Red Plains using Pleistocene volcanic ash deposits: *Geomorphology*, v. 3, p. 471-488.
- Carlson, R.W., and Hart, W.K., 1986, Crustal genesis on the Oregon Plateau: *Journal of Geophysical Research*, v. 92, p. 6191-6206.
- Carlson, R.W. and Hart, W.K., 1988, Flood basalt volcanism in the northwestern United States, in Macdougall, J.D., ed., *Continental Flood Basalts*, Kluwer Academic Publishers, Dordrecht, The Netherlands, p. 35-61.
- Christiansen, R.L., 1982, Late Cenozoic volcanism of the Island Park area, eastern Idaho in Bonnicksen, Bill and Breckenridge, R.M., eds., *Cenozoic Geology of Idaho*: Idaho Bureau of Mines and Geology, Bulletin 26, p. 345-368.
- Christiansen, R.L., 1984, Yellowstone magmatic evolution; Its bearing on understanding large-volume explosive volcanism, in *Explosive volcanism: inception, evolution, and hazards*, National Academy Press, Studies in Geophysics, p. 84-95.
- Christiansen, R.L., and Blank, H.R., 1972, Volcanic stratigraphy of the Quaternary rhyolite plateau in Yellowstone National Park: U.S. Geological Survey Professional Paper 729B, 18 p.
- Christiansen, R.L., and Lipman, P.W., 1972, Cenozoic volcanism and plate-tectonic evolution of the Western United States. II. Late Cenozoic: *Philosophical Transactions of the Royal Society of London*, v., 271, p. 249-284.
- Christiansen, R.L., and Love, J.D., 1978, Connant Creek Tuff, U.S. Geological Survey Bulletin 1435C, 9 p.
- Christiansen, R.L., and McKee, E.H., 1978, Late Cenozoic volcanic and tectonic evolution of the Great Basin and Columbia intermountain regions: *Geological Society of America Memoir* 152, p. 283-311.
- Clawson, S.R., Smith, R.B., and Benz, H.M., 1989, P-Wave attenuation of the Yellowstone caldera from three-dimensional inversion of spectral decay using explosion seismic data: *Journal of Geophysical Research*, v. 94, No. B6, p. 7205-7222.
- Colman, S.M., and Pierce, K.L., 1981, Weathering rinds on andesitic and basaltic stones as a Quaternary age indicator, western United States: U.S. Geological Survey Professional Paper 1210, 56 p.
- Colman, S.M., and Pierce, K.L., 1986, The glacial record near McCall, Idaho—Weathering rinds, soil development, morphology, and other relative-age criteria: *Quaternary Research*, v. 25, p. 25-42.
- Courtilot, V., Besse, J., Vandamme, D., Montigny, R., Jaeger, J.J., and Cappetta, H., 1986, Deccan flood basalts at the Cretaceous/Tertiary boundary?: *Earth and Planetary Sciences Letters*, v. 80, p. 361-374.
- Courtney, R.C. and White, R.S., 1986, Anomalous heat flow and geoid across the Cape Verde Rise: evidence for dynamic support from a thermal plume in the mantle: *Geophysical Journal of the Royal Astronomical Society*, v. 87, p. 815-867.
- Covington, H.R., 1983, Structural evolution of the Raft River basin, Idaho: *Geological Society of America Memoir* 157, p. 229-237.
- Crone, A.J., Machette, M.N., Bonilla, M.G., Leinkaemper, J.J., Pierce, K.L., Scott, W.E., and Bucknam, R.C., 1987, Surface faulting accompanying the Borah Peak earthquake, and segmentation of the Lost River fault, central Idaho: *Seismological Society of America Bulletin*, v. 77, no. 2, p. 739-770.
- Crough, S.T., 1978, Thermal origin of mid-plate hot-spot swells: *Geophysical Journal of the Royal Astronomical Society*, v. 55, p. 451-469.
- Crough, S.T., 1979, Hot spot epeirogeny: *Tectonophysics*, v. 61, p. 321-333.
- Crough, S.T., 1983, Hot spot swells: *Annual Reviews of the Earth and Planetary Sciences*, v. 11, p. 165-193.
- Doser, D.I., 1985, Source parameters and faulting processes of the 1959 Hebgen Lake, Montana, earthquake sequence: *Journal of Geophysical Research*, v. 90, p. 4537-4556.
- Doser, D.I., and Smith, R.B., 1983, Seismicity of the Teton-southern Yellowstone region, Wyoming: *Bulletin of the Seismological Society of America*, v. 73, no. 5, p. 1369-1394.
- Duncan, R.A., 1982, A captured island chain in the Coast Range of Oregon and Washington: *Journal of Geophysical Research*, v. 87, p. 10827-10837.
- Duncan, R.A., 1984, Age progressive volcanism in the New England seamounts and the opening of the central Atlantic Ocean: *Journal of Geophysical Research*, v. 89, p. 9980-9990
- Eaton, G.P., Christiansen, R.L., Iyer, H.M., Pitt, A.M., Mabey, D.R., Blank, Jr., H.R., Zietz, Isidore, and Gettings, M.E., 1975, Magma beneath Yellowstone National Park: *Science*, v. 188, p. 787-796.
- Ekren, E.B., D.H. McIntyre, and E.H. Bennett, 1984, High-temperature, large-volume, lavalike ash-flow tuffs without calderas in southwestern Idaho: U.S. Geological Survey Professional Paper 1272, 76 p.
- Elison, M.W., Speed, R.C., and Kistler, R.W., in press, Geologic and isotopic constraints on the crustal structure of the northern Great Basin: *Geological Society of America Bulletin*.
- Erslev, E.A., 1982, The Madison mylonite zone: a major shear zone in the Archean Basement of southwestern Montana: Wyoming Geological Association, Thirty-third Annual Conference Guidebook, p. 213-221.
- Erslev, E.A., and Sutter, John, in press, Evidence for Proterozoic mylonitization in the northwestern Wyoming Province: *Geological Society of America Bulletin*.
- Evans, J.R., 1982, Compressional wave velocity structure of the upper 350 km under the eastern Snake River Plain near Rexburg, Idaho: *Journal of Geophysical Research*, v. 87, No. B4, p. 2654-2570.
- Evenson, E.B., Cotter, J.F.P., and Clinch, J.M., 1982, Glaciation of the Pioneer Mountains; a proposed model for Idaho, in Bonnicksen, Bill and Breckenridge, R.M., eds., *Cenozoic Geology of Idaho*, Idaho Bureau of Mines and Geology, Bulletin 26, p. 653-665.
- Evernden, J.F., Savage, D.E., Curtis, G.H., and James, G. T., 1964, Potassium-argon dates and the Cenozoic mammalian chronology of North America: *American Journal of Science*, v. 265, p. 257-291.

- Fields, R.W., Rasmussen, D.L., Tabrum, A.R., and Nichol, R., 1985, Cenozoic rocks of the intermontane basins of western Montana and eastern Idaho, in Flores R.M., and Kaplan, S.S., editors, *Cenozoic Paleogeography of the West-Central United States: Society of Economic Paleontologists and Mineralogists, The Rocky Mountain Section, Denver Co.*, p. 9-36.
- Fisher, F.S., and Ketner, K.B., 1968, Late Tertiary syncline in the southern Absaroka Mountains, Wyoming: U.S. Geological Survey Professional Paper 600B, p. B144-B147
- Fisher, F.S., McIntyre, D.H., and Johnson, K.M., 1983, Geologic Map of the Challis 1°x2° Quadrangle, Idaho: U.S. Geological Survey Open File Report 83-523.
- Fritz, W.J., and Sears, J.W., 1989, Late Cenozoic crustal deformation of SW Montana in the wake of the passing Yellowstone hot spot: evidence from an ancient river valley: *Geological Society of America Abstracts with Programs*, v. 21, n. 6, p. A90.
- Fryxell, F.M., 1930, Glacial features of Jackson Hole, Wyoming: Augustana Library Publications, No. 13 (Ira Oliver Nothstein, ed.), Augustana College and Theological Seminary, Rock Island, IL, 129 p.
- Gibbons, A.B., and Dickey, D.D., 1983, Quaternary faults in Lincoln and Uinta Counties, Wyoming and Rich County, Utah: U.S. Geological Survey Open-File Report 83-288.
- Gilbert, J.D., Ostenaar, Dean, and Wood, C., 1983, Seismotectonic study, Jackson Lake Dam and Reservoir, Minidoka Project, Idaho-Wyoming: U.S. Bureau of Reclamation Seismotectonic Report 83-8, 122 p.
- Godson, R.H., 1981, Digital terrain map of the United States: U.S. Geological Survey Miscellaneous Geologic Investigations Map I-____, scale 1:7,500,000
- Greene, R.C. and Plouff, Donald, 1981, Location of a caldera source for the Soldier Meadow Tuff, northwestern Nevada, indicated by gravity and aeromagnetic data: Summary: *Geological Society of America Bulletin, Part I*, v. 92, p. 4-6.
- Greensfelder, R.W., 1976, Maximum probable earthquake acceleration on bedrock in the State of Idaho: Idaho Department of Transportation, Research Project No 79, Boise, Idaho, 69 p.
- Griffiths, R.W. and Richards, M.A., 1989, The adjustment of mantle plumes to changes in plate motion: *Geophysical Research Letters*, v. 16, p. 437-440.
- Hall, R.D., and Michaud, Denis, 1988, The use of hornblende etching, clast weathering, and soils to date alpine glacial and periglacial deposits: A study from southwestern Montana: *Geological Society of America Bulletin*, v. 100, p. 458-467.
- Haller, K.M., 1988, Segmentation of the Lemhi and Beaverhead faults, east-central Idaho, and Red rock fault, southwest Montana, during the late Quaternary: Boulder, University of Colorado, M.S. thesis, 141 p.
- Hamilton, L.J., and Paulson, Q.F., 1968, Geology and ground-water resources of the lower Bighorn valley, Montana: U.S. Geological Survey Water-Supply Paper 1876, 39 p.
- Hamilton, Warren, 1987, Plate-tectonic evolution of the Western U.S.A.: *Episodes*, v. 10, p. 271-276.
- Hamilton, Warren, 1989, Crustal geologic processes of the United States, in Pakiser, L.C., and Mooney, W.D., *Geophysical framework of the continental United States: Geological Society of America Memoir 172*, p. 743-781.
- Hansen, W.R., 1985, Drainage development of the Green River Basin in southwestern Wyoming and its bearing on fish biogeography, neotectonics, and paleoclimates: *The Mountain Geologist*, v. 22, p. 192-204.
- Harrison, R.E., 1969, Shaded Relief map of the United States, Albers equal area projection, U.S. Geological Survey National Atlas, sheet n. 56.
- Helz, R.T., 1973, Phase relations of basalts in their melting range at PH₂O = 5kb as a function of oxygen fugacity. Part I. mafic phases: *Journal of Petrology*, v. 14, 249-302.
- Hildebrand, A.R., and Boynton, W.V., 1990, Proximal Cretaceous-Tertiary boundary impact deposits in the Caribbean: *Science*, v. 24, p. 843-846
- Hildreth, W., 1981, Gradients in silicic magma chambers: Implications for lithospheric magmatism: *Journal of Geophysical Research*, v. 86, p.10153-10192.
- Hill, D.P., 1972, Crustal and upper-mantle structure of the Columbia Plateau from long-range seismic-refraction measurements: *Geological Society of America Bulletin*, v. 83, p. 1639-1648.
- Hooper, P.R., 1988, The Columbia River Basalt, in Macdougall, J.D. (ed.), *Continental Flood Basalts: Dordrecht, The Netherlands, Kluwer Academic Publishers*, p.1-33.
- Houseman, G. and England, P., 1986, A dynamical model of lithospheric extension and sedimentary basins: *Journal of Geophysical Research*, v. 91, p, 719-729.
- Ito, E., and Takahashi, E.J., 1989, Postspinel transformations in the system Mg₂SiO₄-Fe₂SiO₄ and some geophysical implications: *Journal of Geophysical Research*, v. 94, p. 10637-10646
- Iyer, H.M., Evans, J.R., Zant, G, Stewart, R.M., Coakley, J.M, Roloff, J.N., 1981, A deep low-velocity body under the Yellowstone caldera, Wyoming: delineation using teleseismic P-wave residuals and tectonic interpretation- Summary: *Geological Society of America Bulletin, Part I*, v. 92, p. 792-798.
- Izett, G.A., 1990, Cretaceous-Tertiary boundary interval, Raton Basin, Colorado and New Mexico, and its content of shock-metamorphosed minerals: Evidence relevant to the K/T boundary impact-extinction theory: *Geological Society of America Special Paper 249*, 100 p.
- Izett, G.A. and Wilcox, R.E. 1982, Map showing localities and inferred distributions of the Huckleberry Ridge, Mesa Falls, and Lava Creek ash beds (Pearlette Family ash beds) of Pliocene and Pleistocene age in the western United States and southern Canada: U.S. Geological Survey Miscellaneous Investigations Map I-1325, scale 1:4,000,000.
- Kane, M.F., and Godson, R.H., 1989: A crust/mantle structural framework of the conterminous United States based on gravity and magnetic trends in Pakiser, L.C., and Mooney, W.D., *Geophysical framework of the continental United States, Geological Society of America Memoir 172*, p. 383-403.
- Kellogg, in press, The Putnam Thrust, Northern Portneuf Range, Southeastern Idaho: structural complexities caused by upper-plate imbricate thrusting and Neogene block rotation; *Geological Society of America Memoir* ____, p. ____ - ____
- Kellogg, K.S., and Marvin, R.F., 1988, New potassium-argon ages, geochemistry, and tectonic setting of upper Cenozoic volcanic rocks near Blackfoot, Idaho: *U.S. Geological Survey Bulletin* 1086, 19 p.
- Kellogg, K.S., Pierce, K.L., Mehnert, H.H., Hackett, W.R., Rodgers, D.W., and Hladky, F.R., 1989, New ages on biotite-bearing tuffs of the eastern Snake River Plain, Idaho: Stratigraphic and mantle-plume implications: *Geological Society of America Abstracts with Programs*, v. 21, no. 5, p. 101.
- Kelson, K.I., and Swan, F.H., 1988, Recurrent Late Pleistocene to Holocene(?) surface faulting on the Stagner Creek Segment of the Cedar ridge Fault, Central Wyoming; *Geological Society of America, Abstracts with Programs*, v. 20, p. 424.

- Kennedy, B.M., Reynolds, J.H., Smith, S.P., and Truesdell, A.H., 1987, Helium isotopes: Lower Geyser Basin, Yellowstone National Park: *Journal of Geophysical Research*, v. 92, p. 12,477-12,489.
- Ketner, K.B., Keefer, W.R., Fisher, F.S., Smith D.L., and Raabe, R.G., 1966, Mineral resources of the Stratified Primitive Area, Wyoming: U.S. Geological Survey Bulletin 1230-E, 56 p.
- Kistler, R.W., 1983, Isotope geochemistry of plutons in the northern Great Basin: Geothermal Resources Council, Special Report no. 13, p. 3-8.
- Kistler, R.W., and Peterman, Z.E., 1978, Reconstruction of crustal blocks of California on the basis of initial strontium isotopic compositions of Mesozoic granitic rocks: U.S. Geological Survey, Professional Paper 1071, 17 p.
- Kistler, R.W. and Lee, D.E., 1989, Rubidium and strontium isotopic data for a suite of granitoid rocks from the Basin and Range Province, Arizona, California, Nevada, and Utah: U.S. Geological Survey Open-File Report 89-199, 13 pp.
- Kistler, R.W., Ghent, E.D., and O'Neil, J.R., 1981, Petrogenesis of garnet two-mica granites in the Ruby Mountains, Nevada: *Journal of Geophysical Research*, v. 86, p. 10591-10606.
- Kuntz, M.A., in press, An overview of basaltic volcanism of the eastern Snake River Plain: Geological Society of America Memoir.
- Kuntz, M.A., Skipp, B.A., Scott, W.E., and Page, W.R. 1984, Preliminary geologic map of the Idaho National Engineering Laboratory and adjacent areas, Idaho: U.S. Geological Survey Open-File Report 84-281, 23 p., scale 1:100,000.
- Kuntz, M.A., Lefebvre, R.H., Champion, D.E., McBroome, L.A., Mabey, D.R., Stanley, W.D., and Covington, H.R., 1983, Geological and geophysical investigations of the proposed Great Rift Wilderness area, Idaho: U.S. Geological Survey Open-File Report 80-475, 48 p.
- Lageson, D.R., 1987, Laramide controls on the Teton Range, NW Wyoming: Geological Society of America Abstracts with Programs, v. 20, no. 6, p. 426.
- Leeman, W.P., 1989, Origin and Development of the Snake River Plain (SRP) - an Overview in Ruebelman, K.L., ed., Snake River Plain-Yellowstone Volcanic Province: Field Trip Guidebook T305, 28th International Geological Congress, p. 4-13.
- Leeman, W.P., 1982, Development of the Snake River Plain-Yellowstone Plateau province, Idaho and Wyoming: an overview and petrologic model, in Bonnicksen, Bill and Breckenridge, R.M., eds., Cenozoic Geology of Idaho: Idaho Bureau of Mines and Geology, Bulletin 26, p. 155-178.
- Lehman, J.A., Smith, R.B., Schilly, M.M., and Braille, L.W., 1982, Upper crustal structure of the Yellowstone caldera from seismic delay time analyses and gravity correlations: *Journal of Geophysical Research*, v. 87, p. 2813-2730.
- Lipman, P.W., 1980, Cenozoic volcanism in the western United States: Implications for continental tectonics, in Continental Tectonics: National Academy of Sciences, Washington, D.C., p. 161-174.
- Loper, D.E., and Stacey, F.D., 1983, The dynamical and thermal structure of deep mantle plumes: *Physics of the Earth and Planetary Interiors*, v. 33, p. 304-317.
- Love, J.D., 1939, Geology along the southern margin of the Absaroka Range, Wyoming: Geological Society of America Special Paper 20, 137 p.
- Love, J.D., 1961, Reconnaissance study of Quaternary faults in and south of Yellowstone National Park, Wyoming: Geological Society of America Bulletin, v. 72, n. 12, p. 1749-1764.
- Love, J.D., 1977, Summary of upper Cretaceous and Cenozoic stratigraphy, and of tectonic and glacial events in Jackson Hole, northwestern Wyoming: Wyoming Geological Association, Twenty-Ninth Annual Field Conference Guidebook, p. 585-593.
- Love, J.D., and Keefer, W.R., 1975, Geology of sedimentary rocks in southern Yellowstone National Park, Wyoming: U.S. Geological Survey Professional Paper 729-D, 60 p.
- Love, J.D., and Love, J.M., 1982, Road log, Jackson to Dinwoody and return: Wyoming Geological Association, Thirty-fourth Annual Field Conference Guidebook, p. 283-318.
- Love, J.D., and de la Montagne, John, 1956, Pleistocene and recent tilting of Jackson Hole, Teton County, Wyoming: Wyoming Geological Association, 11th Annual Field Conference Guidebook, p. 169-178.
- Love, J.D., Reed, Jr., J.C., and Christiansen, A.C., in press, Geologic Map of Grand Teton National Park, Teton County, Wyoming: U.S. Geological Survey Miscellaneous Geologic Investigations Map I-2031, scale 1:62,500.
- Love, J.D., Simons, F.S., Keefer, W.R., and Harwood, D.S., 1988, Geology in Mineral Resources of the Gros Ventre Wilderness Study Area, Teton and Sublette Counties, Wyoming: U.S. Geological Survey Bulletin, p. 6-20.
- Luedke, R.G., and Smith, R.L., 1981, Map showing distribution and age of late Cenozoic volcanic centers in California and Nevada: U.S. Geological Survey Miscellaneous Geologic Investigations Map I-1091-C.
- Luedke, R.G., and Smith, R.L., 1982, Map showing distribution and age of late Cenozoic volcanic centers in Oregon and Washington: U.S. Geological Survey Miscellaneous Geologic Investigations Map I-1091-D.
- Luedke, R.G., and Smith, R.L., 1983, Map showing distribution and age of late Cenozoic volcanic centers in Idaho, western Montana, west-central south Dakota, and northwestern Wyoming: U.S. Geological Survey Miscellaneous Geologic Investigations Map I-1091-E.
- Lundstrom, S.C., 1986, Soil stratigraphy and scarp morphology studies applied to the Quaternary geology of the southern Madison Valley, Montana: Arcata, California, Humboldt State University, M.S. thesis, 53 p.
- Mabey, D.R., 1982, Geophysics and tectonics of the Snake River Plain, Idaho, in Bonnicksen, Bill and Breckenridge, R.M., eds., Cenozoic Geology of Idaho: Idaho Bureau of Mines and Geology, Bulletin 26, p. 139-153.
- Mabey, D.R., Zietz, I., Eaton, G.P., and Kleinkopf, M.D., 1978, Regional magnetic patterns in part of the Cordillera in the western United States: Geological Society of America Memoir 152, p. 93-109.
- Machette, M.N., Personius, S.F., and Nelson, A.R., 1987, Quaternary geology along the Wasatch Fault zone; segmentation, recent investigations, and preliminary conclusion, in Assessment of regional earthquake hazards and risk along the Wasatch Front, Utah, Gori, P.L. and Hays, W.W. editors: U.S. Geological Survey Open-File Report 87-585 p. A1-A72
- Mackin, J.H., 1937, Erosional history of the Big Horn Basin, Wyoming: Geological Society of America Bulletin, v. 48, p. 813-894.
- MacLeod, N.S., Walker, G.W., and McKee, E.H., 1976, Geothermal significance of eastward increase in age of upper Cenozoic rhyolitic domes in southeastern Oregon in Proceedings of the Second United Nations symposium on the development and use of geothermal resources, v. 1: Washington, D.C., U.S. Government Printing Office, p. 456-474
- Madsen, D.B., and Currey, D.R., 1979, Late Quaternary glacial and vegetation changes, Little Cottonwood area, Wasatch Mountains, Utah: Quaternary Research, v. 12, no. 2, p. 254-270.

- Malde, H.E., 1987, Quaternary faulting near Arco and Howe, Idaho: *Bulletin of the Seismological Society of America*, v. 77, no. 3, p. 847-867.
- Malde, H.E., in press, Quaternary geology and structural history of the Snake River Plain, Idaho and Oregon in R.B. Morrison, ed., *Quaternary nonglacial history of the conterminous U.S.:* Geological Society of America, *The Geology of North America*, v. K-2, Ch. 4.
- Mathiesen, E.L., 1983, Late Quaternary activity of the Madison fault along its 1959 rupture trace, Madison County, Montana: Stanford University, M.S. thesis, 157 p.
- Mayer, Larry, and Schneider, N.P., 1985, Temporal and spatial relations of faulting along the Madison Range fault, Montana—evidence for fault segmentation and its bearing on the kinematics of normal faulting: *Geological Society of America Abstracts with Programs*, v. 17, p. 656.
- McBroome, L.A., 1981, Stratigraphy and origin of Neogene ash-flow tuffs on the north-central margin of the eastern Snake River Plain, Idaho: Boulder, University of Colorado, M.S. thesis, 74 p.
- McCalpin, James, 1987, Quaternary deformation along the East Cache fault, north-central Utah: *Geological Society of America Abstracts with Programs*, v. 19, n. 5, p. 320.
- McCalpin, James, Robison, R.M., and Garr, J.P., 1987, Neotectonics of the Hansel Valley-Pocatello Valley Corridor, northern Utah and southern Idaho, in *Assessment of regional earthquake hazards and risk along the Wasatch Front, Utah*, Gori, P.L. and Hays W.W., eds.: U.S. Geological Survey Open-File Report 87-585, p. G1-G44.
- McCalpin, James, Zhang, Liren, and Khromovskikh, V.S., 1990, Quaternary faulting in the Bear Lake Graben, Idaho and Utah: *Geological Society of America Abstracts with Programs*, v. 22, n. 6, p. 38.
- McCoy, W.D., 1981, Quaternary aminostratigraphy of the Bonneville and Lahontan Basins, western U.S., with paleoclimatic implications: Boulder, University of Colorado, Ph.D. thesis, 603 p.
- McKee, E.H. and Noble, D.C., 1986, Tectonic and magmatic development of the Great Basin of the western United States during late Cenozoic time: *Modern Geology*, v. 10, p. 39-49.
- McKee, E.H., Noble, D.C., and Silberman M.L., 1970, Middle Miocene hiatus in volcanic activity in the Great Basin area of the western United States: *Earth and Planetary Sciences Letters*, v. 8, p. 93-96.
- McKenna, M.C., and Love, J.D., 1972, High-level strata containing Early Miocene mammals on the Bighorn Mountains, Wyoming: *Novitates*, no 2490, 31 p.
- McKenzie, D., and Bickle, M.J., 1988, The volume and composition of melt generated by extension of the lithosphere: *Journal of Petrology*, v. 29, p. 625-679.
- Merrill, R.D., 1973, Geomorphology of terrace remnants of the Greybull River, northwestern Wyoming: Austin, University of Texas, Ph.D. thesis.
- Minor, S.A., Sawatzky, D. and Leszczykowski, A.M., 1986, Mineral Resources of the North Fork Owyhee River Wilderness Study Area, Owyhee County, Idaho: U.S. Geological Survey Bulletin 1719-A, 10 p.
- Minor, S.A., King, H.D. Kulik, D.M., Sawatzky, D. and Capstick, D.O., 1987, Mineral Resources of the Upper Deep Creek Wilderness Study Area, Owyhee County, Idaho: U.S. Geological Survey Bulletin 1719-G, 10 p.
- Minster, J. B., Jordan, T.H., Molnar, P., and E. Haines, E., 1974, Numerical modelling of instantaneous plate tectonics: *Royal Astronomical Society Geophysical Journal*, v. 36, p. 541-576.
- Minster, J.B., and Jordan, T.H., 1978, Present day plate motions: *Journal of Geophysical Research*, v. 83, p. 5331-5354.
- Molnar P., and Chen, W.P., 1983, Focal depths and fault plane solutions of earthquakes under the Tibetan plateau: *Journal of Geophysical Research*, v. 88, p. 1180-1196.
- Montagne, John, and Chadwick, R.A., 1982, Cenozoic history of the Yellowstone Valley south of Livingston Montana: *Field trip Guidebook*, Montana State University, Bozeman, Montana, 67 p.
- Mooney, W.D. and Braille, L.W., 1989, The seismic structure of the continental crust and upper mantle of North America, in Bally, A.W. and Palmer, A.R., eds., *The Geology of North America - An overview:* Geological Society of America, *The Geology of North America*, v. A, p. 39-52.
- Moore, D.W., Oriel, S.S., and Mabey, D.R., 1987, A Neogene(?) gravity-slide block and associated slide phenomena in Swan Valley graben, Wyoming and Idaho: *Geological Society of America, Centennial Field Guide*, v. 2, p. 113-116.
- Morgan, L.A., 1988, Explosive rhyolitic volcanism on the eastern Snake River Plain: Honolulu, University of Hawaii, Ph.D. thesis, 191 p.
- Morgan, L.A., Doherty, D.J., and Bonnicksen, B., 1989, Evolution of the Kilgore caldera: a model for caldera formation on the Snake River Plain-Yellowstone Plateau volcanic province, IAVCEI General Assembly Abstracts, New Mexico Bureau of Mines and Mineral Resources Bulletin 131, p. 195.
- Morgan, L.A. and Bonnicksen, Bill, 1989, Heise volcanic field, in C.E. Chapin and J. Zidek, eds., *Field Excursions to Volcanic Terranes in the western United States, Vol. II: Cascades and Intermountain West:* New Mexico Bureau of Mines and Mineral Resources, *Memoir* 47, p. 153-160.
- Morgan, L.A., Doherty, D.J. and Leeman, W.P., 1984, Ignimbrites of the eastern Snake River Plain: evidence for major caldera forming eruptions: *Journal of Geophysical Research*, v. 89, No. B10, p. 8665-8678.
- Morgan, W.J., 1973, Plate motions and deep mantle convection: *Geological Society of America Memoir* 132, p. 7-22.
- Morgan, W.J., 1981, Hot spot tracks and the opening of the Atlantic and Indian Oceans, in C. Emiliani, ed., *The Sea*, vol. 7: New York, Wiley Interscience, p. 443-487.
- Morris, D.A., Hackett, O.M., Vanlier, K.E., and Moulder, E.A., 1959, Ground-water resources of Riverton irrigation project area, Wyoming: U.S. Geological Survey Water-Supply Paper 1375, 205 p.
- Myers, W.B., and Hamilton, Warren, 1964, Deformation accompanying the Hebgen Lake earthquake of August 17, 1959: U.S. Geological Survey Professional Paper 435, p. 55-98.
- Naeser C.W., Izett, G.A. and Obradovich, J.D., 1980, Fission-track and K-Ar ages of natural glasses: U.S. Geological Survey Bulletin 1489, 31 p.
- Naeser, N.D., 1986, Neogene thermal history of the northern Green River Basin, Wyoming—evidence from fission-track dating in Gautier, D.L., ed., *Roles of Organic Matter in Sediment Diagenesis:* Society of Economic Paleontologists and Mineralogists Special Publication 38, p. 65-72., 1988
- Noble, D.C, McKee, E.H., Smith, J.G. and Korringa, M.K., 1970, Stratigraphy and geochronology of Miocene volcanic rocks in northwestern Nevada: U.S. Geological Survey Professional Paper 700-D, p. D23-D32.
- Okal, E.A., and Batiza, R., 1987, Hot spots: the first 25 years: American Geophysical Union, *Geophysical Monograph* 43, p. 1-11.
- O'Neill, J.M. and Lopez, D.A., 1985, The Great Falls tectonic zone of east-central Idaho and west-central Montana—its character and regional significance: *American Association of Petroleum Geologists Bulletin*, v. 69, no. 3, p. 487-497.

- Oriel, S.S., and Platt, L.A., 1980, Geologic map of the Preston 1 x 2 degree Quadrangle, southeastern Idaho and western Wyoming: U.S. Geological Survey Miscellaneous Investigations Series, Map I-1127.
- Osborne, G.D., 1973, Quaternary geology and geomorphology of the Uinta Basin and the south flank of the Uinta Mountains, Utah: Berkeley, University of California, Ph.D. Dissertation, 266 p.
- Palmquist, R.C., 1983, Terrace chronologies in the Bighorn Basin, Wyoming: Wyoming Geological Association, 34th Annual Field Conference Guidebook, p. 217-231.
- Pankratz, L.W., and Ackerman, H.D., 1982, Structure along the northwest edge of the Snake River Plain interpreted from seismic reflection: *Journal of Geophysical Research*, v. 87, No. B4, p. 2676-2682.
- Pardee, J.T., 1950, Late Cenozoic block faulting in western Montana: *Geological Society of America Bulletin*, v. 61, p. 359-406.
- Perman, R.C., F.H. Swan, and Kelson, K.I., 1988, Assessment of late Quaternary faulting along the south granite Mountains and north Granite Mountains faults of Central Wyoming: *Geological Society of America Abstracts with Programs*, v. 20, p. 462.
- Personius, S.F., 1982, Geologic setting and geomorphic analysis of Quaternary fault scarps along the Deep Creek fault, upper Yellowstone valley, south-central Montana: Bozeman, Montana State University, M.S. thesis, 77 p.
- Pierce, K.L., 1979, History and dynamics of glaciation in the northern Yellowstone National Park area: U.S. Geological Survey Professional Paper 729F, 90 p.
- Pierce, K.L., 1974, Surficial geologic map of the Abiathar Peak and parts of adjacent quadrangles, Yellowstone National Park, Wyoming and Montana: U.S. Geological Survey Map I-646, scale 1: 62,500.
- Pierce, K.L., 1985, Quaternary history of faulting on the Arco segment of the Lost River fault, central Idaho, in Stein, R.S., and Bucknam, R.C., eds., *Proceedings of Workshop XXVIII on the Borah Peak, Idaho, Earthquake*: U.S. Geological Survey Open-file Report 85-290, p. 195-206.
- Pierce, K.L., Obradovich, J.D. and Friedman, I., 1976, Obsidian hydration dating and correlation of Bull Lake and Pinedale glaciations near West Yellowstone Montana: *Geological Society of America Bulletin*, v. 87, p. 703-710.
- Pierce, K.L., and Scott, W.E., 1982, Pleistocene episodes of alluvial-gravel deposition, southeastern Idaho in Bonnicksen, Bill and Breckenridge, R.M., eds., *Cenozoic Geology of Idaho*: Idaho Bureau of Mines and Geology, Bulletin 26, p. 658-702.
- Pierce, K.L., and Scott, W.E., 1986, Migration of faulting along and outward from the track of thermo-volcanic activity in the eastern Snake River Plain region during the last 15 m.y.: *EOS (Transactions of the American Geophysical Union)* v. 67, n. 44, p. 1225.
- Pierce, K.L., Scott, W.E., and Morgan, L.A., 1988, Eastern Snake River Plain neotectonics—faulting in the last 15 Ma migrates along and outward from the Yellowstone "hot spot" track: *Geological Society of America Abstracts with Programs*, v. 20, p. 463.
- Pierce, W.G., 1965, Geologic map of the Deep Lake quadrangle, Park County, Wyoming: U.S. Geological Survey Geologic Quadrangle Map GQ-478, scale 1:62,500.
- Piety, L.A., Wood, C.K., Gilbert, J.D., Sullivan, J.T. and Anders, M.H., 1986, Seismotectonic study for Palisades Dam and Reservoir, Palisades Project: U.S. Bureau of Reclamation Seismotectonic Report 86-3, 198 p.
- Pings, J.C., and Locke, W.W., 1988, A fault scarp across the Yellowstone caldera margin- its morphology and implications: *Geological Society of America, Abstracts with Programs*, v. 20, n. 6, p. 463.
- Pollastro, R.M., and Baker, C.E., 1986, Application of clay mineral, vitrinite reflectance, and fluid inclusion studies to the thermal and burial history of the Pinedale anticline, Green River Basin, Wyoming: *Society of Economic Paleontologists and Mineralogist Special Publication No. 38*, p. 73-83.
- Pollitz, F.F., 1988, Episodic North American and Pacific plate motions: *Tectonics*, v. 7, p. 711-726.
- Porter, S.C., Pierce, K.L., and Hamilton, T.D., 1983, Late Pleistocene glaciation in the Western United States, in H.E. Wright, ed., *Late Quaternary Environments of the United States*: Minneapolis, Minn., University of Minnesota Press, p. 71-111.
- Prostka, H.J., and Embree, G.F., 1978, Geology and geothermal resources of the Rexburg area, eastern Idaho: U.S. Geological Survey Open-File Report 78-1009, 15 p.
- Raisz, Erwin, 1957, Landforms of the United States, available from Kate Raisz, Raisz Landform Map, P.O. Box 2254, Jamaica Plains, MA, 02130.
- Reheis, M.C., 1985, Evidence for Quaternary tectonism in the northern Bighorn Basin, Wyoming and Montana: *Geology*, v. 13, p. 364-367.
- Reheis, M.C., 1987, Soils in granitic alluvium in humid and semiarid climates along Rock Creek, Carbon County, Montana: U.S. Geological Survey Bulletin 1590D, 71 p.
- Reheis, M.C., and Agard, S.S., 1984, Timing of stream captures in the Big Horn Basin, WY and MT, determined from ash-dated gravels: *Geological Society of America Abstracts with Programs*, v. 16, n. 6, p. 632.
- Reheis, M.C., Palmquist, R.C., Agard, S.S., Jaworowski, Cheryl, Mears, B.M., Jr., Madole, R.L., Nelson, A.R., and Osborne, Gerald, in press, Non-glacial Quaternary history of some Rocky Mountain basins, in Morrison, R.B., ed., *Quaternary non-glacial history of the United States*: Geological Society of America, *The Geology of North America*, v. K-2.
- Reilinger, Robert, 1985, Vertical movements associated with the 1959, M=7.1 Hebgen Lake Montana earthquake, in Stein, R.S. and Bucknam, R.C., editors, *Proceedings of Workshop XXVIII on the Borah Peak, Idaho, Earthquake*: U.S. Geological Survey Open-file Report 85-290, p. 519-530.
- Reilinger, R.E., Citron, G.P., and Brown, L.D., 1977, Recent vertical crustal movements from precise leveling data in southwestern Montana, western Yellowstone National Park and the Snake River Plain: *Journal of Geophysical Research*, v. 82, p. 5349-5359.
- Reynolds, M.W., 1979, Character and extent of basin-range faulting, western Montana and east-central Idaho, in Newman, G.W., and Goode, H.D., eds., *1979 Basin and Range Symposium*, Rocky Mountain Association of Geologists and Utah Geological Association Guidebook, p. 185-193.
- Richards, M.A., Duncan, R.A., and Courtillot, V.E., 1989, Flood basalts and hot spot tracks: Plume heads and tails: *Science*, v. 246, p. 103-107.
- Richards, M.A., Hager, B.H., and Sleep, N.H., 1988, Dynamically supported geoid highs over hot spots: observation and theory: *Journal of Geophysical Research*, v. 93, p. 7690-7708.
- Richards, P.W., and Rogers, C.P., 1951, Geology of the Hardin area, Big Horn and Yellowstone Counties, Montana: U.S. Geological Survey Oil and Gas Investigations Map OM-111.
- Richmond, G.M., 1972, Appraisal of the future climate of the Holocene in the Rocky Mountains: *Quaternary Research*, v. 2, p. 315-322.
- Richmond, G.M., 1973, Geologic map of the Fremont Lake South quadrangle, Sublette County, Wyoming: U.S. Geological Survey Geologic Quadrangle Map GQ-1138, scale 1:24,000.

- Richmond, G.M., 1974, Surficial geology of the Frank Island quadrangle, Yellowstone National Park, Wyoming: U.S. Geological Survey Miscellaneous Geologic Investigations Map I-652, scale 1:62,500.
- Richmond, G.M., 1976, Pleistocene stratigraphy and chronology in the mountains of western Wyoming, in W.C. Mahaney, editor, Quaternary stratigraphy of North America: Stroudsburg, Pa., Dowden, Hutchinson, and Ross, Inc., p. 353-379.
- Richmond, G.M., 1983, Modification of Glacial sequence along Big Sandy River, southern Wind River Range, Wyoming: Geological Society of America Abstracts with Programs, v. 15, No. 5, p. 431.
- Richmond, G.M., 1986, Stratigraphy and correlation of glacial deposits of the Rocky Mountains, the Colorado Plateau and the ranges of the Great Basin: Quaternary Science Reviews, v. 5, p. 99-127.
- Richmond, G.M., and Murphy, J.F., 1965, Geologic map of the Bull Lake East quadrangle, Fremont County, Wyoming: U.S. Geological Survey Geologic Quadrangle Map GQ-431, scale 1:24,000.
- Ringwood, A.E., 1982, Phase transformations and differentiation in subducted lithosphere: implications for mantle dynamics, basalt petrogenesis, and crustal evolution: *Journal of Geology*, v. 90, n. 6, p. 611-643.
- Ritter, D.F., 1967, Terrace development along the front of the Beartooth Mountains, southern Montana: Geological Society of America Bulletin, v. 78, p. 467-484.
- Ritter, D. F., and Kauffman, M.E., 1983, Terrace development in the Shoshone River Valley near Powell, Wyoming and speculations concerning the sub-Powell terrace: Wyoming Geological Association, 34th Annual Field Conference Guidebook, p. 197-203.
- Rodgers, D.W., and Zentner, N.C., 1988, Fault geometries along the northern margin of the eastern Snake River Plain, Idaho: Geological Society of America, Abstracts with Programs, v. 20, n. 6, p. 465.
- Rodgers, D.W., Hackett, W.R., and Ore, H.T., 1990, Extension of the Yellowstone Plateau, eastern Snake River Plain, and Owyhee Plateau: *Geology*, v. 18, 1138-1141.
- Roy, W.R., and Hall, R.D., 1980, Re-evaluation of the Bull Lake glaciation through re-study of the type area and studies of other localities: Geological Society of America Abstracts with Programs, v. 12, no. 6, p. 302.
- Rubey, W.W., 1973, Geologic map of the Afton quadrangle and part of the Big Piney quadrangle, Lincoln and Sublette Counties, Wyoming: U.S. Geological Survey Miscellaneous Geologic Investigations Map I-686, scale 1:62,500
- Rubey, W.W., Oriol, S.S., and Tracey, J.I., Jr., 1975, Geology of the Sage and Kemmerer 15-minute quadrangles, Lincoln County, Wyoming: U.S. Geological Survey Professional Paper 855, 18 p.
- Ruppel, E.T., 1967, Late Cenozoic drainage reversal, east-central Idaho, and its relation to possible undiscovered placer deposits: *Economic Geology*, v. 62, p. 648-663.
- Rytuba, J.J., 1989, Volcanism, extensional tectonics, and epithermal mineralization in the northern Basin and Range Province, California, Nevada, Oregon, and Idaho: U.S. Geological Survey Circular 1035, p. 59-61.
- Rytuba, J.J. and McKee, E.H., 1984, Peralkaline ash flow tuffs and calderas of the McDermitt volcanic field, southeast Oregon and north central Nevada: *Journal of Geophysical Research*, v. 89, no B10, p. 8616-8628.
- Sandberg, C.A. and Mapel, W.J., 1967, Devonian of the northern Rocky Mountains and Plains, in Oswald, D.H., ed., International symposium on the Devonian System, Calgary, Alberta, Sept. 1967: Calgary, Alberta Society of Petroleum Geologists, v. 1, p. 843-877.
- Sandberg, C.A. and Poole, F.G., 1977, Conodont biostratigraphy and depositional complexes of Upper Devonian cratonic-platform and continental-shelf rocks in Murphy, M.A., Berry, W.B.N. and Sandberg, C.A., eds., Western North America; Devonian: Riverside, California University Campus Museum Contribution 4, p. 144-182.
- Schmidt, D.L. and Mackin, J.H., 1970, Quaternary geology of Long and Bear Valleys, west-central Idaho: U.S. Geological Survey Bulletin 1311-A, 66 p.
- Schroeder, N.L., 1974, Geologic Map of the Camp Davis Quadrangle, Teton County, Wyoming: U.S. Geological Survey Geologic Quadrangle Map GQ 1160.
- Scott, W.E., 1982, Surficial geologic map of the eastern Snake River Plain and adjacent areas, 111° to 115° W., Idaho and Wyoming: U.S. Geological Survey Miscellaneous Investigations Map I-1372, scale 1:250,000.
- Scott, W.E., Pierce, K.L., and Hait, M.H., Jr., 1985a, Quaternary tectonic setting of the 1983 Borah Peak earthquake, central Idaho: in Stein, R.S., and Bucknam, R.C., eds., Proceedings of Workshop XXVIII on the Borah Peak, Idaho, Earthquake: U.S. Geological Survey Open-file Report 85-290, p. 1-16.
- Scott, W.E., Pierce, K.L., and Hait, M.H., Jr., 1985b, Quaternary tectonic setting of the 1983 Borah Peak earthquake, central Idaho: *Bulletin of the Seismological Society of America*, v. 75, p. 1053-1066.
- Sears, J.W., Hyndman, D.W., and Alt, David, 1990, The Snake River Plain, a volcanic hotspot track: Geological Society of America Abstracts with Programs, v. 22, No. 3, p. 82.
- Shackleton, N.J., 1987, Oxygen isotopes, ice volume, and sea level: *Quaternary Science Reviews*, v. 6, p. 183-190
- Skilbeck, J.N., and Whitehead, J.A., Jr., 1978, Formation of discrete islands in linear island chains: *Nature*, v. 272, p. 499-501.
- Skipp, B.A., 1984, Geologic map and cross-sections of the Italian Peak and Italian Peak Middle Roadless Areas, Beaverhead County, Montana, and Clark and Lemhi Counties, Idaho: U.S. Geological Survey Field Studies Map MF-1601-B.
- Skipp, B.A., 1985, Contraction and extension faults in the southern Beaverhead Mountain, Idaho and Montana: U.S. Geological Survey Open-File Report 85-545, 170 p.
- Skipp, B.A. and Link, P.K., in press, Middle and Late Proterozoic rocks in the southern Beaverhead Mountains: implications for Late Proterozoic tectonics: Geological Society of America Memoir?
- Skipp, B.A., Sando, W.J., and Hall, W.E., 1979, Mississippian and Pennsylvanian (Carboniferous) Systems in the United States-Idaho: U.S. Geological Survey Professional Paper 1110, chap. AA, p. AA1-AA42.
- Sleep, N.H., 1987, An analytical model for a mantle plume fed by a boundary layer: *Geophysical Journal of the Royal Astronomical Society*, v. 90, p. 119-128.
- Sleep, N.H., 1990, Hotspots and mantle plumes: some phenomenology: *Journal of Geophysical Research*, v. 95, n. B5, p. 6715-6736.
- Smedes, H.W., M'Gonigle, M.W., and Prostka, H.J., 1989, Geologic map of the Two Ocean Pass quadrangle, Yellowstone National Park and vicinity, Wyoming: U.S. Geological Survey Geologic Quadrangle Map GQ-1667, scale 1:62,500.
- Smith, R.B., Byrd, J.O.D., Sylvester, A.G. and Susong, D.L., 1990, Neotectonics and earthquake hazards of the Teton fault: Geological Society of America Abstracts with Programs, v. 22, No. 6, p. 45
- Smith, R.B., Nagy, W.C., Doser, D.I., and Leu, L.L., in press, The 1983 Borah Peak, Idaho, earthquake sequence: regional seismicity, seismic moment release, stress field inversion, and

- related seismotectonics of the Snake River Plain: *Bulletin of the Seismological Society of America*, v. __, 48 ms p.
- Smith, R.B., and Sbar, N.L., 1974, Contemporary tectonics and seismicity of the western United States with emphasis on the Intermountain Seismic Belt: *Geological Society of America Bulletin*, v. 85, p. 1205-1218.
- Smith, R.B., Shuey, R.T., Freidline, R.O., Otis, R.M., and Alley, L.B., 1974, Yellowstone, hot spot: new magnetic and seismic evidence: *Geology*, v. 2, p. 451-455.
- Smith, R.B., Richins, W.D., and D.I. Doser, D.I., 1985, The 1983 Borah Peak, Idaho, earthquake: regional seismicity, kinematics of faulting, and tectonic mechanism, in Stein, R.S., and Bucknam, R.C., eds., *Proceedings of Workshop XXVIII on the Borah Peak, Idaho, Earthquake*: U.S. Geological Survey Open-file Report 85-290, p. 236-263.
- Smith, R.B., Shuey, R.T., Pelton, J.P., and Bailey, J.P., 1977, Yellowstone hot spot: contemporary tectonics and crustal properties from earthquake and aeromagnetic data: *Journal of Geophysical Research*, v. 82, p. 3665-3676.
- Smith, R.L. and Luedke, R.G., 1984, Potentially active volcanic lineaments and loci in western conterminous United States, in Boyd, F., ed., *Explosive Volcanism: Inception, Evolution, and Hazards*: National Academy of Sciences, Washington, D. C., p. 47-66.
- Smith, R.P., Hackett, W.R. and Rogers, D.W., 1989, Surface deformation along the Arco rift zone, eastern Snake River Plain: *Geological Society of America Abstracts with Programs*, v. 21, no. 5, p. 146.
- Sonderegger, J.L., Schofield, J.D., Berg, R.B., and Mannich, N.L., 1982, The upper Centennial valley, Beaverhead and Madison Counties, Montana: *Montana Bureau of Mines and Geology Memoir 50*, 54 p.
- Sparlin, M.A., Braille, L.W., and Smith, R.B., 1982, Crustal structure of the eastern Snake River Plain determined from ray trace modeling of seismic refraction data: *Journal of Geophysical Research*, v. 87, no. B4, p. 2619-2633.
- Stanford, L.R., 1982, Glacial geology of the upper South Fork Payette River, south central Idaho: *Moscow, University of Idaho, M.S. thesis*, 83 p.
- Stickney, M.C., and Bartholomew, M.J., 1987a, Seismicity and late Quaternary faulting of the northern Basin and Range province, Montana and Idaho: *Bulletin of the Seismological Society of America*, v. 77, p. 1602-1625.
- Stickney, M.C., and Bartholomew, M.J., 1987b, Preliminary map of late Quaternary faults in western Montana: *Montana Bureau of Mines and Geology Open-File Report 186*.
- Suppe, John, Powell, Christine and Berry, Robert, 1975, Regional topography, seismicity, Quaternary volcanism, and the present-day tectonics of the western United States: *American Journal of Science*, v. 275-A, p. 397-436.
- Susong, D.L., Smith, R.B., and Bruhn, R.J., 1987, Quaternary faulting and segmentation of the Teton fault zone, Grand Teton National Park, Wyoming, report submitted to the University of Wyoming-National Park Service Research Center, 13 p.
- Ten Brink, N.W., 1968, Pleistocene geology of the Stillwater drainage and Beartooth Mountains near Nye, Montana: *Pennsylvania, Franklin and Marshall College, M.S. thesis*, 172 p.
- Tredoux, M, De Wit, M.J., Hart, R.J., Armstrong, R.A., Lindsay, N.M., and Sellschop, J.P.F., 1989, Platinum group elements in a 3.5 Ga Nickel-Iron occurrence: possible evidence of a deep mantle origin: *Journal of Geophysical Research*, v. 94, n. B1, p. 795-813.
- Trimble, D.E. and Carr, W.J., 1976, *Geology of the Rockland and Arbon Quadrangles, Power County, Idaho*: U.S. Geological Survey Bulletin 1399, 115 p.
- U.S. Geological Survey, 1972a, *Geologic map of Yellowstone National Park*: U.S. Geological Survey Miscellaneous Geologic Investigations Map I-711, scale 1:125,000.
- U.S. Geological Survey, 1972b, *Surficial geologic map of Yellowstone National Park*: U.S. Geological Survey Miscellaneous Geologic Investigations Map I-710, scale 1:125,000.
- Vallier, T.L., Brooks, H.C., and Thayer, T.P., 1977, Paleozoic rocks of eastern Oregon and western Idaho, in Stewart, J.H., and other, eds., *Paleozoic paleogeography of the western United States*: Society of Economic Paleontologists and Mineralogists, Pacific section, Pacific Coast Paleogeography Symposium 1, p. 455-466.
- Vander Meulen, D.B., 1989, Intracaldera tuffs and central-vent intrusion of the Mahogany Mountain caldera, eastern Oregon: U. S. Geological Survey Open-File Report 89-77, 69 P.
- Walsh, T.H., 1975, *Glaciation of the Taylor fork Basin area, Madison Range, southwestern Montana*; *Moscow, University of Idaho, Ph.D. thesis*, 193 p.
- Weinstein, S.A., and Olson, P.L., 1989, The proximity of hotspots to convergent and divergent plate boundaries: *Geophysical Research Letters*, v. 16, n. 5, p. 433-436.
- West, M.W., 1986, Quaternary extensional reactivation of the Darby and Absaroka thrusts, southwestern Wyoming and north central Utah: *Geological Society of America Abstracts with Programs*, v. 18, p. 422.
- Westaway, Rob, 1989, Northeast Basin and Range Province active tectonics: an alternate view: *Geology*, v. 17, p. 779-783.
- Wernicke, B.P., Christiansen, R.L., England, P.C., and Sonder, L.J., 1987, Tectonomagmatic evolution of Cenozoic extension in the North American Cordillera, in Coward, M.P., Dewey, J.F., and Hancock, P.L., eds., *Continental Extensional Tectonics*, Geological Society Special Publication No. 28, p. 203-21
- White, R.S. and McKenzie, D.P., 1989, Magmatism at rift zones: the generation of volcanic continental margins and flood basalts: *Journal of Geophysical Research*, v. 94, No. B6, p. 7685-7729.
- White, R.S., Spence, G.D., Fowler, S.R., McKenzie, D.P., Westbrook, G.K., and Bowen, A.D., 1987, Magmatism at rifted continental margins: *Nature*, v. 330, p. 439-444
- Whitehead, J.A. and Luther, D.S., 1975, Dynamics of laboratory diapir and plume models: *Journal of Geophysical Research*, v. 80, p. 705-717.
- Williams, E.J. and Embree, G.F., 1980, Pleistocene movement on Rexburg fault, eastern Idaho: *Geological Society of America Abstracts with Programs*, v. 12, no. 6, p. 308.
- Williams, P.L., Mytton, J.W., and Covington, H.R., 1990, *Geologic map of the Stricker 1 quadrangle, Cassia, Twin Falls, and Jerome Counties, Idaho*: U.S. Geological Survey Miscellaneous Investigations Series Map I-2078, scale 1:24,000.
- Williams, P.L., Covington, H.R., and Pierce, K.L., 1982, Cenozoic stratigraphy and tectonic evolution of the Raft River Basin, Idaho, in Bonnicksen, Bill, and Breckenridge, R.M., eds., *Cenozoic Geology of Idaho*, Idaho Bureau of Mines and Geology, Bulletin 26, p. 491-504.
- Wilson, J.T., 1963, *Continental Drift*: *Scientific American*, v. 208, p. 86-100.
- Wilson, J.T., 1990, On the building and classification of mountains: *Journal of Geophysical Research*, v. 95, n. B5, p. 6611-6628.

- Witkind, I.J., 1975a, Geology of a strip along the Centennial fault, southwestern Montana and adjacent Idaho: U.S. Geological Survey Miscellaneous Investigations Series Map I-890, scale 1:62,500.
- Witkind, I.J., 1975b, Preliminary map showing known and suspected active faults in western Montana: U.S. Geological Survey Open-File Report 75-285, scale 1:500,000.
- Witkind, I.J., 1975c, Preliminary map showing known and suspected active faults in Idaho: U.S. Geological Survey Open-File Report 75-278, scale 1:500,000.
- Witkind, I.J., 1975d, Preliminary map showing known and suspected active faults in Wyoming: U.S. Geological Survey Open-File Report 75-279, scale 1:500,000.
- Witkind, I.J., 1964, Reactivated faults north of Hebgen Lake: U.S. Geological Survey Professional Paper 435, p. 37-50
- Wood, B.J., 1989, Mineralogical phase change at the 670-km discontinuity: *Nature*, v. 341, p. 278.
- Wood, Chris, 1988, Earthquake Data - 1986: Jackson Lake Seismographic Network, Jackson Lake Dam, Minidoka Project, Wyoming: Seismotectonic Report 88-1, U.S. Bureau of Reclamation, 33 p.
- Wood, S.H., 1984, Review of late Cenozoic tectonics, volcanism, and subsurface geology of the western Snake River Plain, Idaho, in Beaver, P.C., ed., *Geology tectonics, and mineral resources of Western and Southern Idaho*, Tobacco Root Geological Society, Dillon, Montana, p. 48-60.
- Wood, S.H., 1989, Silicic volcanic rocks and structure of the western Mount Bennett Hills and adjacent Snake River Plain, Idaho in Smith, R.P., and Downs, W.F., eds., *28th International Geological Congress Field Trip Guidebook T305*, p. 69-77.
- Wood, S.H., and Gardner, J.N., 1984, Silicic volcanic rocks of the Miocene Idavada Group, Bennett Mountain, southwestern Idaho: Final Contract Report to the Los Alamos National Laboratory from Boise State University, 55 p.
- Woodward, N.B., 1988, Primary and secondary basement controls on thrust sheet geometries in Schmidt, C.J., and Perry, W.J., Jr., eds., *Interaction of the Rocky Mountain Foreland and the Cordilleran Thrust Belt: Geological Society of America Memoir 171*, p. 353-366.
- Wyllie, P.J., 1988, Solidus curves, mantle plumes, and magma generation beneath Hawaii: *Journal of Geophysical Research*, v. 93, p. 4171-4181.
- Zoback, M.L., and Thompson, G.A., 1978, Basin and Range rifting in northern Nevada: clues from a mid-Miocene rift and its subsequent offsets: *Geology*, v. 6, p. 111-116.
- Zoback, M.L., and Zoback, Mark, 1980, State of stress in the Conterminous United States: *Journal of Geophysical Research*, v. 85, No. B11, p. 6113-6156.

Plate Caption

PLATE 1. VOLCANIC FIELDS, NEOTECTONIC FAULT TYPES, AND ALTITUDE NEAR THE TRACK OF THE YELLOWSTONE HOTSPOT, IDAHO AND ADJACENT STATES

[Caption] The color spectrum (scale bar) represents altitude, with the warmest colors the highest. Numbers beside color bar are elevations in meters. The track of the Yellowstone hotspot is shown by the increasing age of volcanic fields southwest from Yellowstone. The hotspot track from Yellowstone to the Picabo field has a systematic time/distance progression (Fig. 3) and follows the mountain-bounded eastern SRP, whereas the track from the Twin Falls to the McDermitt field is less systematic and is not bounded by mountains. Neotectonic fault Belt II is defined by *major Holocene* faults and has arms that trends south and west from Yellowstone. Neotectonic Belts I and III occur outside and inside Belt II whereas Neotectonic Belt IV occurs only on the south side of the SRP and is characterized by inactive *major Tertiary* faults. The sources for the volcanic geology compilation are given in Table 1.

Abbreviations for names of fault segments north of the plain (from Haller, 1988; Scott and others, 1985b) are as follows: (1) Lost River fault--, A=Arco, P=Pass Creek, M=Mackay; T=Thousand Springs, and W=Warm Springs; (2) Lemhi Fault--, H=Howe; F=Fallert Springs, S=Sawmill Gulch, G=Goldburg, P=Patterson, and M=May; and (3) Beaverhead Fault--, N=Nicholia, B=Baldy Mountain, L=Leadore, and M=Mollie Gulch.

Sources for fault location and classification:

Montana: General-- Stickney and Bartholomew (1987a, 1987b); Pardee (1950), Reynolds (1979); Centennial fault--Witkind (1975a and 1975b); Deep Creek or Emigrant fault--Personius (1982); Madison fault-- Mayer and Schneider (1985); Sawtooth fault--Fisher and others (1983).
Idaho: General-- Greensfelder (1976), Witkind (1975c, 1975a), Scott (1982), Bond (1978), Scott and others (1985b); basin-range north of plain--Haller (1988); Skipp (1984, 1985); Swan-Grand Valley faults--Piety and others 1986); Thatcher Basin and Blackfoot volcanic field faults-- Oriel and Platt, 1980; Bear Lake fault-- McCalpin, 1990); fault near Rexburg--Williams and Embree (1980); fissures on Snake River Plain- Kuntz (in press).
Wyoming: General--Witkind, 1975d; Yellowstone area--U.S. Geological Survey (1972a, 1972b), R. L Christiansen, written commun. (1987); Snipe

Point fault extending into Yellowstone Lake-- Pings and Locke (1988); Teton Fault--Gilbert and others (1983); Mt. Glory fault and parts of Teton fault--K.L. Pierce, field observations, 1988; Star Valley fault--Piety and others (1986); Rock Creek and fault to west--Oriel and Platt (1980), Rubey, Oriel, and Tracy (1975); southwest Wyoming--Gibbons and Dickey, 1983; Bear River fault zone and fault zone to east--West, 1986 and written commun., 1987; Boulder-Nye lineament--Reheis, 1985; south side of Owl Creek Mountains--Kelson and others, 1988; and north and south Granite Mountains faults--Perman and others, 1988.

Utah: Wasatch fault-- Machette and others (1987); Hansel Valley- Pocatello Valley faults--McCalpin and others (1987); East Cache fault--McCalpin (1987); faults near Wyoming line--Gibbons and Dickey (1983).

Volcanic geology compilation

Idaho: Christiansen, 1984, Morgan and others, 1984; Morgan, 1988; Kellogg and Marvin, 1988; Williams and others, 1982; Wood and Gardner, 1984; Bonnichsen, 1982; Bonnichsen and Kauffman, 1987; Ekren and others, 1984; Minor and others, 1986, 1987.

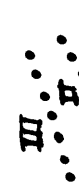
Oregon: Rytuba, 1989; Rytuba and McKee, 1984; Vander Muellen, 1989.

Nevada: Rytuba, 1989; Rytuba and McKee, 1984; Ach and others, 1987; Greene and Plouff, 1981; Noble and others, 1970

Wyoming: Christiansen, 1984

Plate 1. VOLCANIC FIELDS, NEOTECTONIC FAULT TYPES, AND ALTITUDE NEAR THE TRACK OF THE YELLOWSTONE HOT SPOT, IDAHO AND ADJACENT STATES.

EXPLANATION

-  OBLATE CRESCENT OF HIGH TERRAIN, central dashed blue line along axis of high elevations
-  CALDERAS AND VOLCANIC CENTERS [white dashed lines]. White numbers are ages in Ma for major eruptions; italic numbers for inception ages of volcanic fields
-  BOUNDARIES OF NEOTECTONIC FAULT BELTS [white dots] I, II, III, and IV
-  VOLCANIC FISSURES of late Quaternary age

TYPES OF LATE CENOZOIC NORMAL FAULTS

FAULT TYPE	ESCARPMENT	LAST OFFSET	CHARACTERIZES NEOTECTONIC BELT
MAJOR HOLOCENE	>700 m relief, high steep facets	Holocene <15 ka	II
LESSER AND REACTIVATED HOLOCENE	absent or >200 m rejuvenated facets	Holocene <15 ka	I
MAJOR LATE PLEISTOCENE	>500 m relief moderate facets	late Pleistocene 15-120 ka	III
LESSER LATE PLEISTOCENE	<200 m relief, low or absent facets	late Pleistocene 15-100 ka	
MAJOR TERTIARY	>500 m, muted escarpment	Tertiary or older Quaternary	IV
<i>Italic numbers in white</i>	<i>for age of major interval of activity on fault</i>		
LESSER TERTIARY	absent or low (<200 m) and muted	Tertiary or older Quaternary	

Figure Captions

Figure 1. Location map showing geographic features in the region of the Yellowstone hotspot track, Idaho and adjacent states. Adapted from Raisz (1957) with minor additions.

Figure 2. Sketch of experimental plume showing head and tail (chimney) parts. Drawn from photograph shown in Richards and others (1989, Fig. 2). The large bulbous plume head is fed by a much narrower tail or chimney. In this scale model, the plume head was 1.3 cm across. For the Yellowstone hotspot track, we postulate that a plume head about 300 km across intercepted the lithosphere 16-17 Ma and produced widespread volcanism and deformation whereas from 10 Ma to present a much narrower chimney (tail) 10-20 km across has produced more localized volcanism, faulting, and uplift .

Figure 3. Plot of age of silicic volcanic centers with distance southwestward from Yellowstone. Trough-shaped lines represent caldera widths. For different volcanic fields, stars designate centers of first caldera whereas dots designate subsequent calderas. As defined by stars, silicic volcanism since 10 Ma has progressed at a rate of 2.9 cm/yr N 54°E. From 16 to 10 Ma, the apparent trend and velocity is roughly N 75° E at 7 cm/yr, although both the alignment of the trend and age progression is not as well defined (Plate 1 and Fig. 4). Zero distance is at northeast margin of 0.6 Ma caldera in Yellowstone. Open triangle for Steens Mountain Basalt, one of the Oregon Plateau flood basalts.

Figure 4. Plot of volcanic centers showing marked increase in dispersion (shaded area) about hotspot centerline with distance from Yellowstone. Vertical axis is the distance of volcanic centers away from the hotspot centerline; horizontal axis is the distance from Yellowstone. The numbers represent the age of a center, given in italics for centers south of the centerline (Plate 1). From 0 to 300 km, the centers (0.6 and 10.3 Ma) are within 20 km of the centerline. But from 600 to 800 km, the centers (mostly 13 and 16 Ma) are up to 160 km off the centerline. Although rhyolites 13-16 Ma are common south of the centerline in north-central Nevada (Luedke and Smith, 1981), they are not plotted here because centers have not been located.

Figure 5. The front of the Teton Range, showing a post-glacial fault scarp 35 m high produced by a vertical offset of 20 m. Note the high, steep front of the Teton Range and high partially dissected triangular facets. Based on post-glacial activity and the abruptness of the range front, this is the most active *major Holocene* fault in Belt II. For the Teton and the other *major Holocene* faults, we infer that the high, precipitous range fronts, with high, steep, relatively undissected facets reflect high Quaternary offset rates ($>0.3?$ mm/yr). Photograph of fault scarp just west of String Lake by R.C. Bucknam.

Figure 6. Inferred late Cenozoic history of the Teton fault based on tectonic rotation into the fault of beds in the Signal Mountain area. Signal Mountain is 13 km east of the central part of the Teton fault. Differences in rate between 2 and 6 Ma (shaded area) result from three options given for the age of the older tuff on Signal Mountain: A-- our preferred correlation with the $4.2 \pm$ tuff of Kilgore, B-- a fission track age from Signal Mountain of 5.5 ± 1 M.y., and C- correlation with the 5.99 ± 0.06 Ma Connant Creek Tuff. The present episode of tilting started after 6 Ma and high tilt rates have persisted since at least 2 Ma. Cross sections by Gilbert and others (1983) and by us indicate downfaulting of 2.5 ± 0.4 km of the 2.0 Ma tuff opposite Signal Mountain. Thus, offset rate since 2 Ma has been about 1.25 ± 0.2 mm/yr (solid line). In the 15 ka since glacial recession near String Lake (Fig. 5), 19.2 m vertical offset (Gilbert and others, 1983) yields a rate of 1.3 ± 0.3 mm/yr (dashed line).

Figure 7. Photograph looking south along "new" fault on Baldy Mountain 32 km east of the Teton fault, Wyoming. The 5-m-high scarp offsets Pinedale moraines probably about 20 ka. The fault trends north-south and the east (left) side is down. The bedrock escarpment south of here is only a few times higher than the scarp, suggesting the fault is a new, late Quaternary fault.

Figure 8. History of the recently reactivated Emigrant fault, a fault in Belt I about 75 km north of the Yellowstone calderas (Plate 1). Estimated fault offset is approximated from the tectonic rotation assuming a hinge line 10 km northwest of the fault based on the present valley width. [Assuming a 20-km-hinge-line as for the Teton fault, offset length would be doubled]. About 4

km northwest of the fault, white tuffaceous beds about 15 Ma dip 8-10° into the fault, but overlying basalt flows 8.4 and 5.4 Ma (Montagne and Chadwick, 1982) dip no more than 0.5° into the fault. Late Quaternary scarps along the Emigrant fault indicate an offset rate of about 0.25 mm/yr (Personius, 1982), but this rate can be extended back to no more than 0.5 Ma because of the nearly horizontal basalts. Thus, an interval of quiescence (shaded area) from about 0.5 Ma to 8.4 Ma separates Neogene faulting from late Quaternary faulting.

Figure 9. Late Quaternary history of the Arco segment of the Lost River fault, a fault in Belt III just north of the Snake River Plain. A 160-ka datum defines an overall rate (dotted line) of about 0.1 mm/yr (Pierce, 1985). Local back tilting affects this rate, and actual vertical tectonic displacement between the mountain and basin blocks is estimated to be 0.07 mm/yr. The 6 control points define a more irregular history, including no offsets since 30 ka (Pierce, 1985).

Figure 10. Late Cenozoic offset history of the Grand Valley fault, Idaho, based on tectonic rotation of volcanic layers (from Anders and others, 1989). Paleomagnetic studies of ignimbrites show that only the 2-Ma unit has a significant non-tectonic dip. Cumulative displacement represents total dip slip movement. The great majority of offset occurred between 4.3 and 2 Ma; before and after this interval, rates were one or more orders of magnitude slower. Error bars are one sigma for age and two sigma for displacement as explained in Anders and others (1989, Fig. 14). The regional nomenclature of Morgan (1988) and Kellogg and others (1989) has been substituted for local stratigraphic nomenclature used by Anders and others (1989) as follows: tuff of Blacktail = tuff of Spring Creek; tuff of Kilgore = tuff of Heise; and tuff of Arbon Valley = tuff of Cosgrove Road.

Figure 11. Deformation history of the Raft River valley and adjacent ranges showing about 15 km of sub-horizontal detachment faulting since 10 Ma (from Covington, 1983). Quaternary deformation has been minor, and silicic domes and tuffs exposed around the basin margins suggest deformation and valley filling was largely complete by 6-8 Ma. Silicic volcanic activity in the adjacent Snake River Plain is not well dated,

but probably started between 12 and 10 Ma (Plate 1).

Figure 12. Correlation between belts of neotectonic faulting and historic earthquake locations in the Snake River Plain region. Belts are separated by dashed lines and variously shaded except Belt II which is unshaded. Epicenters map kindly provided by R.L. Smith (written commun., 1990). The earthquake record samples a much shorter time interval than our fault studies, probably explaining the differences described in the text. Dotted line is "thermal shoulder" of Smith and others (1985) inside of which earthquakes are rare and outside of which earthquakes are concentrated. The solid lines with carrots are the inner and outer parabolas of Anders and others (1989) between which earthquakes have been concentrated and inside of which is their "collapse shadow".

Figure 13. Profiles across three oceanic hotspot swells showing their large-scale topographic expression with heights of 1-2 km and diameters of 800-1200 km (from Crough, 1978). The smoothed line removes small scale variations and the volcanic edifice and its associated isostatic depression. Although the Yellowstone hotspot is beneath continental rather than oceanic lithosphere, these profiles are given to show the scale of uplift that may be involved.

Figure 14. Gray-scale digital topography showing expression of the Yellowstone crescent of high terrain (solid line) that wraps around the Yellowstone Plateau. The higher the terrain, the lighter the shading. The Yellowstone crescent stands about ½-1 km higher than the surrounding terrain. The crest of the western arm of the crescent (long-dashed line with arrows) coincides with the belts of neotectonic faulting, whereas the crest of the southern arm is just east of these belts (Plate 1). The effects of Laramide uplifts such as the Wind River, Bighorn, and Beartooth Ranges as well as the associated basins are older features that need to be discounted to more clearly define altitude anomalies associated with the Yellowstone Hotspot. The numbers are the altitudes, in hundreds of meters of selected high remnants of 2-Ma Huckleberry Ridge Tuff mapped by R.L. Christiansen (written commun., 1985), which at the margin of its caldera (oval area) is now generally between 2000 and 2500 m. Altitude differences exceeding 500 m between the

caldera source and sites near the axis of the Yellowstone crescent indicate uplift of the Yellowstone crescent and/or subsidence of the caldera. Dotted line encloses a broader bulge of higher terrain that may also be associated with Yellowstone.

Figure 15. Historic vertical uplift across the western arm of the Yellowstone crescent of high terrain (from Reilinger, 1985). Lines with small dots indicate resurveyed benchmarks along highways. The interval between surveys was 30 to 60 yrs between 1903 and 1967 (Reitlinger, and others, 1977, Table 1). Area of map shown on Fig. 15.

- A.** Contours on historic uplift in mm/yr based entirely on highway survey lines almost all located along topographic lows. Contours based on this data almost entirely from basins show three domes of uplift roughly coincident both with the axis of the Yellowstone crescent and fault Belt II (shaded), excepting Emigrant fault. The highest basin uplift rates of (>2 mm/yr) are associated with the downthrown sides of the active Red Rock, Madison-Hebgen, and Emigrant faults (see text).
- B.** Vertical movements along repeat leveling line between Idaho Falls, ID, and Butte, MT. A arch of uplift about 200 km wide centers near the boundary of Belts I and II (see part A).

Figure 16. Ratios of the length of Pinedale to Bull Lake glaciers in the Yellowstone crescent of high terrain and nearby mountains. Pinedale terminal moraines are about 20 to 35 ka and Bull Lake ones are about 140 ka. Uplift would result in high ratios (triangles) and subsidence would result in low ratios (circles), although several non-tectonic factors could also result in departures from the "normal" ratio. Area of high ratios (light shading) suggests uplift on outer slope of the Yellowstone crescent of high terrain. Area of low ratios for the Yellowstone ice sheet (darker shading) suggests subsidence of the west part of Yellowstone.

Sources of data (capital letters indicate location by state on figure):

Montana: (A) East and West Rosebud, West and main fork, Rock Creek (Ritter, 1967); (B) West and main fork, Stillwater River (TenBrink, 1968); (C) north side Beartooth uplift (Pierce, field notes); (D) Yellowstone River, west side of Beartooth uplift, northwest Yellowstone (Pierce, 1979); (E) west side of Beartooth uplift

(Montagne and Chadwick, 1982); (F) Taylor Fork (Walsh, 1975, with modifications by Pierce); (G) Tobacco Root Mtns. (Hall and Michaud, 1988, and other reports by Hall referenced therein); (H) Centennial Range (Witkind, 1975a)

Wyoming: (A) Bighorn Mtns. (Lon Drake and Steven Esling, written commun., 1989); (B) east side Bighorn Mtns. (Pierce, 1965); (C) Sunlight Basin (K.L. Pierce, unpublished mapping); (D) North Fork Shoshone River (John Good, written commun., 1980); (E) Wood River (Breckenridge, 1975, reinterpreted by Pierce after consulting with Breckenridge); (F) southern Absaroka Range and Wind River (Helaine Markewich, oral commun., 1989; K.L. Pierce, field notes, 1989); (G) Bull Lake Creek (Richmond and Murphy, 1965; Roy and Hall, 1980); (H) Dinwoody Cr., Torrey Cr., Jackeys Fork, Green River (Pierce, field notes); (I) Fremont Lake, Pole Creek (Richmond, 1973); (J) Big Sandy River (Richmond, 1983); (K) Granite Creek and Dell Creek (Don Eschman, written commun., 1976); (L) west side of Tetons (Fryxell, 1930; Scott, 1982); (M) Jackson Hole (K.L. Pierce and J.D. Good, unpublished mapping); (N) southwestern Yellowstone (Richmond, 1976; Colman and Pierce, 1981).

Idaho: (A) drainages adjacent to the eastern Snake River Plain not designated "B" (Scott, 1982); (B) Copper Basin and area to west (Evenson and others, 1982; E.B. Evenson, written commun., 1988); (C) South Fork Payette River (Stanford, 1982); (D) Bear Valley and Payette River (Schmidt and Mackin, 1970; Colman and Pierce, 1986); (E) Albion Range (Scott, 1982; R.L. Armstrong, written commun.; K.L. Pierce, unpublished mapping).

Utah: (A) Raft River Range (K.L. Pierce, unpublished mapping); (B) Little Cottonwood and Bells Canyons (Madsen and Currey, 1979); (C) Uinta Mtns (Osborne, 1973; K.L. Pierce, field notes).

Figure 17. Direction of Quaternary unidirectional stream migrations by either slip off or capture, Bighorn Basin and adjacent areas. Note that streams have generally migrated away from the outer margin of the Yellowstone crescent of high terrain (arcuate dashed line). Base map from Mackin (1937).

Compiled from: Ritter, 1967; Reheis, 1985; Reheis and Agard, 1984; Agard, 1989; Palmquist, 1983; Mackin, 1937; Andrews and others, 1947; Ritter and Kauffman, 1983; Morris and others, 1959; Hamilton and Paulson, 1968; Richards and

Rogers, 1951; Agard, written commun., 1989; and Palmquist, written commun., 1989; mostly using ash-based chronology from Izett and Wilcox, 1982.

Figure 18. Terraces profiles along three selected streams, Bighorn Basin, Wyoming. A., Shoshone River; flows east away from the Yellowstone crescent and terraces and stream profile diverge upstream. Shoshone River terraces from Mackin (1937) where solid line is altitude of top of gravel beneath variable capping of overbank and sidestream alluvium; dashes indicate top of terraces with such fine sediment. Upstream divergence of about 0.1 m/km based on lower most continuous Cody terrace represented by heavy line. Light solid line-- upper Cody terrace. B. Paint Rock Creek and C., Tensleep Creek, both flow west towards the crescent, terraces converge upstream. Terrace profiles and designations from Palmquist (1983); stipples below floodplains represent depth of glaciofluvial fill.

Figure 19. Northeast migration away from Yellowstone crescent and Beartooth Mountain front of the convergence/divergence points between pairs of terrace profiles, Rock Creek, Montana. Solid circle, closest place between older terrace and younger terrace; small arc, place where terrace profiles visibly diverge. Based on terrace and stream profiles drawn by Reheis (1987, Fig. 3). Terrace symbols: M- Mesa, UR- Upper Roberts, IR- lower Roberts, BL- Bull Lake, and Pd- Pinedale. Other symbols: c- channel of Rock Creek; < - convergence point lies left of dot.

Figure 20. Decrease in the altitude of the upper limit of calcareous soils with terrace age along Rock Creek at northwest margin of Bighorn Basin, Montana (from Reheis, 1987). Regional uplift of about 0.5 mm/yr could explain this change, although it may also be explained by non-tectonic causes, including increase in soil fines through time and increased aridity of some increasingly older interglacial climates. Terrace names as in Reheis (1987); two age-options are shown for Boyd terrace: R- Reheis, 1987; P- Palmquist, written commun., 1989. The data point for 2-Ma Mesa terrace not included.

Figure 21. Selected Quaternary rates of stream incision in the Rocky Mountain area. Incision

rates generally reflect uplift rates, although other factors like the relation between stream orientation and tilt are also involved. High incision rates of greater than 15 mm/100 yrs extend from just east of Yellowstone south through Colorado to New Mexico. Incision rates are based on terrace heights whose age is known from volcanic ashes erupted between 0.6 and 2.0 Ma (Izett and Wilcox, 1982; Reheis and others, in press Carter and others, 1991). R.L. Palmquist suggested this compilation and noted that the high incision rates correspond with the axis of uplift in the tandem Yellowstone-Raton hotspot hypothesis of Suppe and others (1975, Fig. 7) .

Figure 22. Stress distribution in the Snake River Plain region showing extensional (T-axis) orientations. Extension is subparallel to the length of the SRP-YP trend rather than, as expected for a rift origin, perpendicular to it .

Compiled from: north of SRP, (Stickney and Bartholomew 1987a); normals to fissures on SRP, (Kuntz , in press); Yellowstone-Teton area (Doser and Smith, 1983 Doser, 1985 Wood, 1988); Grand-Star Valley area (Piety and others, 1986); other areas south of SRP (Smith and Sbar, 1974); and general region (Zoback and Zoback, 1980).

Figure 23. Major geologic features in the western U.S. associated with the late Cenozoic track of the Yellowstone hotspot.

Compiled from: Blakely, 1988; Blakely and others, 1989; Luedke and Smith, 1981, 1982, 1983; Smith and Luedke, 1984; Hooper, 1988; Carlson and Hart, 1988; Elison and others, in press; Kistler and Lee, 1989; Kistler and others, 1981. Base map from Harrison, 1969

Figure 24. Postulated development of the Yellowstone thermal plume from its inception phase, through its huge head and transition phases, to its present chimney phase. Inspired from Richards and others (1988, 1989) and Griffiths and Richards (1989). Only the hottest part of the plume is shown-- that part > 1400°C based on the schematic isotherms of Courtney and White (1986) and Wyllie (1988). As the mantle plume rises, decompression melting produces basaltic melt which rises through the mantle lithosphere to the lower crust and may vent as flood basalts or be emplaced in the lower crust where it exchanges its heat to produce silicic magma that

rises to higher in the crust. Scale does not permit showing the entire, approximately 1000-km-diameter, lower-temperature plume, based on the 800-1200-km diameter of oceanic hotspot swells (Courtney and White, 1986). Volumes (minimum estimates) show flood basalts are 100 times greater than ignimbrites. The schematic crustal section showing major lithologic phases (rhyolitic calderas, granitic batholiths, and mid-crustal basalts) along the hotspot track is consistent with seismic refraction data modeled for the SRP (Sparlin and others, 1982). Rhyolites and their associated calderas are exposed at Yellowstone, but beneath the SRP are covered by a veneer of basalt and intercalated sediments. Magma and zones of partial melt presently under the Yellowstone caldera are at depths ranging from several kilometers (not shown; Clawson and others, 1989) to 250-300 km (Iyer and others, 1981). Stars, centers of volcanic fields. Mid-crustal basalts have not been detected seismically beneath Yellowstone (Iyer and others, 1981) but evidence of their presence may be the later post-0.6-Ma basalts that now fill much of the Henry's Fork caldera (Christiansen, 1982). Line marked 0.706 (initial $^{87}\text{Sr}/^{86}\text{Sr}$ isopleth) approximates the western edge of the Precambrian sialic crust (Armstrong and others, 1977; Kistler and Peterman, 1978); that marked 0.704 marks the western edge of Paleozoic mafic crust (Kistler, 1983; Elison and others, in press).

Table 1. Volcanic fields, calderas, and ignimbrites and their ages along the track of the Yellowstone hotspot

VOLCANIC FIELD	CALDERA	IGNIMBRITE	AGE (Ma)	REFERENCE
<u>Yellowstone Plateau</u>				
	Yellowstone	Lava Creek Tuff	0.6	1
	Henry's Fork	Mesa Falls Tuff	1.2	1
	Huckleberry Ridge	Huckleberry Ridge Tuff	2.0	1
<u>Heise</u>				
	Kilgore	tuff of Kilgore	4.3	2, 3
	Blue Creek	Walcott Tuff	6.0	2, 3
	Blacktail Ck.	tuff of Blacktail Ck.	6.5	2, 3
<u>Picabo</u>				
	Blackfoot	*tuff of Arbon Valley	10.3	5
<u>Picabo or Twin Falls</u>				
	?	City of Rocks Tuff	6.5	4
	?	Fir Grove Tuff	?	4
	?	Gwin Spring Fm.	?	4
	?	older welded tuff	?	4
<u>Twin Falls</u>				
	?	tuff of McMullen Ck.	8.6	6
	?	tuff of Wooden Shoe Butte	10.1	6
	?	tuff of Sublett Range	10.4	7
	?	tuff of Wilson Ck.	11.0	8
	?	tuff of Browns Ck.	11.4	8
	?	tuff of Steer Basin	12.0	6
<u>Bruneau-Jarbridge</u>				
	?	rhyolite of Grasmere escarpment	11.2	9
	?	Cougar Point Tuff III	11.3	9
	?	Cougar Point Tuff VII	12.5	9
<u>Owyhee-Humboldt</u>				
	Juniper Mtn. volcanic center	tuff of the Badlands	12.0	8
	Juniper Mtn. volcanic center	lower Lobes Tuff	13.8	8
	Juniper Mtn. volcanic center	upper Lober Tuff	13.9	8
	Boulder Creek	Swisher Mtn. Tuff	13.8	8, 10
<u>McDermitt</u>				
	Whitehorse	tuff of Whitehorse Ck.	15.0	11
	Hoppin Peaks	tuff of Hoppin Peaks	15.5	11

	Long Ridge	tuff of Long Ridge 5	15.6	11
	Jordan Meadow	tuff of Long Ridge 2	15.6	11
	Calavera	tuff of Double H	15.7	11
	Pueblo	tuff of Trout Ck. Mts.	15.8	11
	Washburn	tuff of Oregon Canyon	16.1	11
unnamed volcanic fields	Three-Finger	?	15.4	12, 13
	Mahogany Mtn.	Leslie Gulch Tuff	15.5	12, 13
	Hog Ranch	?	15.4	12
	Soldier Meadow	Soldier Meadow Tuff	15.0	14, 15

* The age of the tuff of Arbon Valley has been determined to be about 10.3 Ma at several sites on the south side of the plain over a distance of 120 km (Kellogg and Marvin, 1988; Kellogg and others, 1989; Armstrong and others, 1980). Two unpublished ages for the tuff of Arbon Valley in Rockland Valley also yield ages of about Ma (Karl Kellogg and Harold Mehnert, written Communication, 1989). The previously accepted age of 7.9 Ma on a similar biotite-bearing ignimbrite (Armstrong and others, 1980) was based only on one sample and is either too young or represents a more local unit. An age of about 10.3 was also obtained on the north side of the SRP in the southern Lemhi Range (John Sutter and Falma Moye, oral commun., 1989).

1. Christiansen, 1984
2. Morgan et al., 1984
3. Morgan, 1988
4. Leeman, 1982b
5. Kellogg and others, 1989
6. Williams and others, 1990
7. Williams and others, 1982
8. Ekren and others, 1984
9. Bonnicksen, 1982
10. Minor and others, 1986, 1987
11. Rytuba and McKee, 1984
12. Rytuba, 1989
13. Vander Muelen, 1989
14. Noble and others, 1970
15. Greene and Plouff, 1981; Kellogg and Marvin, 1988; Armstrong and others, 1980

Table 2. A Classification of late Cenozoic normal faults. For the fault-type designation, the first word applies to the escarpment height and the second to the recency of offset.

FAULT TYPE	ESCARPMENT	LAST OFFSET	CHARACTERIZES NEOTECTONIC BELT
MAJOR HOLOCENE	>700 m relief, high steep facets	Holocene <15 ka	II
LESSER AND REACTIVATED HOLOCENE	absent or >200 m rejuvenated facets	Holocene <15 ka	I
MAJOR LATE PLEISTOCENE	>500 m relief moderate facets	late Pleistocene 15-120 ka	III
LESSER LATE PLEIST.	<200 m relief, low or absent facets	late Pleistocene 15-100 ka	
MAJOR TERTIARY	>500 m, muted escarpment	Tertiary or older Quaternary	IV
LESSER TERTIARY	absent or low (<200 m) and muted	Tertiary or older Quaternary	

[Ohstab2, August 1, 1990, set print options to HPLANS, divisions to 11 inches wide]

Table 3. Differences between Silicic Volcanism on the Eastern Snake River Plain and the Southeast Oregon Rhyolite Belt

Factor	Eastern Snake River Plain	Southeast Oregon Rhyolite Belt	
1. Time of inception	16-17 Ma ¹	-10 Ma (majority 8 Ma) ²	
2. Point of origin	northern Nevada near McDermitt volcanic field	<u>Northern belt</u> SE of Harney Basin	<u>Southern belt</u> Beaty Butte (S. Oregon)
3. Length of province	700 km ¹	250-300 km *	
4. Style of volcanism	generally large-volume ignimbrites from large calderas	generally small-volume rhyolite domes	
5. Manner in which volcanism migrated	northeast-trending wide belt 10-16 Ma and narrow belt 0-10 Ma ¹	northwest-trending wide swath along two broad belts ²	
6. Migration rate of volcanism	-7.0 cm/yr, 10-16 Ma ¹ 2.9 cm/yr, 0-10 Ma ¹	<u>Northern belt</u> 4.4 cm/yr, 5-10 Ma ² 1.5 cm/yr, 0-5 Ma ²	<u>Southern belt</u> 2.6 cm/yr
7. Volume of erupted products	100's to >1000 km ³	one to a few tens of km ³	
8. Faults or other structure associated with volcanic trend	downwarp	northwest-trending en echelon faults defining the Brothers fault zone ²	

¹this study

²MacLeod and others, 1976

*Walker and Nolf, 1981

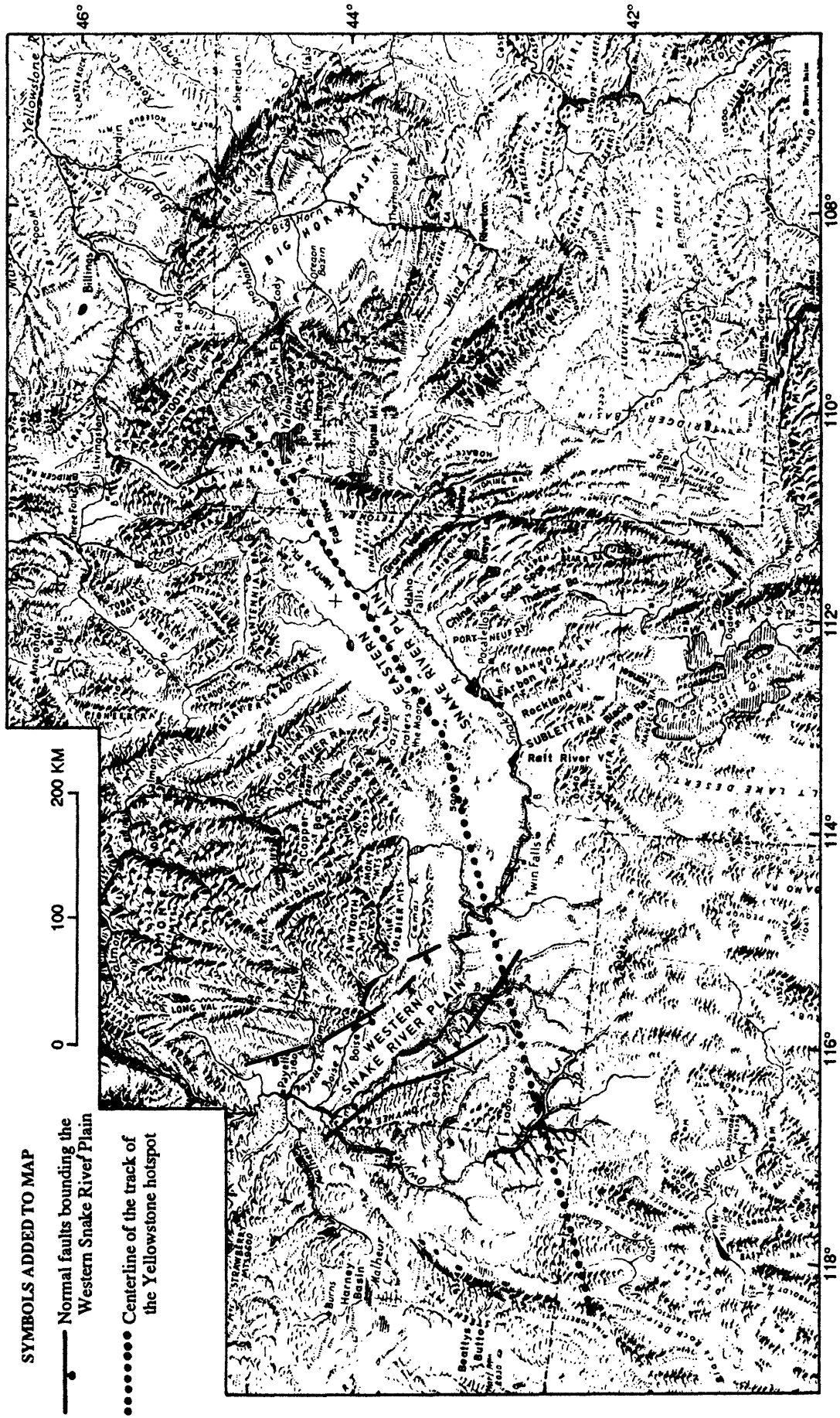


Figure 1. Location map showing geographic features in the region of the Yellowstone hotspot track, Idaho and adjacent states.



Figure 2. Sketch of experimental plume showing head and tail (chimney) parts.

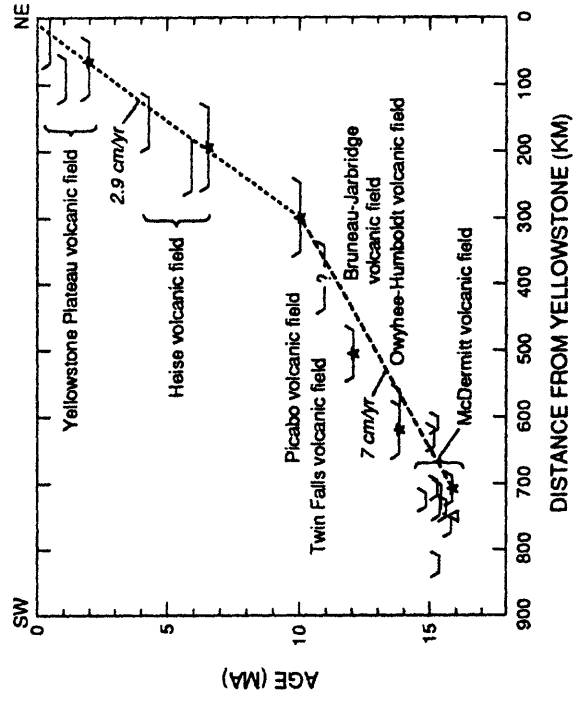


Figure 3. Plot of age of silicic volcanic centers with distance southwestward from Yellowstone.

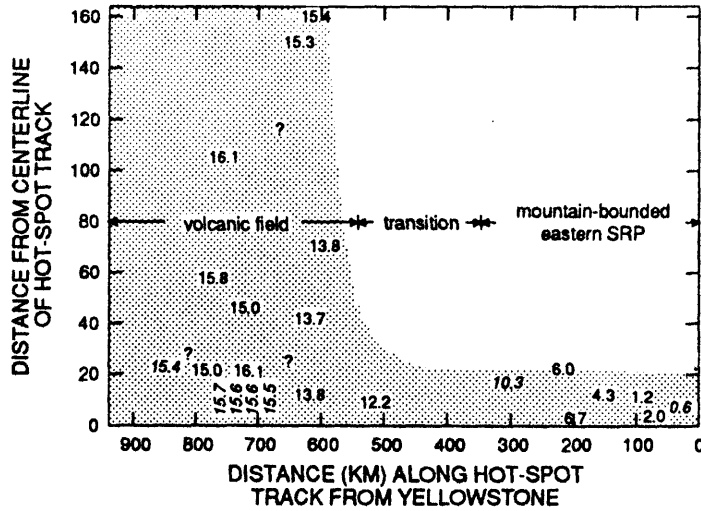


Figure 4. Plot of volcanic centers showing marked increase in dispersion (shaded area) about hotspot centerline with distance from Yellowstone.

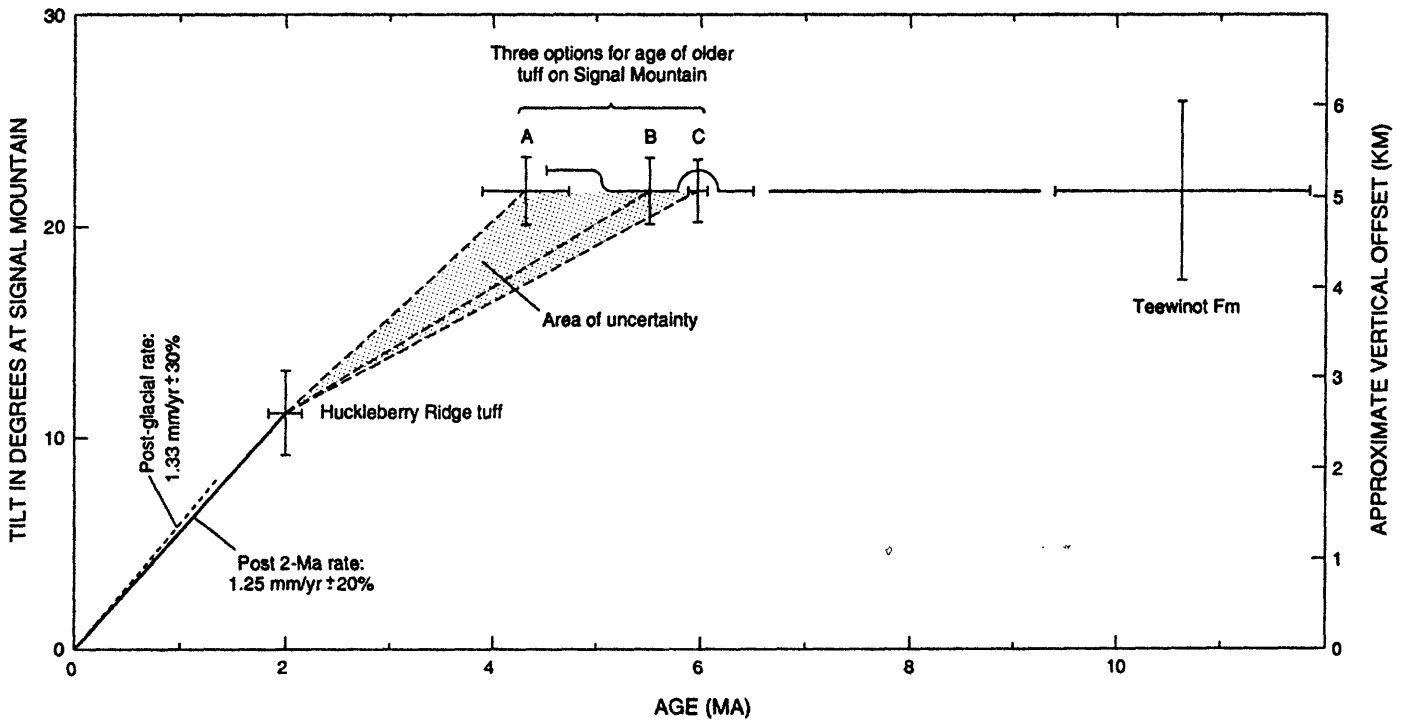


Figure 6. Inferred late Cenozoic history of the Teton fault based on tectonic rotation into the fault of beds in the Signal Mountain area.



Figure 5. The front of the Teton Range, showing a post-glacial fault scarp 35 m high produced by a vertical offset of 20 m.

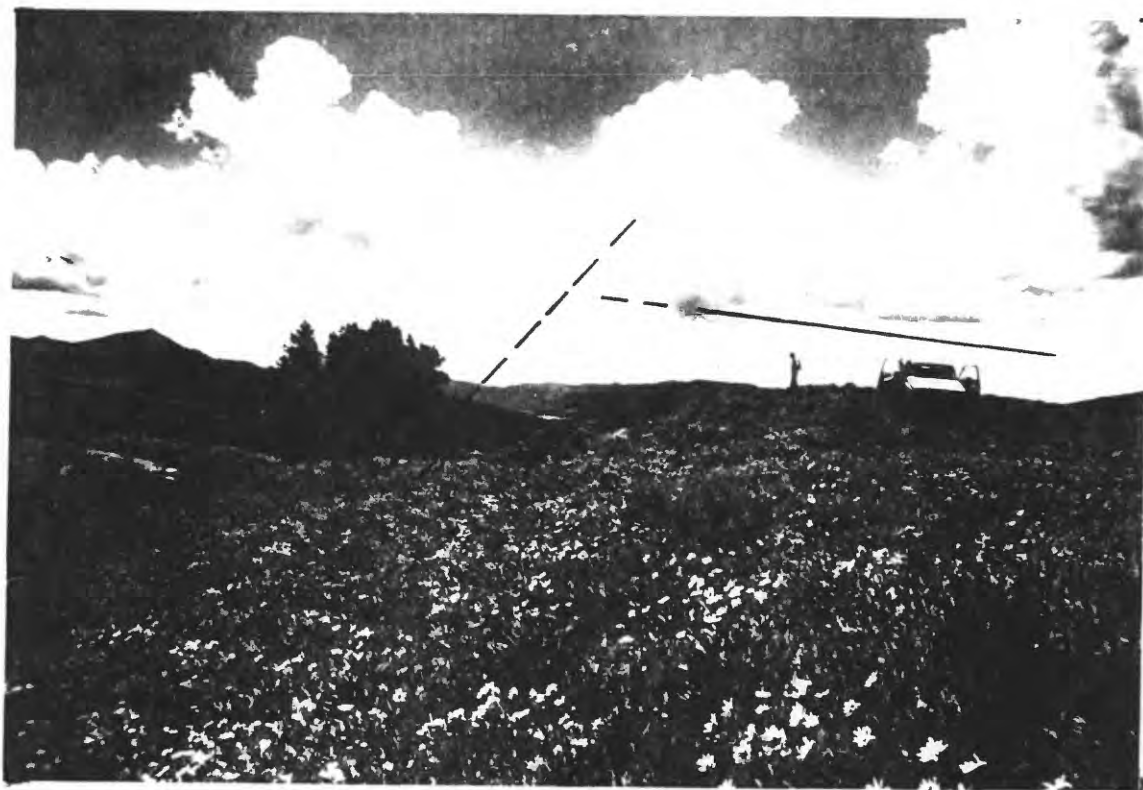


Figure 7. Photograph looking south along "new" fault on Baldy Mountain 32 km east of the Teton fault, Wyoming.

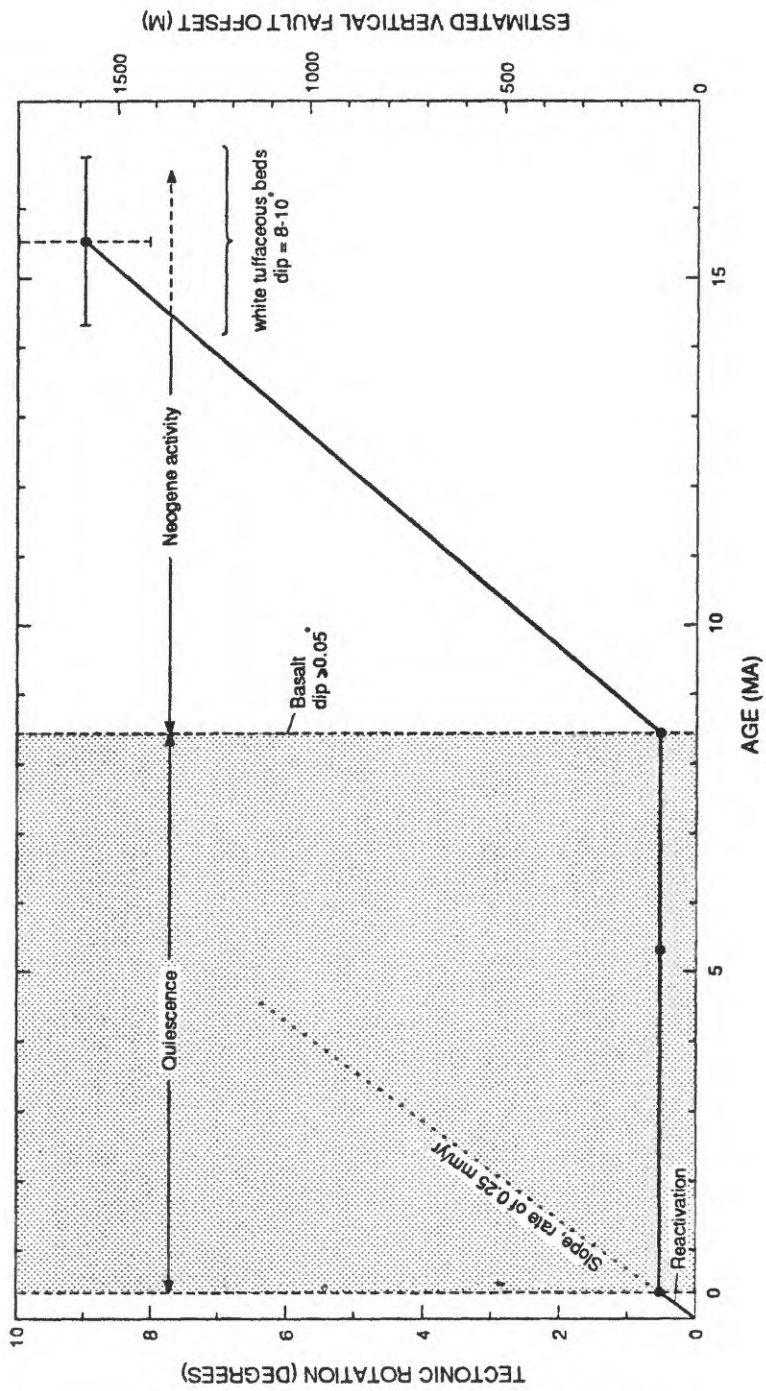


Figure 8. History of the recently reactivated Emigrant fault, a fault in Belt I about 75 km north of the Yellowstone calderas (Plate 1).

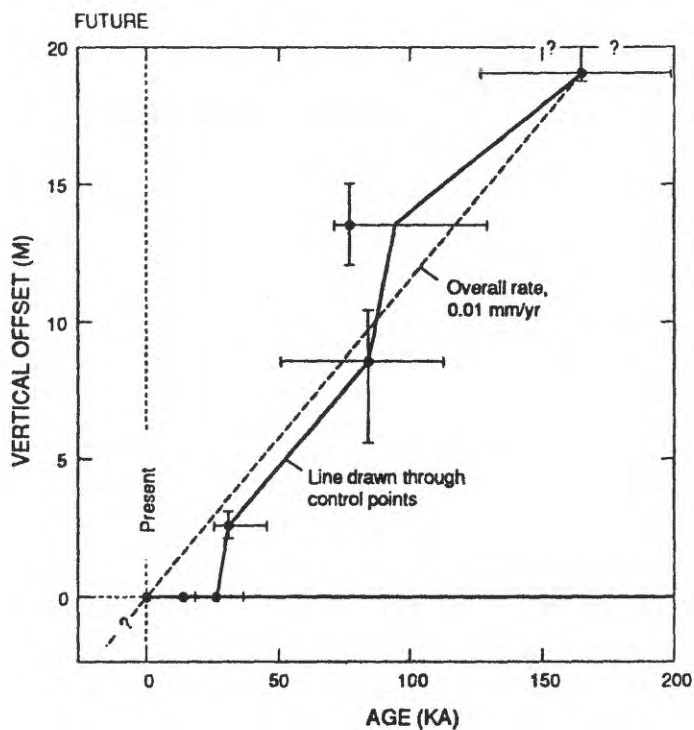


Figure 9. Late Quaternary history of the Arco segment of the Lost River fault, a fault in Belt III just north of the Snake River Plain.

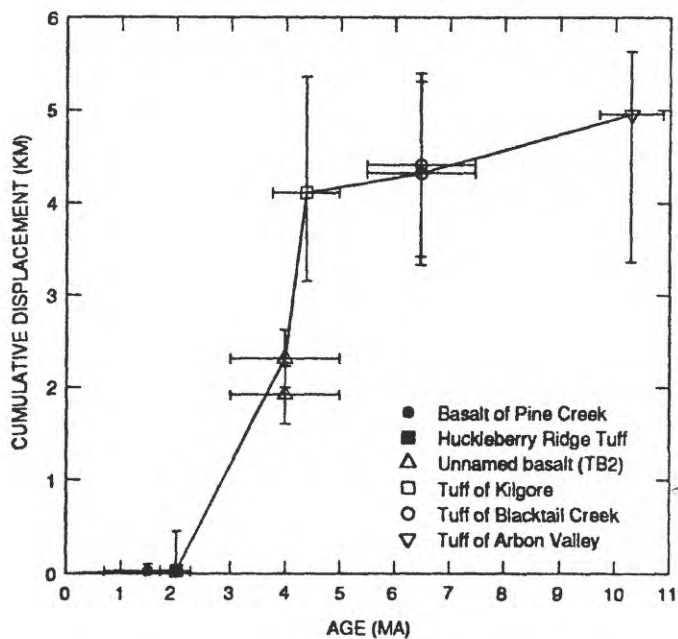


Figure 10. Late Cenozoic offset history of the Grand Valley fault, Idaho, based on tectonic rotation of volcanic layers (from Anders and others, 1989).

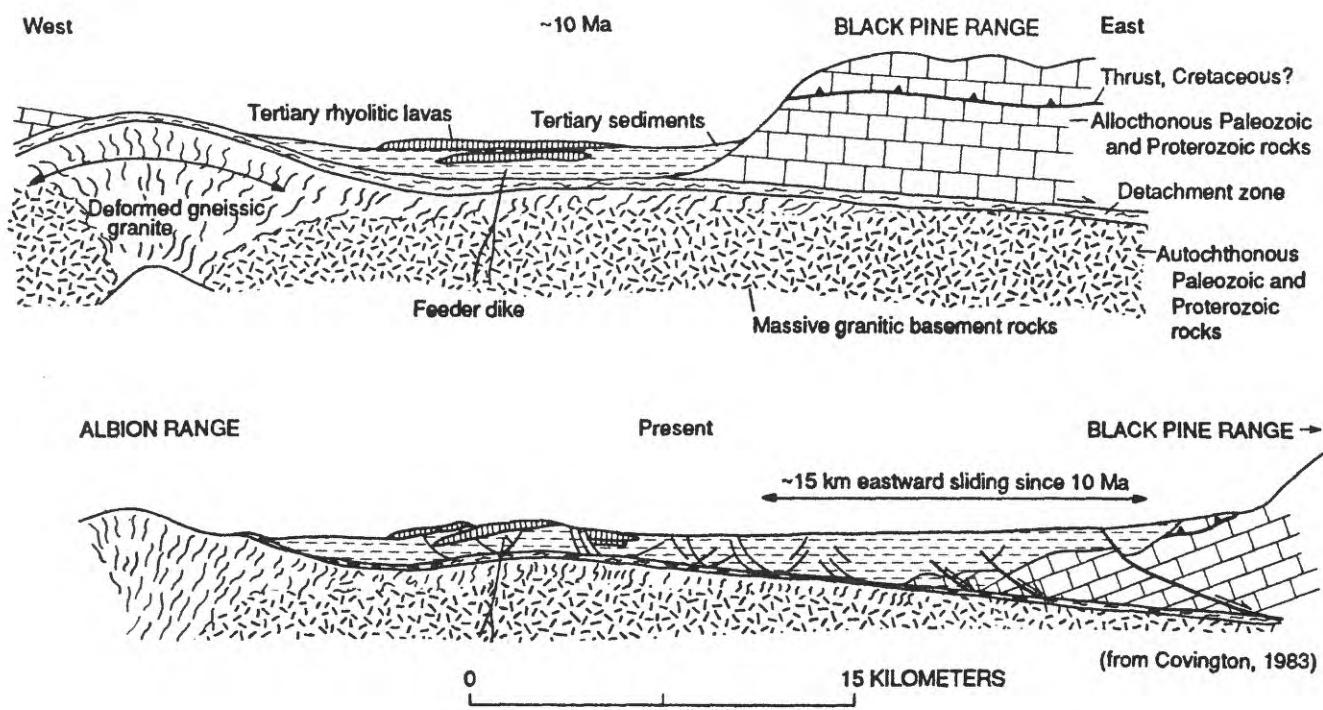


Figure 11. Deformation history of the Raft River valley and adjacent ranges showing about 15 km of sub-horizontal detachment faulting since 10 Ma (from Covington, 1983).

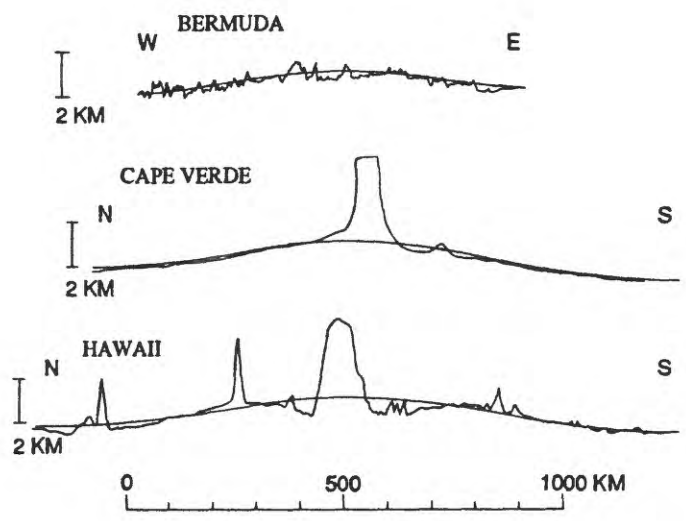


Figure 13. Profiles across three oceanic hotspot swells showing their large-scale topographic expression with heights of 1-2 km and diameters of 800-1200 km (from Crough, 1978).

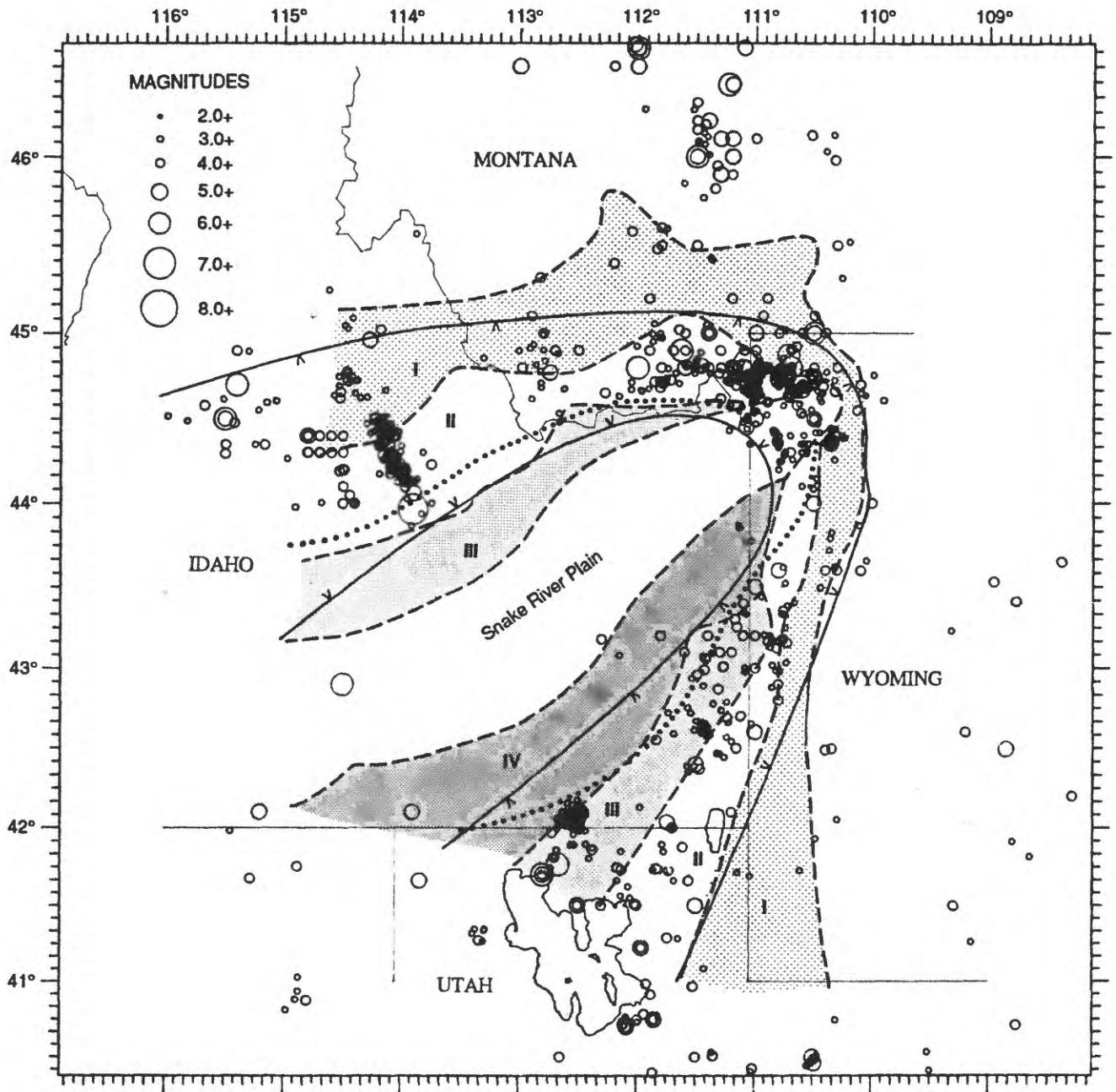


Figure 12. Correlation between belts of neotectonic faulting and historic earthquake locations in the Snake River Plain region.

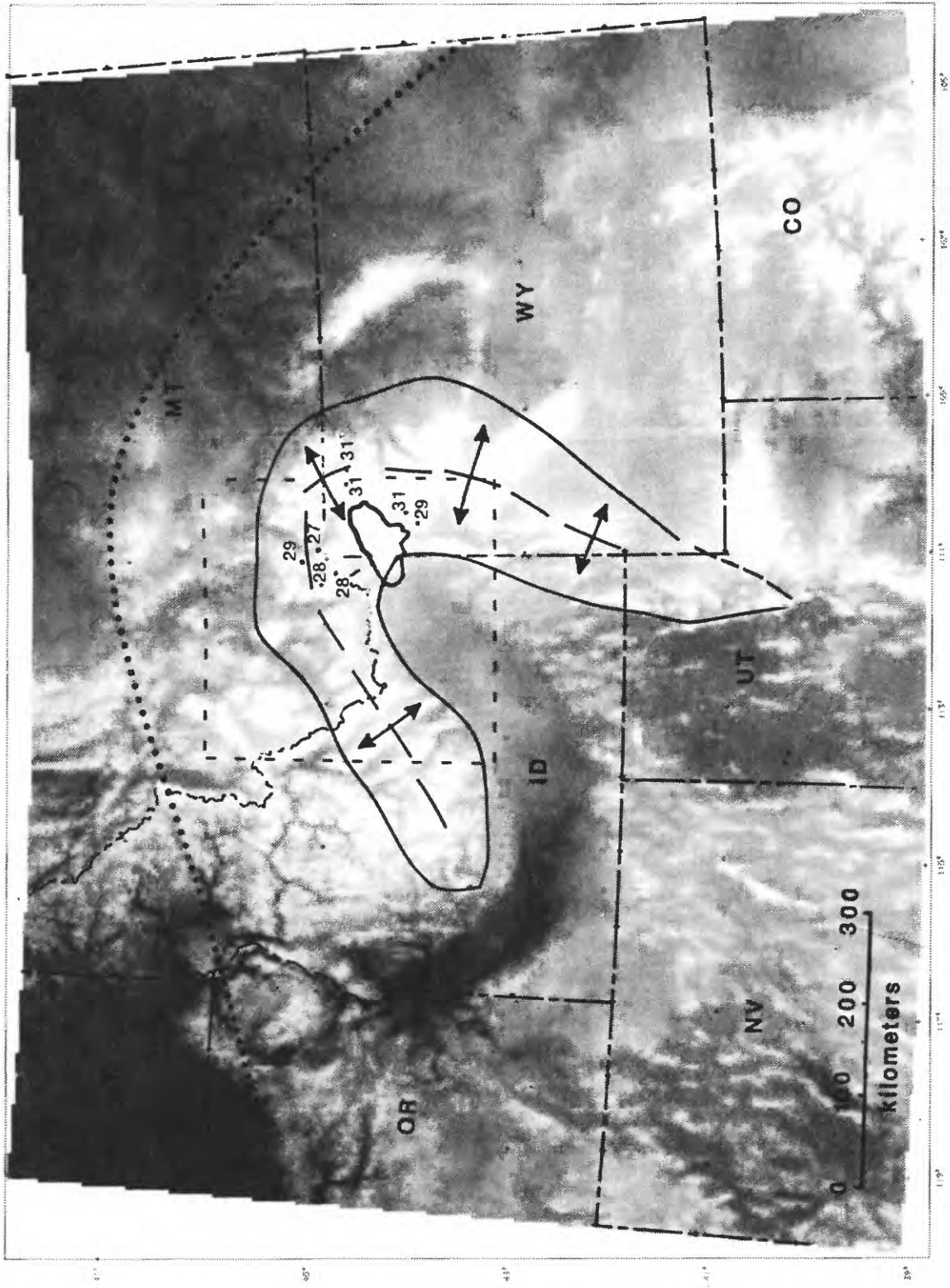
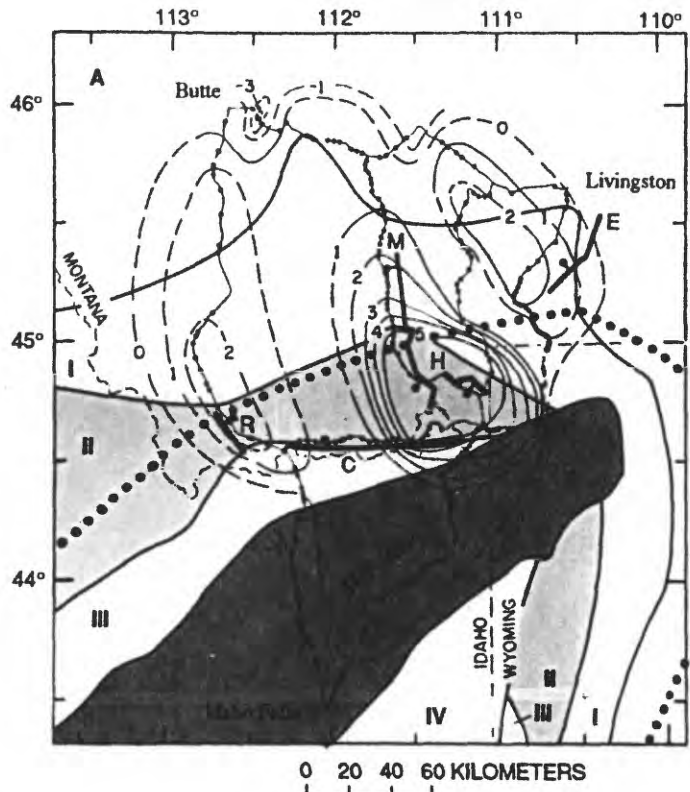


Figure 14. Gray-scale digital topography showing expression of the Yellowstone crescent of high terrain (solid line) that wraps around the Yellowstone Plateau.



EXPLANATION

- Axis of Yellowstone Crescent
- R— Red Rock Fault
- C— Centennial Fault
- M— Madison Fault
- H— Hebgen Fault
- E— Emigrant Fault

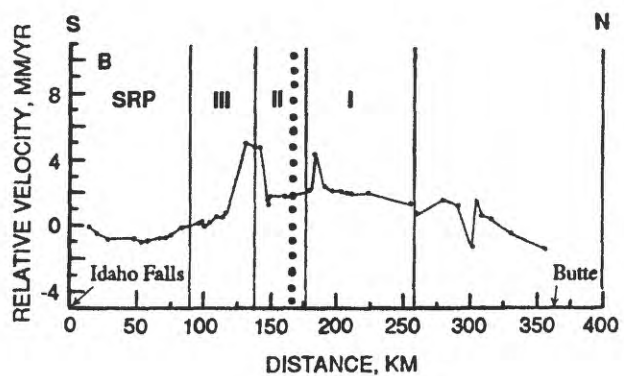


Figure 15. Historic vertical uplift across the western arm of the Yellowstone crescent of high terrain (from Reilinger, 1985).

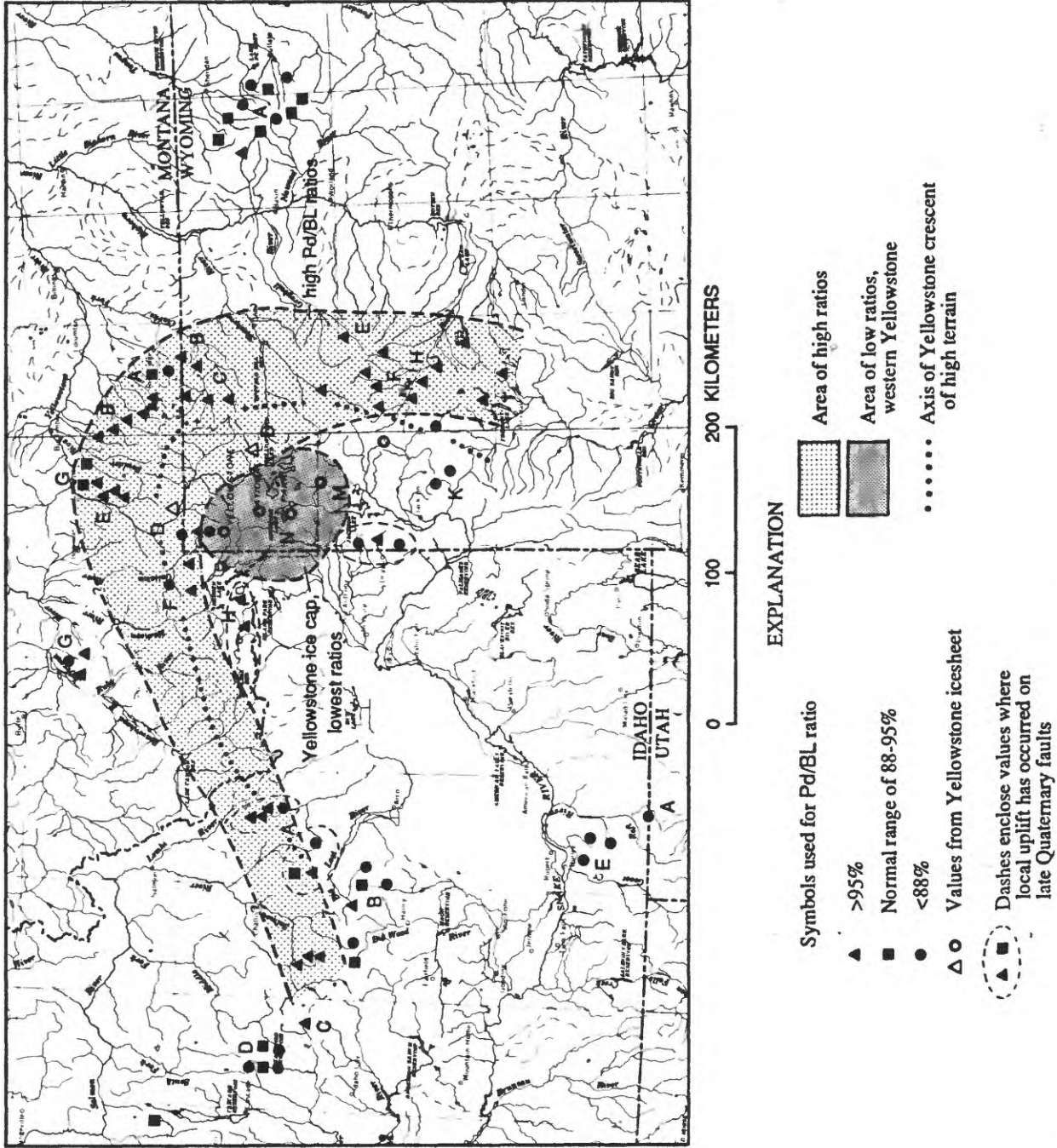
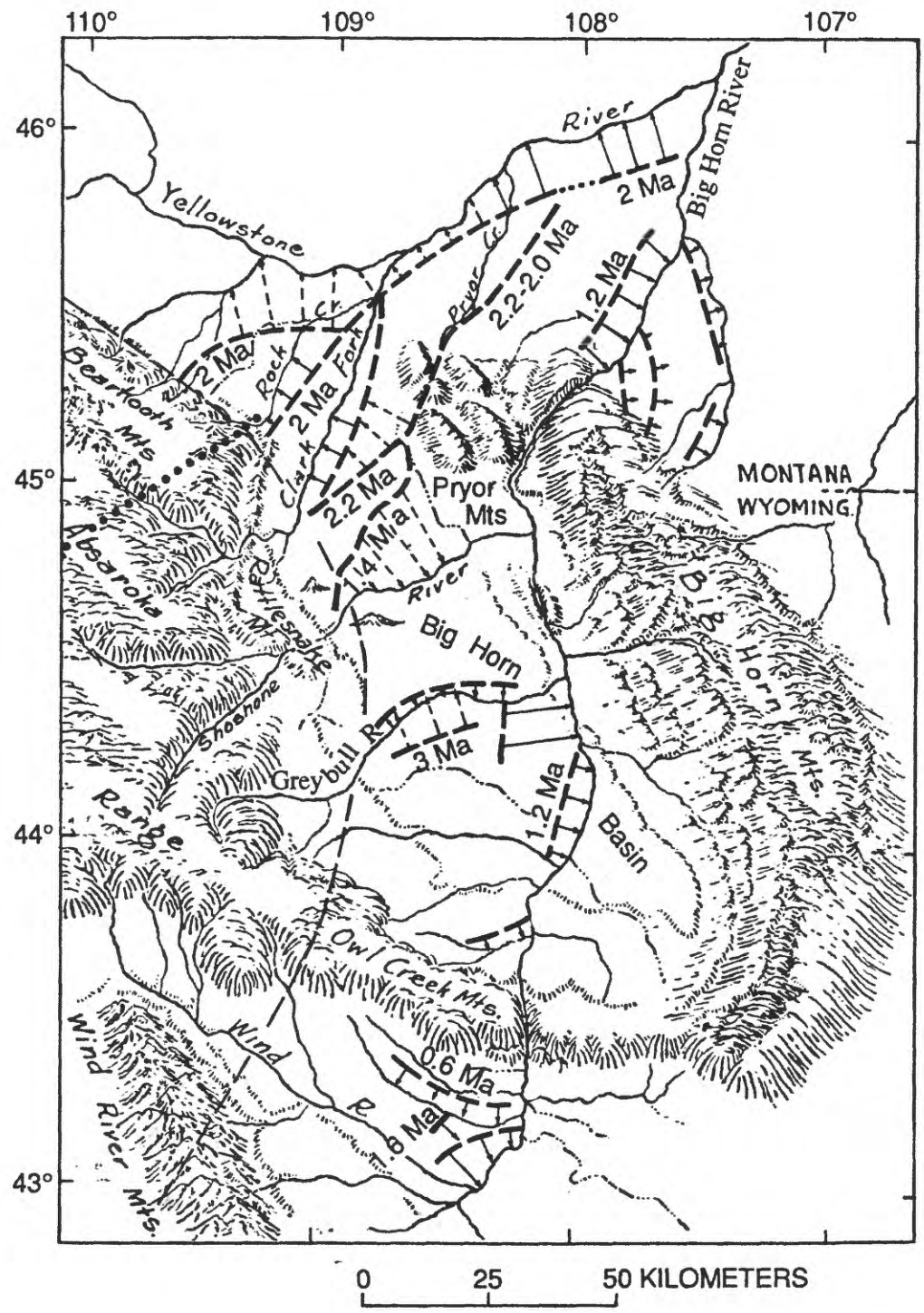


Figure 16. Ratios of the length of Pinedale to Bull Lake glaciers in the Yellowstone crescent of high terrain and nearby mountains.



EXPLANATION

- 1.6 Ma Ancestral stream courses with ages
- Migration by slip-off
- - - - -> Change due to capture
- Projected centerline of the Yellowstone hotspot

Figure 17. Direction of Quaternary unidirectional stream migrations by either slip off or capture, Bighorn Basin and adjacent areas.

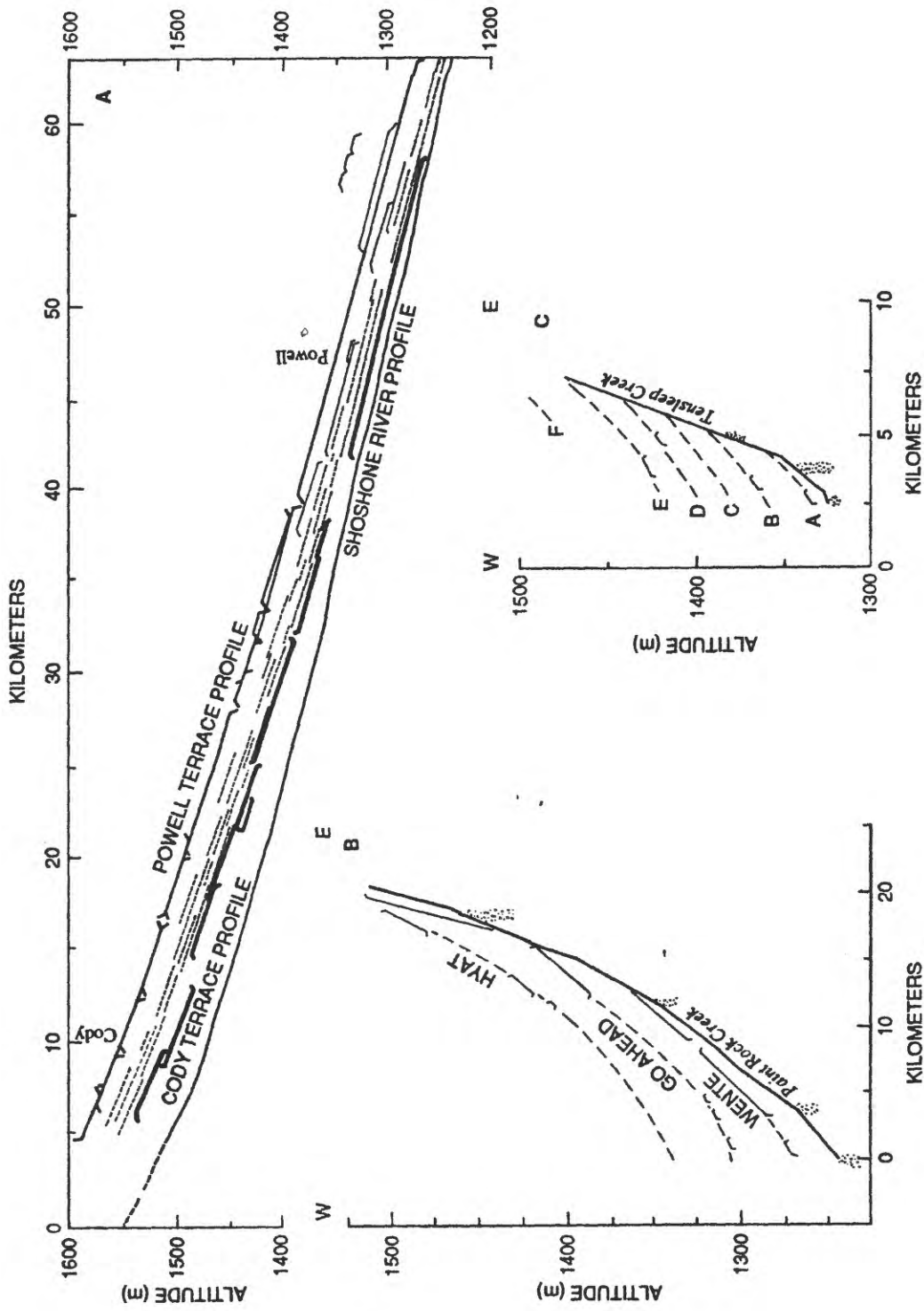


Figure 18. Terraces profiles along three selected streams, Bighorn Basin, Wyoming.

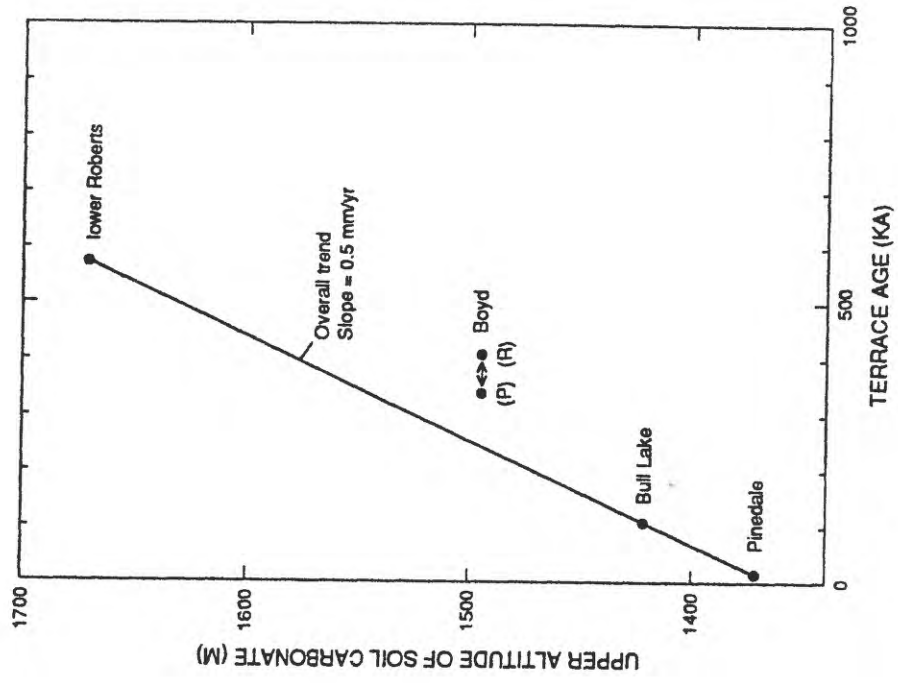


Figure 20. Decrease in the altitude of the upper limit of calcareous soils with terrace age along Rock Creek at northwest margin of Bighorn Basin, Montana (from Reheis, 1987).

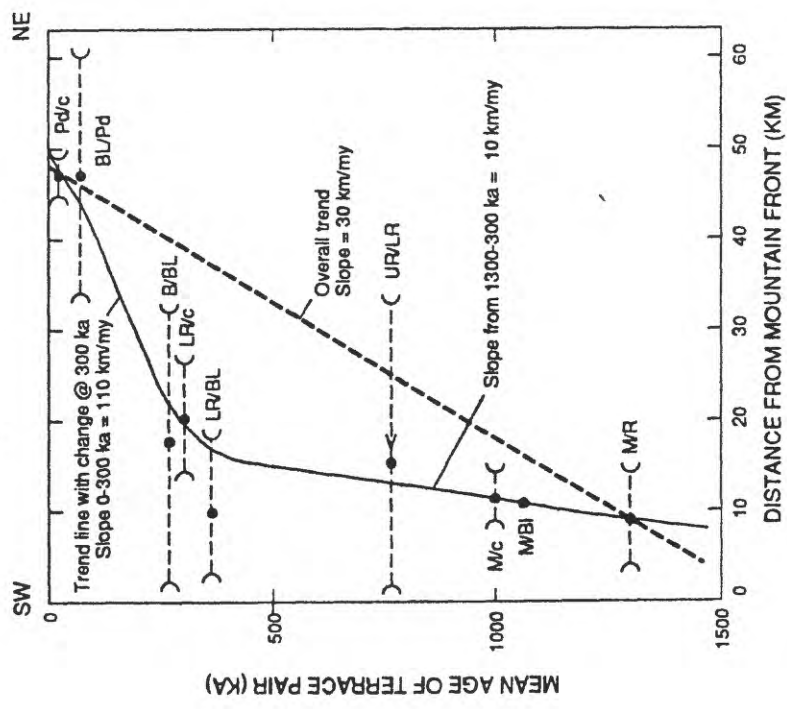


Figure 19. Northeast migration away from Yellowstone crescent and Beartooth Mountain front of the convergence/divergence points between pairs of terrace profiles, Rock Creek, Montana.

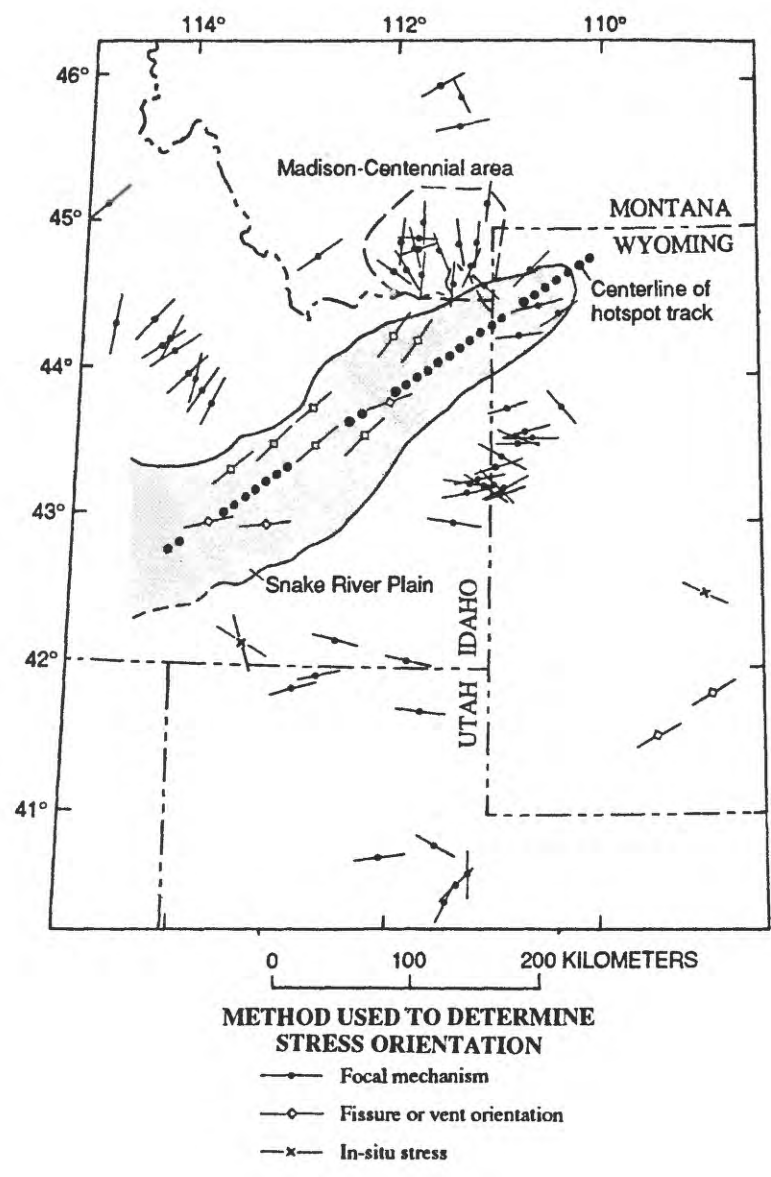
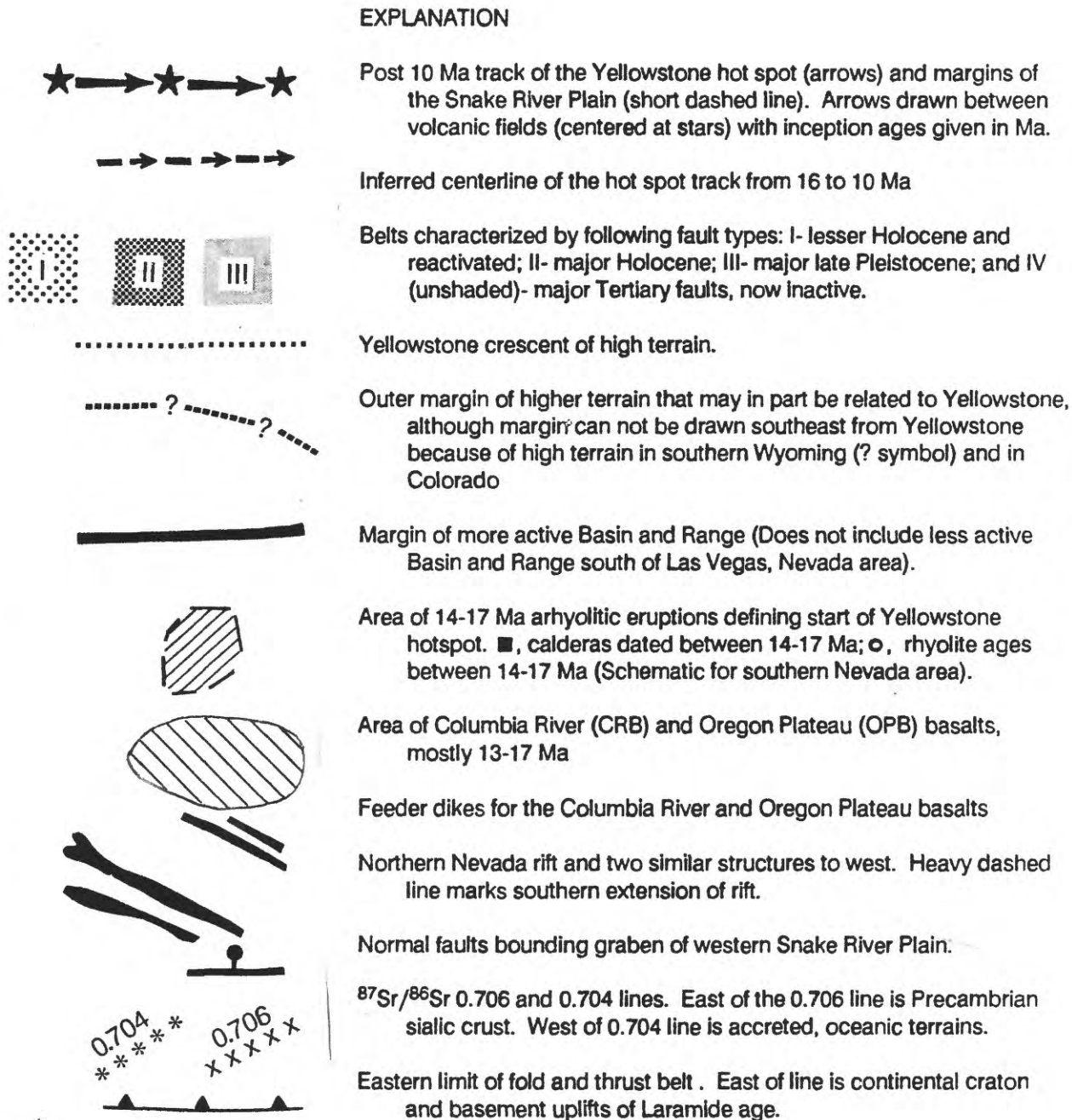


Figure 22. Stress distribution in the Snake River Plain region showing extensional (T-axis) orientations.



Part A

Figure 23. Major geologic features in the western U.S. associated with the late Cenozoic track of the Yellowstone hotspot.

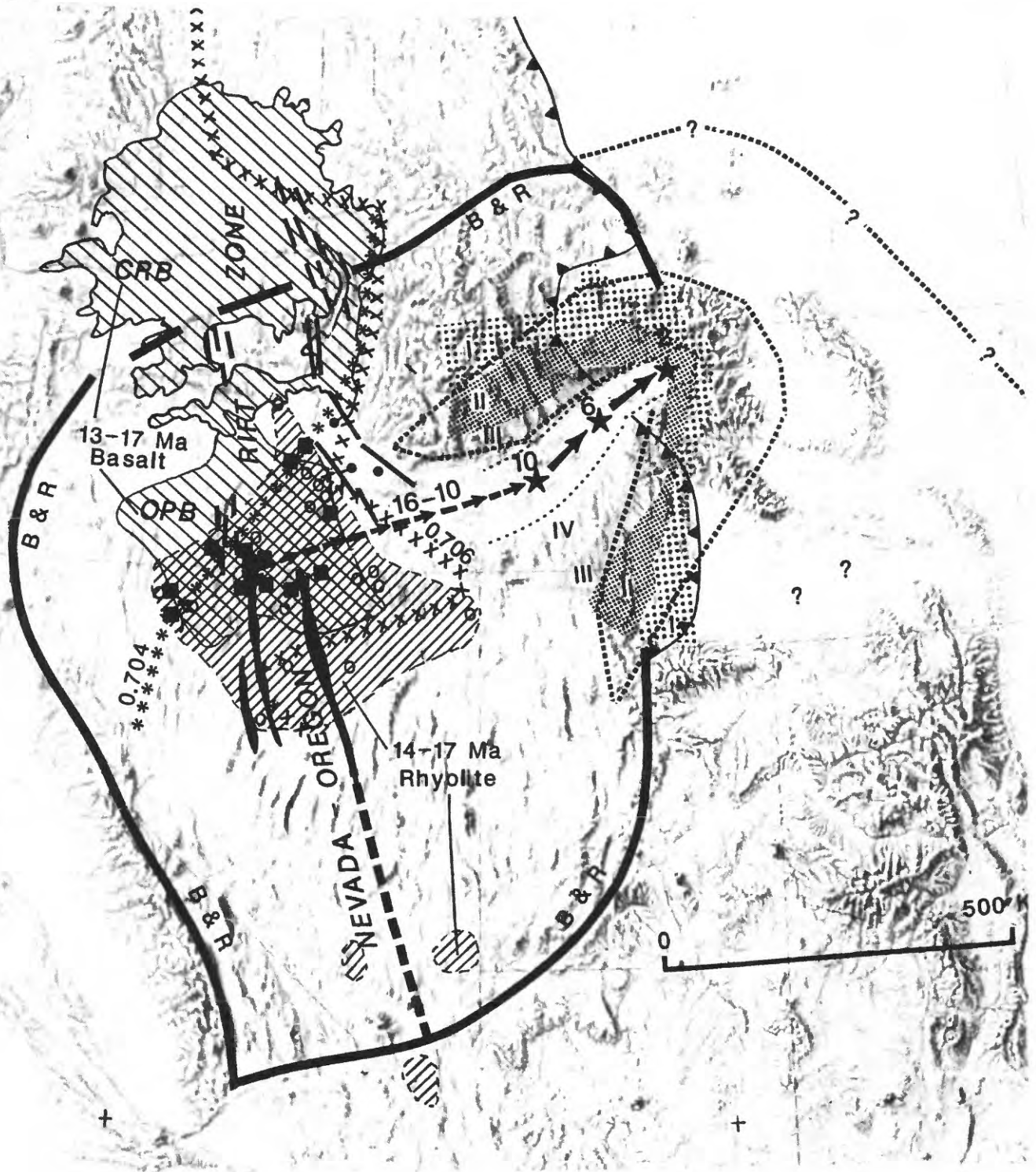


Figure 23. Major geologic features in the western U.S. associated with the late Cenozoic track of the Yellowstone hotspot. *Part B*

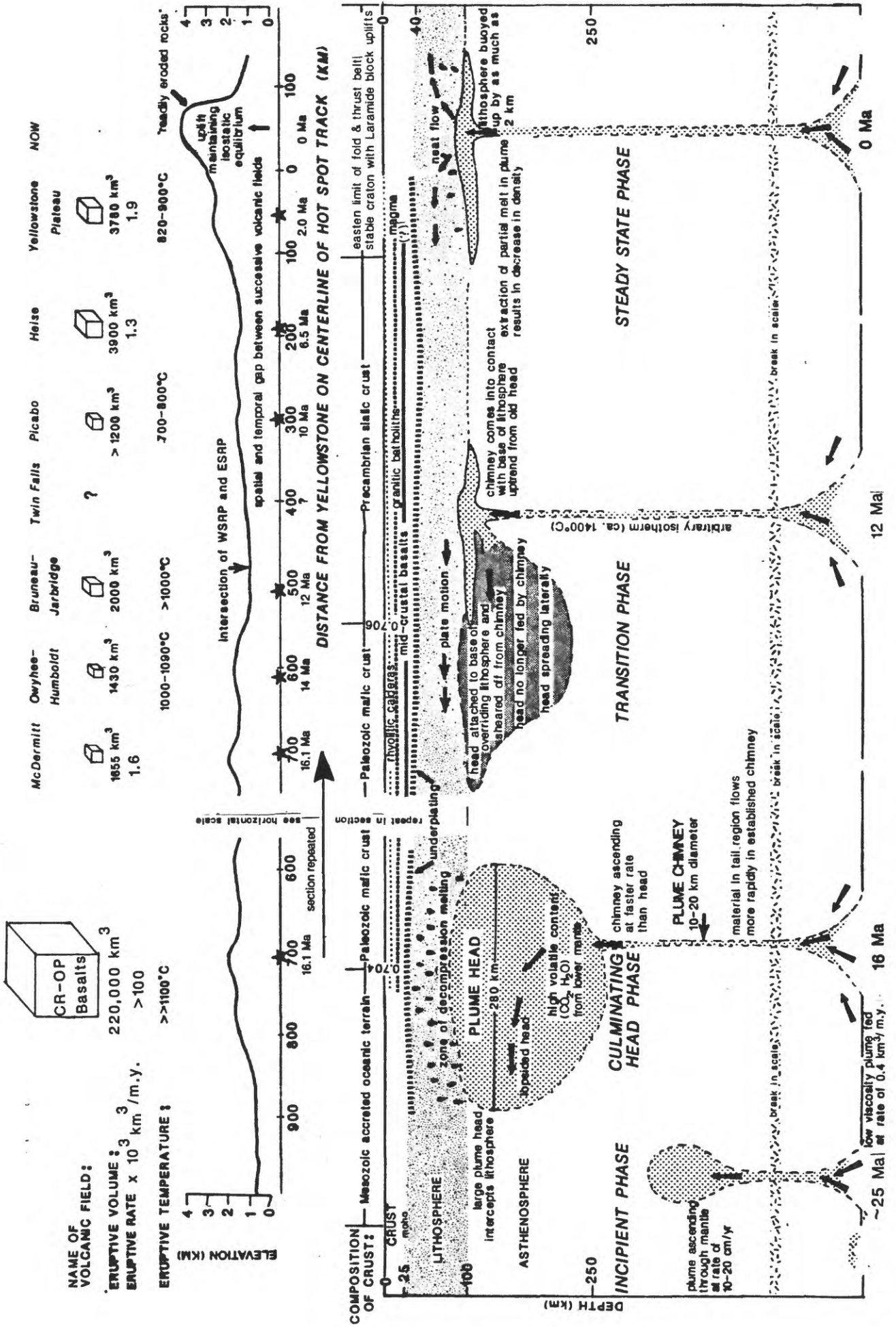


Figure 24. Postulated development of the Yellowstone thermal plume from its inception phase, through its huge head and transition phases, to its present chimney phase.

p 67

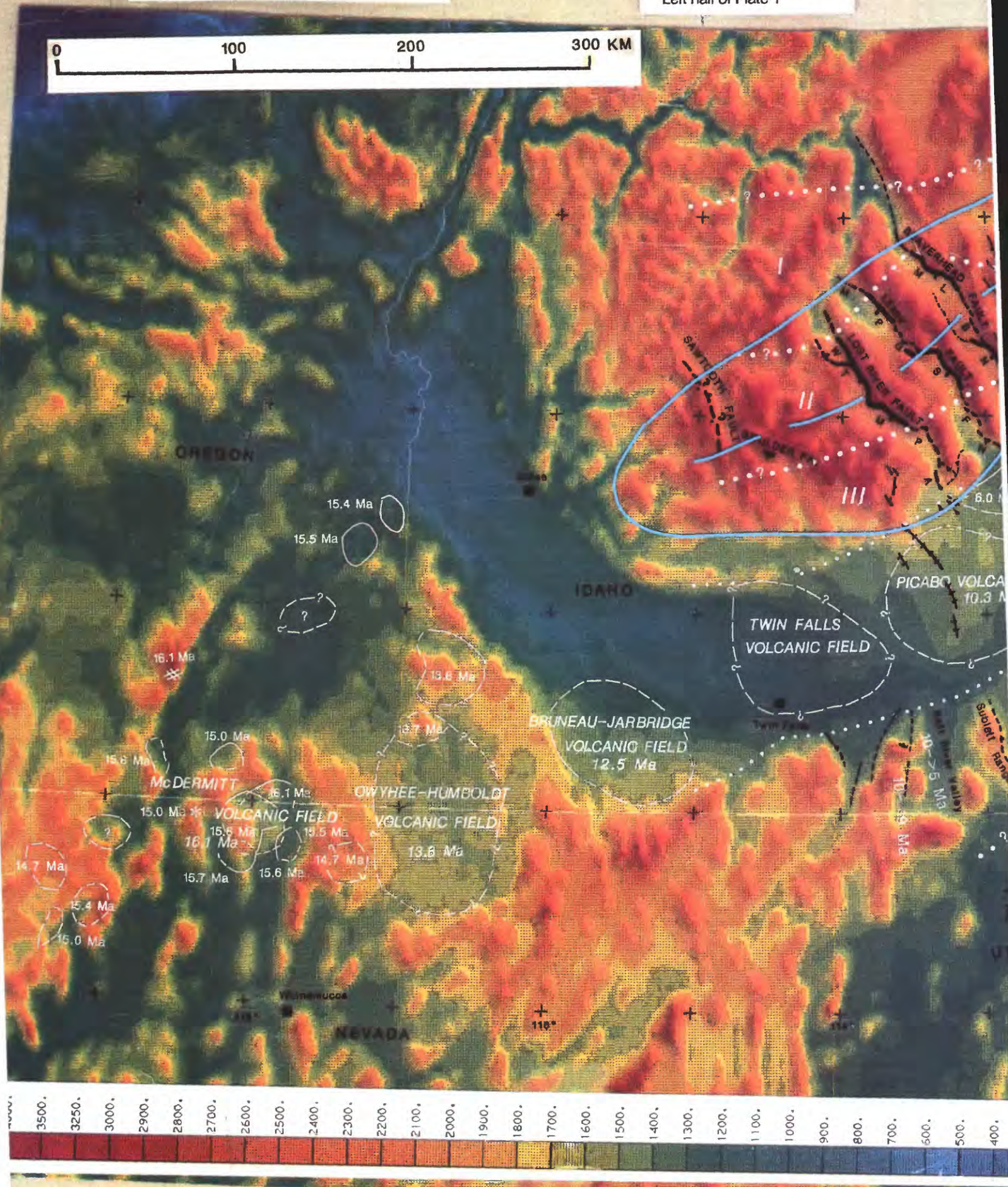


Plate 1. Volcanic fields, neotectonic fault types, and altitude near the track of the Yellowstone hot spot, Idaho and adjacent states.
Kenneth L. Pierce and Lisa A Morgan

This report is preliminary and has not been reviewed for conformity with U.S. Geological Survey editorial standards.

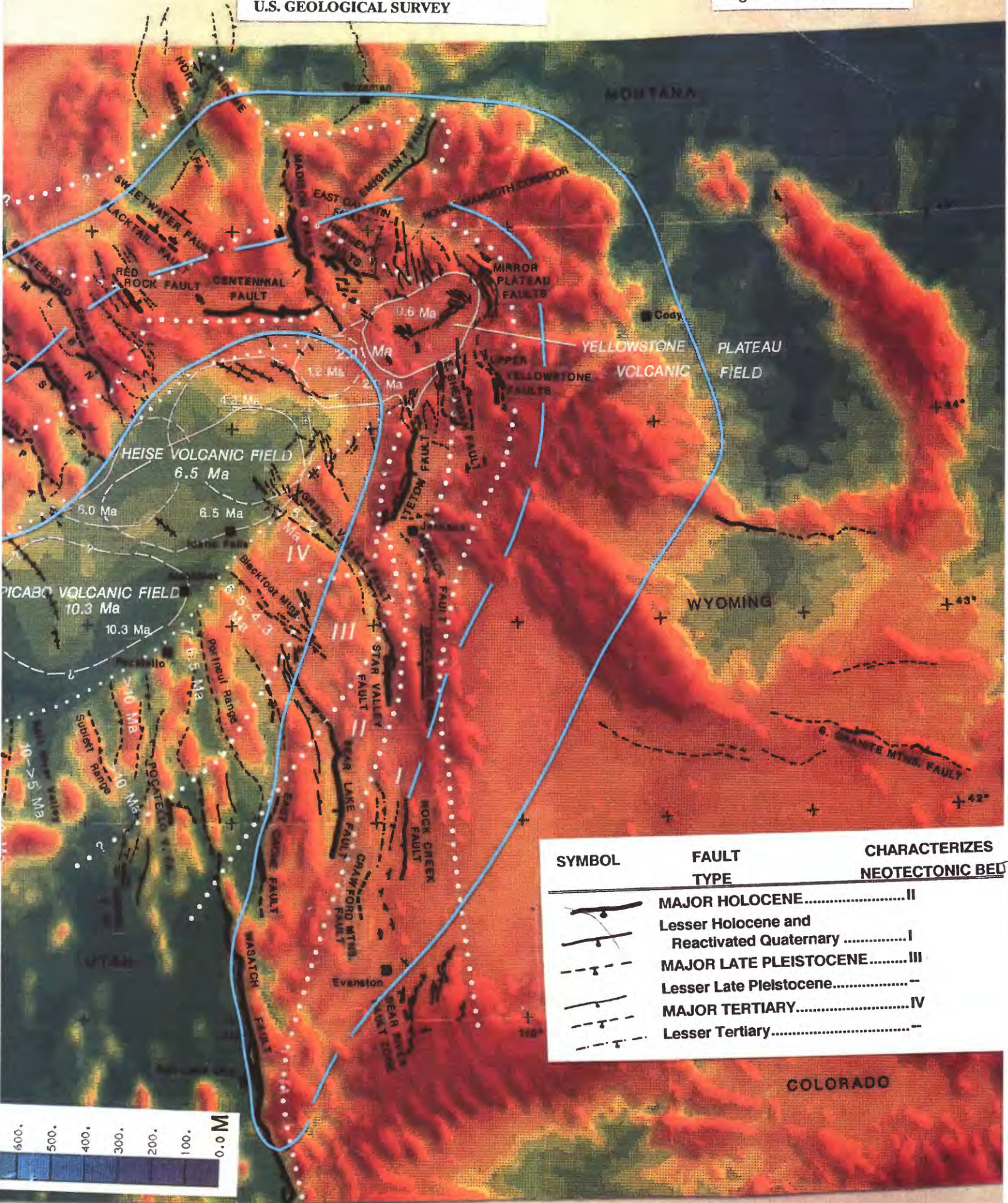


Plate 1. Volcanic fields, neotectonic fault types, and altitude near the track of the Yellowstone hot spot, Idaho and adjacent states.
Kenneth L. Pierce and Lisa A Morgan

This report is preliminary and has not been reviewed for conformity with U.S. Geological Survey editorial standards.